LUT University
School of Energy Systems
Degree program in Energy Technology
BH10A1101 Master's Thesis

Jere Kouvo

TECHNICAL REVIEW OF THERMAL ENERGY STORAGE TECHNOLOGIES FOR WASTE HEAT RECOVERY AND RELATED APPLICATIONS

Instructor: M.Sc. (Tech) Markku Kakko

Examiner: D.Sc. (Tech) Prof. Esa Vakkilainen

ABSTRACT

LUT University
School of Energy Systems
Degree program in Energy Technology

Jere Kouvo

Technical review of thermal energy storage technologies for waste heat recovery and related applications

Master's Thesis 2021
85 pages, 15 figures, 12 equations and 4 appendices

Examiners: D.Sc. (Tech) Prof. Esa Vakkilainen, D.Sc. (Tech) Juha Kaikko
Instructor: M.Sc. (Tech) Markku Kakko (Alfa Laval Aalborg Oy)

Keywords: Thermal Energy Storage TES, Waste Heat Recovery WHR, energy efficiency, process heat, power generation, sensible heat, latent heat

In this work different thermal energy storage technologies are reviewed and compared in their usefulness to be used in conjunction with waste heat recovery applications. Thermal energy storages can be categorized to sensible and latent heat storages, along with thermochemical storages which are not reviewed in this work. Sensible heat storages store energy by increasing the temperature of the storage material. Latent heat storages store energy in latent heat of phase change, usually melting.

Sensible heat storages are quite simple and commonly use cheap materials. Latent heat storages can store more energy in a smaller mass or volume than most sensible heat storages and have an additional benefit of doing so at a constant temperature level. However, they are generally more expensive than sensible heat storages and require further research in certain areas until they can be fully commercialized.

Sensible heat storage systems are identified as viable and also safer options for most applications, while latent heat storage technology offers more chances for development.

TIIVISTELMÄ

LUT University
School of Energy Systems
Energiatekniikan koulutusohjelma

Jere Kouvo

Termiset energiavarastot lämmön talteenoton yhteydessä

Diplomityö 2021
85 sivua, 15 kuvaa, 12 yhtälöä and 4 liitettä

Tarkastajat: TkT Prof. Esa Vakkilainen, TkT Juha Kaikko
Ohjaaja: DI Markku Kakko (Alfa Laval Aalborg Oy)

Hakusanat: Termiset energiavarastot, hukkalämmön talteenotto, energiatehokkuus, prosessilämpö, sähköntuotanto, tuntuva lämpö, latenttilämpö

Työssä tarkastellaan erilaisia termisiä varastoteknikoita ja vertaillaan niiden soveltuvuutta käytettäväksi hukkalämmön talteenoton yhteydessä. Termiset energiavarastot voidaan jaotella tuntuvaa lämpöä hyödyntäviin varastoihin, latenttilämpövarastoihin ja termokemiallisiin varastoihin, joista viimeisiä ei käsitellä tässä työssä. Tuntuva lämpö viittaa materiaalin sisäenergian kasvattamiseen sen lämpötilaa nostamalla. Latenttilämpövarastot taas sitovat ja vapauttavat energiaa varastoaineen olomuodonmuutoksissa.

Tuntuvat lämpövarastot ovat yksinkertaisia toimintaperiaatteeltaan ja hyödyntävät usein halpoja materiaaleja. Latenttilämpövarastot puolestaan kykenevät varastoimaan energiaa pienempään massaan ja tilavuuteen kuin tuntuvat lämpövarastot. Lisäksi latenttilämpövaraston lämpötila ei juuri muutu varastoa ladatessa tai purkaessa, mikä voidaan nähdä etuna. Latenttilämpövarastot ovat kuitenkin yleisesti ottaen kalliimpia kuin tuntuvat lämpövarastot, ja vaativat jatkotutkimusta tietyillä osa-alueilla ennen kuin niitä voidaan täysin hyödyntää kaupallisesti.

Tuntuvat lämpövarastot havaitaan käyttökelpoisiksi vaihtoehdoiksi useimpiin käyttökohteisiin ja ovat tässä vaiheessa niin teknisesti kuin taloudellisestikin varmempia vaihtoehtoja. Latenttilämpövarastoissa on puolestaan enemmän potentiaalia kehitykselle ja tätä myötä aseman luomiselle lämpövarastomarkkinoilla.

FOREWORD

I have never been a man of many words, so I won't break character too much if I keep this relatively short as well.

First and foremost, I would like to thank my parents, my brother and other close family members who have all supported me throughout the years all the way up to this point.

Thank you to my instructor, managers and co-workers at Alfa Laval Aalborg who gave me the opportunity to do this thesis in the first place and supported me through thick and thin to see it finished.

And finally, a warm thank you to all the great people who I had the pleasure of sharing my time as a student at LUT university with.

The global pandemic that we have been enduring for the past year has definitely spiced things up in terms of our everyday lives and is sure to leave a mark in history. While I do not expect this thesis to do quite the same, I at least hope that all this time the pandemic allowed me to spend alone in my apartment working on it will be worth the outcome. After a long and bumpy journey into the world of thermal energy storage I am very proud (and probably even more so relieved) to present to you, my thesis.

May 3rd, 2021, Rauma

Jere Kouvo

TABLE OF CONTENTS

LIST OF SYMBOLS AND ABBREVIATIONS

Roman alphabet

C	heat capacity	[kJ/K]
c_p	specific heat capacity at constant pressure	[kJ/kgK]
c_v	specific heat capacity at constant volume	[kJ/kgK]
H	enthalpy	[kJ]
h	specific enthalpy, latent heat	[kJ/kg]
k	thermal conductivity	[W/mK]
m	mass	[kg]
P	power	[W]
p	pressure	[bar]
Q	energy, (energy density)	[kJ, kWh]
q	heat flow	[W]
q_m	mass flow	[kg/s]
T	temperature	[K, °C]
U	internal energy	[kJ]
u	specific internal energy	[kJ/kg]
V	volume	[m^3, l]
v	specific volume	[m^3/kg]

Greek alphabet

η	efficiency	[-]
μ	dynamic viscosity	[kg/ms]
v	kinematic viscosity	[m^2/s]
ρ	density	[kg/m^3]

Subscripts

amb	ambient
b	bulk, gravimetric
f	fluid
g	gas, gaseous
in	input
l	liquid
loss	(heat) loss
mol	molar
out	output
s	solid, solidification
vol	volumetric
x	exergy, exergetic

Abbreviations

ALA	Alfa Laval Aalborg OY
CHP	Combined Heat and Power
CSP	Concentrated Solar Power
ES	Energy Storage
GT	Gas Turbine
HTF	Heat Transfer Fluid
ICE	Internal Combustion Engine
MSTG	Modular Steam Turbine Generator
PCM	Phase Change Material
PFG	Process Flue Gas
TES	Thermal Energy Storage
WHR	Waste Heat Recovery

1 INTRODUCTION

Global warming is a hotter topic day by day. A crucial part of finding solutions to this problem is increasing the share of renewable energy sources in the global energy system. An equally important goal is to reduce unnecessary consumption and loss of energy. Population growth and continuous increase in standards of living and industrialization mean the total global energy consumption will increase in the future, so the usage of energy must be made as effective as possible and alternative ways of covering our energy consumption must be found. (Dincer et al. 2018, 35-36)

The storage of energy is not a new concept by any means. Water has been used for hundreds of years as a means to store both cold and heat for later use, cold in the form of latent energy of ice blocks and heat tied to hot water (Stadler et al. 2019, 589). Other forms of energy storage can be seen in nature as well, as the reaction of photosynthesis can be considered a form of chemical energy storage (Sterner 2019, 4).

An interesting observation during the covid-19 pandemic by many engineers, economics, and other followers of the energy market, including people at Wärtsilä Oy, is how the pandemic and resulting changes in social behavior have effectively simulated a global energy system model from the future, with reduced energy consumption that leads to a higher fraction of renewable energy production as renewable sources are prioritized over fossil ones. On Sunday 5th of July 2020, a record share of 55% renewable energies of all production was observed in Europe, something that was not expected until five to ten years in the future. These observations were performed in this case using the Wärtsilä Energy Transition Lab webtool which is publicly available. (Wärtsilä 2020a; b; c)

The increase in the share of renewable energy sources is often associated with increase in demand for balancing power and flexible production to compensate for fluctuations in renewable energy production, in order to keep the power grid stable. (Dincer et al. 2018, 37; Sterner et al. 2019b, 53; 68-69; Wärtsilä 2020b) This demand also opens business opportunities for the energy storage sector. While most renewable energy sources will most directly benefit from electricity storage, thermal energy storage will also have its

place in the future energy system. (Stadler et al. 2019, 588; Sterner et al. 2019b, 68-69; Stevanovic et al. 2020, 1)

In order to accommodate renewable energy production to power grid, existing high-priority Combined Heat and Power (CHP) plants also need to be made more flexible so they can more individually follow demands of power and heat side by side with renewable production instead of being baseline production that acts as a barrier to increasing the usage of renewable capacity. Thermal energy storage can assist in reaching this goal by helping separate the power and heat end-production of CHP plants. (Sterner et al. 2019b, 54; 69; 133; Sterner et al. 2019c, 153; Sterner et al. 2019e, 668; Sterner et al. 2019g, 758; 761-762)

The effects of relying on large power plants as baseload power in times of renewable-dominated production can already be seen. On certain days in June and July of 2020, due to the aforementioned increase in share of renewables caused by lockdowns of covid-19, Germany had to pay nearly 1m€/h to neighboring countries to take away excess electricity to avoid shutting down and restarting their baseload plants; this could have partially been avoided with larger electricity- and thermal energy storage capacities. (Wärtsilä 2020b)

Even disregarding these eventual issues with grid balance and concentrating on present moment, thermal energy storage together with waste heat recovery can significantly increase the efficiency and flexibility of conventional thermal energy systems, including but not limited to different power plants, resulting in reductions to emissions and costs. According to Miró et al., the energy and industrial sectors together are the largest consumers of energy in the world, so increasing their efficiency and cutting down their energy losses and emissions would be integral in slowing down climate change. (Dincer et al. 2018, 37-38; 85; Miró et al. 2016, 284-285)

The objective of this thesis is to review thermal energy storage technologies based on their technical suitability for use with Alfa Laval Aalborg catalogue. This is done by answering the following questions:

- Operational temperature range
- Storage capacity

- Heat transfer properties
- Material limitations and hazards
- Simplicity
- Modularity
- Economic feasibility

It should be noted that while part of the review is seeing any indication towards economic feasibility, detailed economic assessment is not an objective of this work.

2 BASIS OF WASTE HEAT RECOVERY

The foundation of Waste Heat Recovery (WHR) is to increase the thermal efficiency of a given power plant or industrial plant application by capturing excess heat from its flue gas or another heat source and converting it to a usable form. This leads to economic savings and reductions in emissions as more benefit is gained from the same amount of primary energy. The utilization possibilities of the recovered heat depend on the temperature level of the heat source, with higher temperature waste heat having a wider scope of usefulness. (Miró et al. 2016, 284-286)

Internal combustion engines (ICEs), and by extension gas turbines (GTs), are prime candidates for waste heat recovery. Even with some of the highest efficiency machinery, less than half of the energy content of fuel of an internal combustion engine is converted to power output, the rest is released with flue gases. A good portion of this waste heat can be recovered by a waste heat recovery boiler. ICEs generate sufficiently high amounts of high-temperature flue gas to act as a heat source for a boiler system. (Pandiyarajan et al. 2010, 78; 87; Pandiyarajan et al. 2011, 6011; Shu et al. 2016, 693-694)

Applying WHR on an engine or gas turbine, or any other power production process, should be non-disruptive for the main appliance's operation, as that is the main economical drive. Possible disruptions include increased backpressure and more complex control of the system, particularly in transient operating conditions and startup/shutdown. (Boretti 2012, 18; Pandiyarajan et al. 2010, 78; 87) At times of no/reduced heat demand it is common to use a damper to bypass the WHR boiler in exhaust gas duct or adjust the amount of fed exhaust gas, effectively wasting the heat.

Waste heat in the industrial sector is underutilized in comparison to its potential. This is likely because industrial processes are more sensitive to disruptions that applying WHR might bring than direct power generation applications. The mismatch between heat supply and demand that power generation applications suffer from is amplified in industrial applications, as those operate based on their own unique technical and economic criteria and often have high inherent slowness in starting up and slowing down the process. Furthermore, industrial processes may have other technical features that might cause

difficulties for WHR, such as challenging flue gas compositions. (Miró et al. 2016, 284-285)

In both power production and industrial applications, the challenging mismatch between supply and demand of heat could be remedied using a thermal energy storage (TES) system. TES improves the flexibility of an energy system so that WHR can be applied even if it is otherwise seen as potentially disruptive for the operation of the main process. (Miró et al. 2016, 284-286) The aim of this thesis is to explore possible options for TES to be used together with WHR applications.

2.1 WHR applications in Alfa Laval Aalborg

Alfa Laval Aalborg OY is part of the Alfa Laval Corporate AB, and a global leader at Waste Heat Recovery (Alfa Laval 2015a). The main product is the Aalborg AV-6N, a finned tube heat recovery boiler that is capable of recovering waste heat from flue gases from a wide range of engine fuels as well as process flue gases (Alfa Laval 2015b).

The typical heat recovery area for AV-6N ranges to flue gas temperatures up to 530 °C. Typical product is either saturated or superheated steam up to 40 bar(g) in pressure and 400 °C in temperature, or hot water. The result steam and hot water can be used for a wide range of applications, including power generation with a steam turbine. (Alfa Laval 2015b) The Alfa Laval Aalborg catalogue also includes the Modular Steam Turbine Generator (MSTG), which is designed to be compatible with the AV-6N.

3 BASIS OF THERMAL ENERGY STORAGE

Energy storage (ES) is the process of converting usable energy into another form where it can be held for later use and then reverting it back to a usable form when needed. The act of converting for storage and reverting for use are called “charging” and “discharging” in this context. The concept of energy storage is demonstrated in Figure 3.1. (Sterner et al. 2019a, 24)

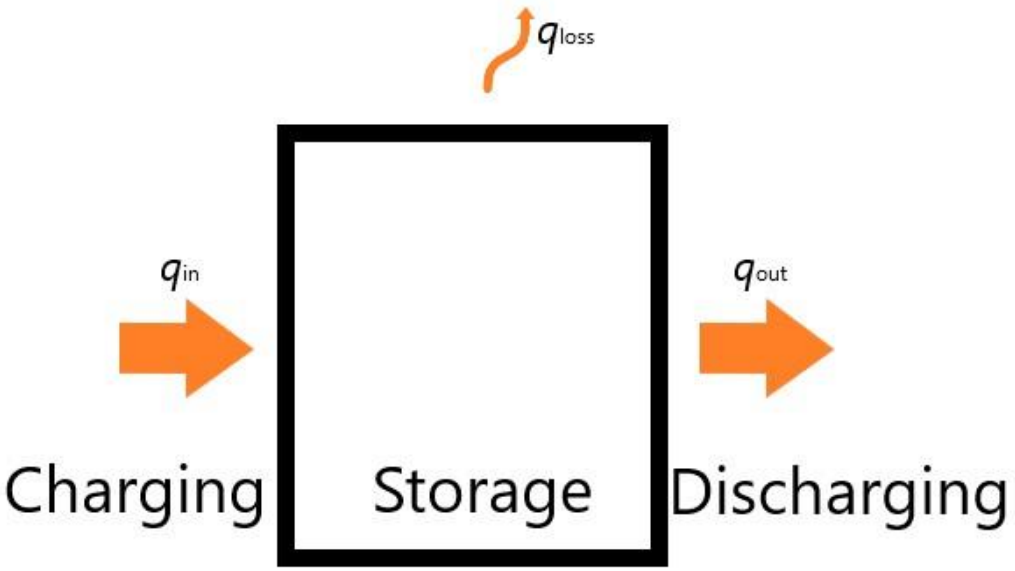

Figure 3.1. Concept of energy storage, demonstrated with thermal energy. (Sterner et al. 2019a, 25; Dincer et al. 2018, 138)

Thermal Energy Storage (TES) applies this same principle for thermal energy, or heat. Technically speaking, heat is not a state variable but only exists when thermal energy is being transferred from one system to another. In other words, thermal energy storages do not in fact contain any heat but possess a thermodynamic potential to transfer heat. However, it is common practice to call thermal energy storages “heat storages” (or “cold storages” where applicable). (Stadler 2019, 571-572)

3.1 Thermodynamic definitions

Energy and exergy

Energy is a state variable describing the thermodynamic, mechanical, or chemical potential of a system. According to the first law of thermodynamics, energy is never created nor consumed, but rather converted to other forms. (Stadler 2019, 571-572) A generic energy balance for a thermal energy storage unit, such as one in Figure 3.1, can be displayed as

$$\frac{\Delta Q}{\Delta t} = q_{\text{in}} - q_{\text{out}} + \frac{\Delta Q_{\text{gen}}}{\Delta t} + q_{m,\text{in}} \cdot h_{\text{in}} - q_{m,\text{out}} \cdot h_{\text{out}}, \quad (1)$$

where	ΔQ	change in energy content	[kJ]
	Δt	change in time	[s]
	q_{in}	heat flow in	[kW]
	q_{out}	heat flow out	[kW]
	ΔQ_{gen}	heat generated inside storage volume	[kJ]
	$q_{m,\text{in}}$	mass flow in	[kg/s]
	$q_{m,\text{out}}$	mass flow out	[kg/s]
	h_{in}	specific enthalpy of input flow	[kJ/kg]
	h_{out}	specific enthalpy of output flow	[kJ/kg].

In thermal energy storage systems, energy is not generated inside the storage volume; that term is normally reserved for use with chemical and nuclear reactions that generate heat from potential of matter. Additionally, in a closed TES system the in- and output mass flows are removed, and if heat losses are separated from heat output the balance can be displayed as

$$\frac{\Delta Q}{\Delta t} = q_{\text{in}} - q_{\text{out}} - q_{\text{loss}}, \quad (2)$$

where	q_{loss}	energy storage loss flow	[kW].

In an open system, on the other hand, mass can be transported to and from the volume. In TES this happens at direct charging, and commonly in this case it is the heat flow terms apart from heat loss that are removed from the balance equation, leading to

$$\frac{\Delta Q}{\Delta t} = q_{m,\mathrm{in}} \cdot h_{\mathrm{in}} - q_{m,\mathrm{out}} \cdot h_{\mathrm{out}} - q_{\mathrm{loss}}. \quad (3)$$

Kinetic and potential energy terms of the mass flow are not considered. In a cold storage application, the heat loss term in both above balances would be negative as it would be heat gain instead of removal. (Dincer et al. 2018, 8-12; 138; Incropera et al. 2007, 13-18)

Exergy, on the other hand, is the amount of energy that is possible to be converted to another form through a conversion process. Unlike energy, exergy is destroyed in processes due to irreversible losses. The unusable part of energy that is left when exergy is removed is called anergy. (Stadler 2019, 571-572; Dincer et al. 2018, 16-17)

The change of exergy in a system is defined as (Dincer et al. 2018, 141-142)

$$\Delta Q_{\mathrm{x}} = Q_{\mathrm{x},2} - Q_{\mathrm{x},1} = m \cdot \big((u_2 - u_1) - T_{\mathrm{amb}} \cdot (s_2 - s_1)\big), \quad (4)$$

where	$Q_{\mathrm{x,i}}$	exergy content at time i	[kJ]
	m	mass of the system	[kg]
	u	specific internal energy of the system	[kJ/kg]
	s	specific entropy of the system	[kJ/kgK]
	T_{amb}	ambient temperature	[K].

Entropy (or in this case, specific entropy) describes the level of thermodynamic disorder in a system. More specifically, the change of exergy in a purely sensible heat system can be written as (Dincer et al. 2018, 142)

$$\Delta Q_{\mathrm{x}} = Q_{\mathrm{x},2} - Q_{\mathrm{x},1} = mc_p \cdot \left((T_2 - T_1) - T_{\mathrm{amb}} \cdot \ln\left(\frac{T_2}{T_1}\right)\right), \quad (5)$$

where	c_p	specific heat of the system	[kJ/kgK]
	T_{i}	temperature of the system at time i	[K].

Change of exergy in a latent heat -based system that also experiences some change in sensible heat can be written as (Dincer et al. 2018, 146-148)

$$\Delta Q_{\mathrm{x}} = Q_{\mathrm{x},2} - Q_{\mathrm{x},1} = mc_{p,1} \cdot \left(\left(T_{\mathrm{pc}} - T_1 \right) - T_{\mathrm{amb}} \cdot \ln\left(\frac{T_{\mathrm{pc}}}{T_1} \right) \right)$$

$$+\Delta m h_{\mathrm{pc}} \cdot \left(\frac{T_{\mathrm{amb}}}{T_{\mathrm{pc}}} - 1 \right) + mc_{p,1} \cdot \left(\left(T_2 - T_{\mathrm{pc}} \right) - T_{\mathrm{amb}} \cdot \ln\left(\frac{T_2}{T_{\mathrm{pc}}} \right) \right), \qquad (6)$$

where	$Q_{\mathrm{x,i}}$	exergy content at time i	[kJ]
	m	mass of the system	[kg]
	$c_{p,\mathrm{i}}$	specific heat of the system at phase i	[kJ/kgK]
	h_{pc}	latent heat of the system	[kJ/kg]
	T_{i}	temperature of the system at time i	[K]
	T_{pc}	phase change temperature	[K]
	T_{amb}	ambient temperature	[K].

The above equation has been simplified by assuming that phase change happens completely between the two phases.

Energy and exergy efficiency

Energy efficiency in thermal energy storages is defined as the ratio of returned energy to stored energy (Dincer et al. 2018, 140)

$$\eta_{\mathrm{TES}} = \frac{Q_{\mathrm{out}}}{Q_{\mathrm{in}}}, \qquad (7)$$

where	η_{TES}	energy efficiency of TES system	[-]
	Q_{in}	stored energy input	[kJ]
	Q_{out}	discharged product energy output	[kJ].

The difference between Q_{out} and Q_{in} is the energy lost in heat losses during storage (Dincer et al. 2018, 138-140).

As the usefulness of thermal energy storage systems is strongly tied to the temperature they manage to maintain and output after a storage period, a better measure of performance would be exergy efficiency (Dincer et al. 2018, 142-145)

$$\eta_{\mathrm{x,TES}} = \frac{Q_{\mathrm{x,out}}}{Q_{\mathrm{x,in}}}, \tag{8}$$

where	$\eta_{\mathrm{x,TES}}$	exergy efficiency of TES system	[-]
	$Q_{\mathrm{x,in}}$	stored exergy input	[kJ]
	$Q_{\mathrm{x,out}}$	discharged product exergy output	[kJ].

Density

Density (ρ) is the weight of a material per unit of volume. It is normally displayed in kg/m^3. Density is a function of temperature, and as such thermal expansion needs to be considered when designing thermal energy storage systems. Large variations in density can even cause damage to storage vessels. With fluids, thermal change in density is the driving force for natural convection as well as causes layering for some liquids. The inverse value of density is called “specific volume” which is also commonly used in engineering calculations. (Dincer et al. 2018, 4; 218)

Heat capacity

Heat capacity (C) is an attribute of a system that reflects its ability to store thermal energy and resist change in temperature while doing so. Heat capacity of a system is the product of the mass of the system and its specific heat capacity and is commonly displayed in J/K. (Incropera et al. 2007, 258; 323; 680)

Specific heat capacity (c_p or c_v, also called “specific heat”) in turn is a physical characteristic of the storage material that is defined as the amount of heat in kilojoules [kJ] that a kilogram of said material must be subjected to in order to increase its temperature by one kelvin. The unit of specific heat capacity is thus kJ/kgK. (Dincer et al. 2018, 4-6; 60; Stadler et al. 2019, 574)

Specific heat capacity can be defined in either constant pressure (c_p) or constant volume (c_v); these values are equal for solids and liquids as their density is generally not affected by pressure. Therefore, only specific heat at constant pressure is considered in this thesis. (Dincer et al. 2018, 5) Specific heat capacity is also a function of temperature (Dincer et al. 2018, 218-219; 235; Stadler et al. 2019, 580).

Volumetric heat capacity (C_{vol}) is also a characteristic of a material and is found by multiplying the specific heat capacity with the density of the material. The unit of volumetric heat capacity is kJ/m^3K. This is not to be confused with specific heat capacity in constant volume. (Dincer et al. 2018, 4-6; 60; Incropera et al. 2007, 67) As both density and specific heat capacity are functions of temperature, the volumetric heat capacity is also.

Latent heat

The sensible heat is not the only form of energy storage capacity of a material. In order to undergo phase change, after reaching the temperature of phase change a material must absorb a certain amount of heat per unit of mass to loosen the bonds between the material's molecules and reach a more disordered state, during which its temperature does not generally change. This amount of heat is called the latent heat, and it is commonly displayed in kJ/kg, but sometimes also as a molar value in kJ/mol. It is different for all materials, and also different for the change between solid and liquid (latent heat of fusion) and the change between liquid and gaseous forms (latent heat of vaporization). Changing to a more fluid phase requires energy and changing to a more stable phase releases it. The temperature of phase change also differs between materials. (Dincer et al. 2018, 72-73; Fleischer 2015, 1; 75)

Energy density

Since the objective is to compare both sensible and latent heat storage technologies, a common unit of storage should be defined. Energy density is a measure that can be used to compare all types of energy storages to each other, including different types of thermal energy storages. (Sterner et al. 2019a, 40)

Energy density is defined as the usable storage capacity of a system divided by its mass,

$$Q_{\mathrm{b}} = \frac{Q}{m}, \tag{9}$$

where	Q_{b}	(gravimetric) energy density	[kWh/kg]
	Q	energy storage capacity of the system	[kWh]
	m	mass of the system	[kg],

or alternatively its volume in the case of volumetric energy density

$$Q_{\mathrm{vol}} = \frac{Q}{V}, \tag{10}$$

Where	Q_{vol}	volumetric energy density	[kWh/m^3]
	Q	energy storage capacity of the system	[kWh]
	V	gross volume of the system	[m^3].

Thus, the unit of energy density is commonly displayed as [kWh/kg] or [kWh/m^3] as kilowatt-hours are a commonly used unit of energy content for energy storages. (Sterner et al. 2019a, 38; 40; Ushak et al. 2015, 49)

The energy storage capacity of a sensible heat -based storage system can be calculated with (Stadler et al. 2019, 574; Ushak et al. 2015, 49)

$$\Delta Q = m \cdot c_p \cdot \Delta T, \tag{11}$$

where	Q	stored energy	[kJ]
	m	mass of the system	[kg]
	c_p	specific heat of the system	[kJ/kgK]
	ΔT	change of temperature	[K].

The energy storage capacity of a latent heat -based system can be calculated with (Stadler et al. 2019, 589)

$$\Delta Q = m \cdot \left(c_{p,\mathrm{s}} \cdot \Delta T_{\mathrm{s}} + \Delta h + c_{p,\mathrm{l}} \cdot \Delta T_{\mathrm{l}}\right), \quad (12)$$

where	Q	stored energy	[kJ]
	m	mass of the system	[kg]
	c_p	specific heat at solid or liquid state	[kJ/kgK]
	h	latent heat of phase change	[kJ/kg]
	ΔT_{i}	change of temperature in phase i	[K].

The gravimetric or volumetric energy densities can be calculated directly using formulas (11) and (12) by either omitting the mass or replacing it with the density of the storage material, respectively (Ushak et al. 2015, 49). The classification of sensible and latent heat -based systems is defined in chapter 3.2.1 Classification.

Since temperature is a factor in amount of sensible heat stored as well as applicability of latent heat, energy density should ultimately be considered specific to a given system, not overarching technological solution or a given storage material (Cabeza et al. 2015, 9).

Thermal conductivity

Thermal conductivity (k) is a material property that determines the amount of conductive heat transfer inside a material. It is also an important constituent in heat transfer to and from the material. Higher thermal conductivity in the storage material improves the dynamic response of the storage system. (Dincer et al. 2018, 22; 218) Like most material properties, thermal conductivity is a function of temperature (Stadler et al. 2019, 573; 580). Thermal conductivity is commonly displayed in W/mK (Stadler et al. 2019, 573).

The thermal conductivity of the heat exchanger surface also has an important effect on heat transfer, but not as large as fluid properties (Incropera et al. 2007, 674).

Viscosity

Viscosity is a material property specific to fluids that reflects internal friction of a fluid (or in common terms, the "thickness" of a fluid) and thus largely determines flow properties of the fluid. As such it is also an important factor in heat transfer along with the other thermal properties mentioned in this chapter. (Dincer et al. 2018, 218; 224) Viscosity can be defined as dynamic viscosity (μ) or kinematic viscosity (ν), which is dynamic viscosity divided by density of the fluid. The unit of dynamic viscosity is kg/ms (or Pa·s), while the unit of kinematic viscosity is m^2/s. (Dincer et al. 26-27; 218) As with most other thermal properties, viscosity is a function of temperature (Dincer et al. 2018, 218; 221).

As viscosity fundamentally affects both flow dynamics and heat transfer of fluids, it is a rather important factor for thermal energy storage system response speed. It affects both natural convection and onset of thermal layering in a liquid thermal energy storage medium. (Dincer et al. 2018, 218-219)

3.2 Characteristics and classification of Thermal Energy Storage

In comparison to other forms of energy storage, thermal energy storages have medium energy density. Their volumetric storage capacity is significantly higher than mechanical storages but significantly lower than chemical storages. They are on par with battery storages, although the comparability of the value of stored product (electricity versus heat or cold) is debatable. (Sterner et al. 2019a, 40; Sterner et al. 2019e, 651) Thermal energy storages are capable of storing energy for a medium to long term storage period (Sterner et al. 2019a, 43; Sterner et al. 2019e, 646; Dincer et al. 2018, 53).

Thermal energy storages are among the cheapest forms of energy storage in terms of system capital cost, especially sensible heat storages (Sterner et al. 2019e, 651-653; 660-661). However, storage efficiency is mediocre due to heat losses and conversion losses. Latent heat -based storage has slightly better efficiency than sensible heat storage, but also higher costs, albeit still in the cheaper end in comparison to other types of storage technologies. (Sterner et al. 2019e, 651-653; 660-661; Dincer et al. 2018, 53)

3.2.1 **Classification**

Thermal energy storages can be classified in terms of:

- storage mechanism
- charging/discharging type (direct or indirect)
- temperature level
- storage duration
- application
- scale
- spatial considerations

(Sterner et al. 2019a, 35; Stadler et al. 2019, 565-567)

Thermal energy storage technologies can be divided into three main groups in terms of storage mechanism: sensible heat storage, latent heat storage and thermochemical storage. Sensible heat storage refers to storage of heat in a storage material using its heat capacity by increasing the temperature of the material, thus increasing the energy content of the storage. Latent heat storage in turn uses the latent heat of a phase change in the storage material to increase the energy content of the storage without changing the temperature of the system. Thermochemical energy storage generally refers to storage of thermal energy through reversible chemical reactions, but can also include systems based around sorption technologies, even if those are more physical than chemical in nature. The categorization of thermal energy storage technologies by thermodynamic phenomena they are based on is further illustrated in Figure 3.2. (Stadler et al. 2019, 567-571)

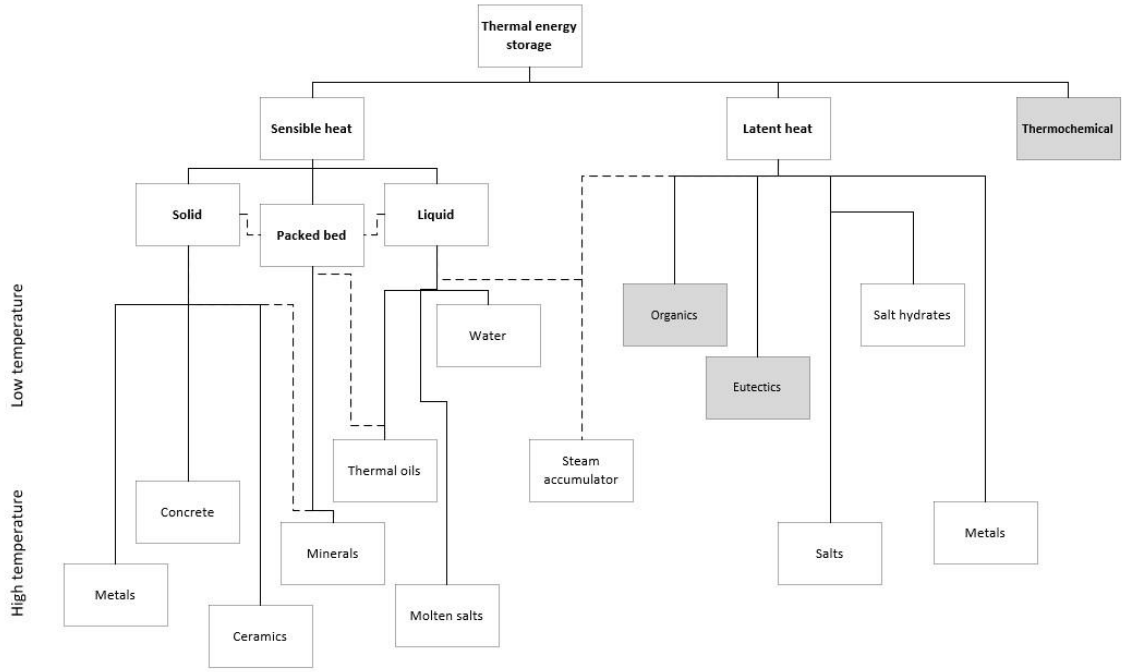

Figure 3.2. Overview of thermal energy storage technologies, categorized by governing thermodynamic phenomenon. Technologies that are mentioned but not focused on in this thesis are grayed out.

The charging and discharging method of a thermal energy storage system can be either direct or indirect. In direct charging, the heat transfer fluid doubles up as the storage material and is physically stored in the storage container. (Stadler et al. 2019, 566; 581-582; Dincer et al. 2018, 62) This method is common in water-based sensible heat storage units (Stadler et al. 2019, 581-582) and molten salt systems (Ushak et al. 2015, 53; Strasser et al. 2014, 393). The main advantages of the direct charging approach are its simplicity and potential for high charging and discharging rate. (Stadler et al. 2019, 581-582).

Indirect charging/discharging, on the other hand, has a heat exchanger separating the heat transfer fluid and the storage material. The advantages of this approach are that because the two materials are ideally never in contact with each other, there is less worry of the materials mixing or reacting with each other, they can be tailored for separate purposes and the storage material can be isolated from the environment (Stadler et al. 2019, 582; 597; Dincer et al. 2018, 62). However, the heat exchanger required for indirect charging

generally leads to additional exergy losses as opposed to direct charging method due to temperature difference necessary for heat transfer (Aga et al. 2013, 1100).

Different charging concepts are demonstrated in Figure 3.3. Only charging methods are displayed for the sake of conciseness, the respective discharging methods follow the same principles but with flow directions reversed. It is possible to mix different charging and discharging methods together if this is useful for the application.

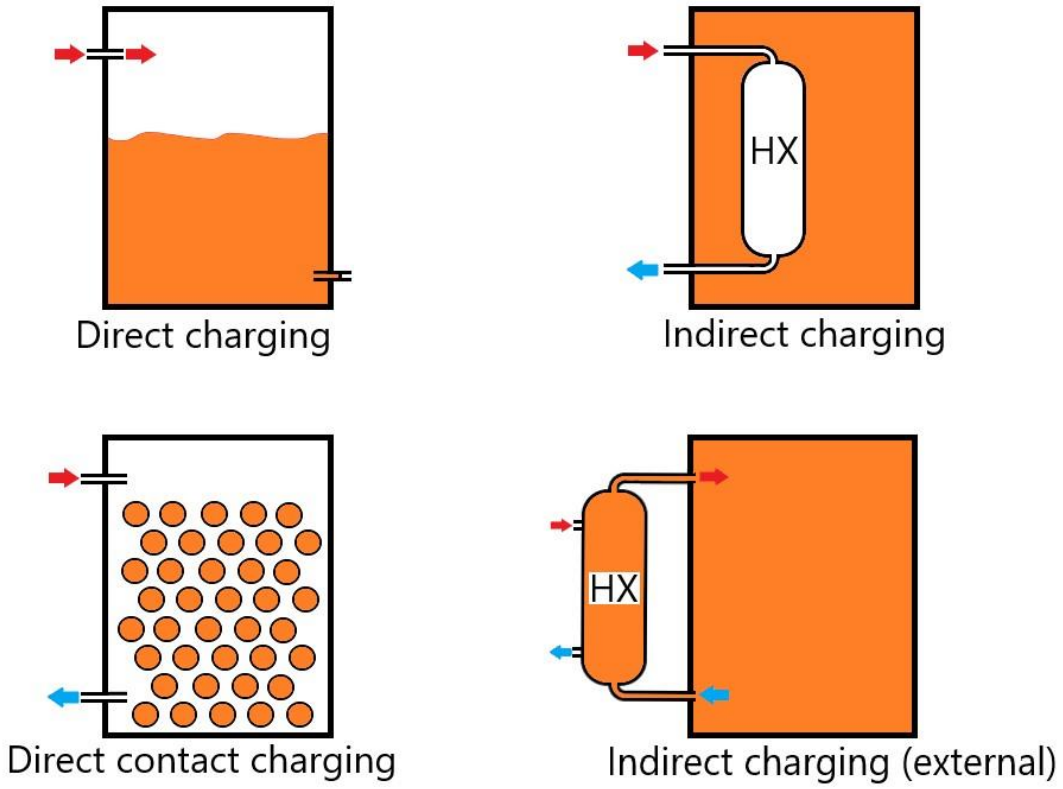

Figure 3.3. Demonstration of different charging (and discharging) concepts for TES systems.

There is a third method of charging and discharging a TES system that falls somewhere between the definitions of direct and indirect charging and seems to divide opinions of its exact classification between different sources. This is charging a TES system through direct contact heat transfer between a heat transfer fluid and the storage material that are known to not mix or react with each other. An example of this interaction is a TES where the storage material is solid and the heat transfer medium is fluid, as depicted in bottom left corner of Figure 3.3, and either of the two materials is chemically inert. The advantage

is, that the lack of heat exchanger simplifies and reduces the cost of the system, but the system remains relatively well separated from the environment. (Stadler et al. 2019, 566; 597-599; Dincer et al. 2018, 62)

The temperature level of a thermal energy storage system is a convenient way of classification as its often closely connected to the application of the storage system. Low and medium temperature storages between ambient temperature and 90 ℃ are often used for space heating (20-50 ℃) and water heating (60-90 ℃) purposes. Storages used in process heating applications are typically between 100 ℃ and 250 ℃, which is also the prime temperature range for Waste Heat Recovery products. Higher temperature applications include power generation (both conventional power plants and Consentrated Solar Power plants, in the range of 300-600 ℃) and high-temperature industrial processes (such as steel manufacturing which produces temperatures in excess of 1000 ℃). (Stadler et al. 2019, 565) Rough categorization of various TES technologies based on general temperature level is displayed in Figure 3.2. Cold storage for air conditioning and cooling applications deals in temperatures between 5 ℃ and ambient conditions, although storage applications for temperatures as low as under -18 ℃ for freezing systems aren't uncommon (Stadler et al. 2019, 566).

In terms of storage duration, thermal energy storages can be divided to short-term and long-term storages. Short term storages deal with timeframes ranging from minutes and hours up to a day and are generally used as buffer storages for balancing fluctuating supply or demand or as temporary storage for recovered waste heat. For this reason, short-term storages require decent heat transfer capabilities for a good dynamic response time. Long term storages last from days to months up to seasonal storages that balance differences in supply and demand between hot and cold seasons. Long-term storages thus require good insulation to reduce heat losses over extended time. (Sterner et al. 2019a, 43-44; Stadler et al. 2019, 566-567)

Physical size of the storage unit is a very tangible way to compare and classify storages. Storages range from small scale units in residential and functional applications to medium storage units in industrial applications to the largest storage tanks and aquifer storage. Overall scale of storage is naturally tied to other classifications, smaller storage units tend

to be confined to short term storage while long term storages are often larger to take full advantage of the storage potential (Sterner et al. 2019a, 44; Stadler et al. 2019, 566-567).

The final common way to categorize thermal energy storages is spatial characteristics. Energy storages are often divided in centralized and decentralized applications, although no clear-cut definition exists between the two. For example, a large hot water storage tank at a district heating plant would be considered a centralized storage unit, while a domestic water heater's tank would be an example of a decentralized one. (Sterner et al. 2019a, 44; Stadler et al. 2019, 567) Furthermore, albeit rare, certain thermal energy storages can be transported from one place to another during their operation cycle, so a clear distinction exists between mobile and stationary storage applications (Cabeza et al. 2015, 21-22; Sterner et al. 2019a, 45; Stadler et al. 2019, 567; Miró et al. 2016, 294-299).

3.2.2 Common characteristics

This chapter lists general characteristics common to all Thermal Energy Storage systems.

Storage materials

As different thermal energy storage methods are primarily set apart by their energy storage material, the materials themselves are convenient to categorize in the same manner. Some materials can, however, be used for either of these two thermal storage applications. Regardless of type of thermal energy storage, certain requirements stand for a good storage material.

Common requirements for all energy storage materials include large energy density, thermal and chemical stability over extended use and multiple charging/discharging cycles, affordable price, high availability, and manageable density changes over temperature or phase change. The material should also be easy and safe to handle, i.e., non-toxic, non-corrosive (also to reduce cost of storage vessel and heat exchangers), non-flammable, non-explosive and environmentally friendly (in both use and production phases). (Stadler et al. 2019, 571; Dincer et al. 2018, 60; 74; Fleischer et al. 2015, 38)

Case specific requirements that must be considered when choosing a storage material include suitable operational temperature and thermal conductivity. While high thermal conductivity is important for efficient heat transfer, in the case of sensible heat storages low thermal conductivity allows for thermal layering of storage materials as heat transfer inside the material is slowed down (Stadler et al. 2019, 575; Dincer et al. 2018, 74). For latent heat storages, the temperature of phase change of the storage material should be such that phase change occurs within the operational range, while sensible heat storages should ensure that the material does not experience phase changes or loss of thermal stability in the established operational temperature range. (Stadler et al. 2019, 565; 574; Fleischer et al. 2015, 37-38)

Heat losses

Sensible and latent heat storages will always suffer some heat (or cold) losses, as long as their temperature differs from ambient temperature. The scale of thermal losses is determined primarily by the temperature difference to the environment. Other affecting factors include insulation, storage surface area, surface-to-volume ratio, thermal conductions of the storage material and the storage tank, operational conditions, and environmental conditions (e.g., wind speed and humidity in addition to ambient temperature). Since thermal losses can only be reduced and not completely prevented, they are usually economically optimized against costs of the storage tank, its insulation, and the storage material. It is, however, possible to manufacture TES systems with minimal heat losses, leading up to 99% efficiency. (Stadler et al. 2019, 566, Dincer et al. 2018, 60)

The main way for reducing thermal losses in a thermal energy storage is insulation. Having adequate insulation is more essential for sensible heat storage than latent heat storage due to commonly higher temperature difference to environment. (Stadler et al. 2019, 573) Common insulation materials used for sensible thermal systems include mineral- and glass-based wools and foams (Stadler et al. 2019, 581). Among the most powerful insulation methods is vacuum as its thermal conduction coefficient is 0. This leaves radiation as the only form of heat loss, which can also be reduced with powder or

fiber additives (super-vacuum) (Stadler et al. 2019, 573). A list of common insulation materials can be found in Appendix IV - Table of insulation materials.

The energy density of the storage material is an important factor even if available space for the storage system is not particularly limited. The higher the energy density of the storage material is, the smaller the volume of the storage will be. Smaller volume leads to smaller surface area for the storage and thus smaller heat losses. (Dincer et al. 2018, 60) Reducing the surface area of the tank also generally makes it cheaper to manufacture and similarly reduces the surface area that needs to be covered with insulation (Dincer et al. 2018, 218).

Optimizing the surface-to-volume ratio in terms of heat losses means finding the minimum amount of surface area for a given volume of storage. In essence, a single large storage has smaller heat losses than multiple smaller storages with equal total volume. The geometry of the storage unit also affects the surface-to-volume ratio; the optimal shape in this regard would be a sphere. Spherical tanks, however, are considerably more complicated and expensive to manufacture. A common compromise is a cylindrical vessel with a height-to-diameter ratio between 2:1 and 5:1. (Stadler et al. 2019, 581)

Heat transfer fluids

Aside from the storage material of a thermal energy storage, the Heat Transfer Fluid (HTF) is also an important part of the system. Heat transfer fluids pose similar requirements to sensible storage materials in terms of temperature range, thermal capacity, thermal and chemical stability, corrosion, and cost; in addition, high thermal conductivity and low viscosity are emphasized compared to storage materials. The HTF can be the same material as the storage material if the material suits both purposes. The benefits of having the same material act as storage and heat transfer fluid include simplicity of the system and having the option to use the direct charging/discharging method, which provides high heat rates. (Stadler et al. 2019, 566; Vignarooban et al. 2015, 385)

Despite these benefits it is often better to use a separate HTF and storage material, for example if the price of the HTF is high in comparison to an applicable storage material,

if the HTF has a low volumetric energy density, if the storage material is solid or if the HTF is used as a process fluid that either is used for a chemical reaction or is under high pressure when the storage material could be in atmospheric or lower pressure state. (Stadler et al. 2019, 566)

In the scope of this thesis, heat transfer fluids are not of particular interest, unless they double up as storage materials.

3.3 Points of focus in Thermal Energy Storage

Point of focus in this thesis will be in the first two of the three main groups of thermal energy storage listed in chapter 3.2.1 Classification, namely sensible and latent heat storages. This definition is made because thermochemical storage is not strictly based on thermodynamic reactions or properties of matter but instead is mainly based on reaction heat of chemical reactions (Stadler et al. 2019, 568) and as such is outside the current main expertise area of Alfa Laval Aalborg and thus the scope of this thesis. Moreover, thermochemical storage is still in very early development, so there would not even be much commercially relevant information to share about it (Dincer et al. 2018, 58). A distinction is to be made between thermochemical energy storage and chemical energy storage, in which the latter mostly refers to binding energy into different chemical substances (also known as Power-to-X -technologies), and thus is entirely out of the scope of this thesis (Sterner et al. 2019d, 325-327).

In addition to ruling out energy storage technologies based on chemical reactions, the scope of this thesis will also be limited in terms of temperature and pressure range as well as the scale of thermal energy storage system.

The energy storage systems reviewed in this thesis are intended to be used mainly in conjunction with existing items in the ALA catalogue, so the pressure range considered shall be limited to a similar level to common operating pressure levels those items, broadly spoken atmospheric to 40 bar(g).

ALA main business area is industrial applications, so residential and space heating applications are ruled outside the scope of this thesis. Cooling applications and other cold

storages will also be left outside the scope of this thesis. This effectively sets the considered temperature range to such that energy storage systems below roughly 60 °C temperature will not need to be reviewed. As an exception, a basic hot water storage tank shall be reviewed as a very fundamental case.

As most items in ALA catalogue are aimed to be relatively easy to transport, the energy storage systems considered should also be somewhat modular. In effect, this rules out aquifer/geological storages as well as storage systems with very low volumetric storage capacity compared to scale of storage itself.

Technologies that fall clearly outside the scope in terms of these variables can be mentioned but will not be delved into too deeply nor exhaustively.

3.4 Potential of Thermal Energy Storage in different applications

Generally speaking, the main use of thermal energy storage in industrial scale lies in leveling out the differences between supply and demand of heat or cold, in various timeframes ranging from hours to months. This will lead to increases in flexibility and efficiency, which will turn into reductions in costs and emissions. (Dincer et al. 2018, 37-38; 85; Cabeza et al. 2015, 1-2)

3.4.1 TES in conjunction with Waste Heat Recovery

Main draw of TES in WHR applications around small-scale power plants and industrial processes is to act as buffer storage between the heat source and consumer. Engine power plants do not always operate steadily, causing fluctuations in waste heat recovery output which can lead to operational inconveniences on system level. Incorporating TES in the WHR system helps in adapting to load changes in the heat source to bring inertia to heat output. (Shu et al. 2016, 693-694; 697; 704-705; Pandiyaran et al. 2011, 6012; Sun et al. 2016, 14) Also, WHR from batch-type industrial processes in particular is much less complicated if TES is used to hold onto the heat and discharge it based on need instead of having to use it at once periodically (Gadd et al. 2015, 469).

According to Sterner, the demand for industrial primary process heating would be possible to be reduced by 42% by increasing utilization of heat recovery and energy storage (Sterner et al. 2019b, 71). Heat recovery would be especially useful in steel and other metal industries, where temperature levels are notably high, but other industries as well. By utilizing a thermal energy storage system, the high temperature waste heat could be used to preheat the next batch of an applicable manufacturing process, or other parts of the process that require heat. Many plants already utilize Waste Heat Recovery in some form or another. (Miró et al. 2016, 287-288; 300; Martin et al. 2013, 159)

Thermal energy storage is already established and considered essential for the operation of Concentrated Solar Power (CSP) plants, where the intermittency and uncontrollability of the heat source is an inherent factor in design. Studies show the same technical advances can be applied to conventional power plants and WHR for both operational and economic benefits. (Stadler et al. 2019, 588; Fleischer 2015, 15-16; Farid et al. 2003, 1598)

The heat load of the consumer can also fluctuate (Pandiyarajan et al. 2011, 6012). Normally in engine power plant WHR, in situations when heat demand is decreased or does not exist, WHR boilers are either partially or completely bypassed using a flue gas damper, which simply lets flue gases uncooled into the chimney. In this case the energy recovery potential of the flue gases is wasted. Incorporating TES into the system would allow to store the surplus heat to be then used at a time of peak load or an engine outage.

Heat and power producers may also want to follow feed-in-tariffs. Utilizing TES allows to take full advantage of the incentive by selling heat and producing power when their prices are the highest. (Aga et al. 2013, 1098; Läiskä 2020)

The temperature level of waste heat varies widely depending on the heat source. The usefulness of the recovered heat depends heavily on its temperature level with higher temperature heat being more useful and thus valuable. (Miró et al. 2016, 286) The TES method should be chosen so that it can utilize the recovered heat to the highest degree without a significant drop in temperature level over the storage.

Flue gases from engine power plants are commonly around 400-500 ℃ (Pandiyarajan 2011, 6011; Miró et al. 2016, 292), whereas waste heat from industrial sources frequently surpasses 1000 ℃ (Miró et al. 2016, 286-289; 291). Lower temperature heat can also be utilized with systems such as heat pumps and Organic Rankine Cycle (ORC), but those increase costs and are not as efficient as utilizing higher temperature heat to begin with (Shu et al. 2016, 693).

Frequency and duration of charge-discharge cycles affects the performance of TES systems and higher frequency cycling poses additional requirements for the design and materials of the TES. WHR applications tend to go through multiple cycles in a week or even day in some cases, which would typically increase the cost of the TES system. (Stadler et al. 2019, 607)

Lastly, energy storage systems in marine-based WHR applications will not be as important of a focus in this thesis than those in land-based WHR applications but shall be mentioned regardless. For marine-based applications, the storage density in terms of both volume and weight is a much more critical parameter than in land-based applications due to space and weight restrictions of cruise ships (Takasuo 2020).

3.4.2 **TES as a separate system in a power plant or an industrial plant**

Power production- and industrial plants are typically more stable sources of heat than WHR applications. In these applications it would be preferred to keep both the production and load of the plant as stable as possible to increase efficiency and economic predictability. In addition to reducing power generation efficiency of power plants, constantly fluctuating loads speed up aging of various components due to thermal and mechanical stresses. Larger plants also often respond slowly to load changes, in particular industrial processes. Using TES to respond to intermittent load changes would allow to keep the power plant at a more constant load, reducing the occurrence and magnitude of start-up and partial load losses and wear. (Gadd et al. 2015, 469; Sala 2015, 493; 495-496; 498; 504; Stevanovic et al. 2020, 1; Miró et al. 2016, 286)

Spreading the peak load more evenly over a longer period of time using TES would allow to design power plants to a lower maximum output, reducing capital costs (Gadd et al. 2015, 469; Farid et al. 2003, 1598; Miró et al. 2016, 286; Sala 2015, 504). Alternatively, flattening the peak would allow to forego using a separate back-up boiler for peak production where applicable (Sala 2015, 497). On the other hand, at times of lower heat loads such as summertime, many power plants struggle to maintain operation of the process at loads below a certain minimum point. In this situation TES could be used to increase system efficiency and reduce operational difficulties by operating the power plant for a relatively short period at a higher load that allows for acceptable efficiency of production and charging the TES during that time and then discharging the TES slowly over an extended period to spread the peak of heat production over a longer consumption period, an operation that is effectively the reverse of flattening the consumption peak. (Gadd et al. 2015, 473)

Thermal energy storage can be used to increase the flexibility of operation and economic efficiency of a CHP plant by decoupling the power and heat generation. This allows the plant to fully take advantage of peaks of both heat and power demands, which do not always occur simultaneously. (Sterner et al. 2019b, 133; Sterner et al. 2019c, 153; Sterner et al. 2019g, 761-762; Gadd et al. 2015, 469; Sala 2015, 493; 495-496; 500; 505) The storage temperature can be under or around 100 °C if the CHP plant is used for district heating purposes, but if the heat is produced for industrial applications, the required temperature level for the storage is likely higher.

Dedicated district heating plants also experience seasonal variation in addition to their daily load variation. Seasonal variation is caused by the difference in temperature and thus heating demand between summer and winter. In theory, large scale seasonal TES would allow to concentrate production and delivery of heat to times when production cost is low and heating price is high, respectively. (Gadd et al. 2015, 468) However, according to Gadd et al., seasonal large-scale energy storages are uncommon in district heating systems due to the cost of the large storage often outweighing the attainable economic benefit (Gadd et al. 2015, 473). An option exists to use seasonal storage to cover the extended peak load of heating over midwinter in cooperation with a baseload heating plant and charge the storage at time of lesser heating need. This allows to dimension the

plant for lower peak capacity and to utilize the capacity to a higher degree around the entire heating season (Gadd et al. 2015, 476)

In addition to using thermal energy storage in direct conjunction with a heat source, they can also be used to absorb electricity surpluses from the power grid in times of low electricity prices using Power-to-Heat -technologies (electric heaters, heat pumps etc.) The stored heat can then be used in times of high heat prices, but returning the absorbed power to the power grid is generally not viable. (Sterner et al. 2019a, 28; Sterner et al. 2019c, 148-149; 156-157; Sterner et al. 2019e, 648-649; 668; Gadd et al. 2015, 476).

3.4.3 Considered reference applications

A common example of an industrial application that could utilize thermal energy storage would be a factory that uses process heat from a connected power plant with waste heat recovery, where the power plant has constant electricity production and thus also constant waste heat generation, but the factory would either idle at nighttime and weekends or drastically vary production based on demand. A common process steam pressure for such factory would be around 7-12 bar. Another example would be an industrial process with waste heat recovery combined with a steam turbine that is operated following a tariff and idles part of the time, while the main process does not. (Läiskä 2020)

Both above applications would require the ability to generate steam from the stored energy. This would require a storage temperature level high enough as well as a suitable heat exchanger solution to produce a heat output high enough for steam generation. In the case of the factory that utilizes process heat generated by WHR, the applicable temperature level would be around 165 ℃ to 190 ℃ based on the estimated saturated steam pressures of 7-12 bar. Although the main focus in both examples would be in saturated steam generation, out of interest the further capability to produce superheated steam is also considered as that is also a common feature in ALA scope of supply.

An example of thermal energy storage in a cruise ship environment would be to level out heat demand between the time spent at sea and the time spent at port. At sea there is usually plenty of usable heat from the ship’s engines’ WHR boilers, but at port there is

always deficit that must be covered with an auxiliary boiler. Excess heat could be stored at sea and then used at port to avoid having to use the auxiliary boiler. Normally, the excess heat is dumped into sea water using a dumping condenser. The temperature levels are commonly between 90 ℃ and 180 ℃. (Takasuo 2020)

An option that also needs to be considered in applications for thermal energy storage is the ALA MSTG (modular steam turbine generator) that uses either saturated or superheated steam to generate electricity (Jäpölä 2020). However, stored energy does not need to always be output as steam, but can also be used as, for example, feedwater preheating. This sort of an approach increases the range of exergy utilization in terms of temperature levels. (Fleischer 2015, 19-20)

In light of all of the above considerations, the applications that will primarily be considered in terms of temperature level, heat transfer and general viability while comparing different technologies are:

- Saturated steam generation at ~160-250 ℃
- Superheated steam generation at up to 350 ℃
- Process heating at various temperatures using water or other heat transfer fluids if applicable

4 STUDY ON APPLICABLE TECHNOLOGICAL SOLUTIONS

In this chapter different thermal energy storage solutions are reviewed in terms of fulfilling the requirements for feasibility to use in combination with different process applications and in terms of general usefulness in scope of Alfa Laval Aalborg catalogue. The technologies are organized by main thermodynamic storage phenomenon and then by storage material/method, as per Figure 3.2.

4.1 Sensible Heat -based solutions

Sensible heat storage technologies store thermal energy by increasing the energy content of the storage material by increasing its temperature. The amount of heat stored in the system is determined by the heat capacity of the system and the possible temperature range of the system. (Dincer et al. 2018, 59-60; Stadler et al. 2019, 567; 574)

The temperature range of a sensible heat storage system is normally limited in the higher end either by the temperature of phase change of the storage material or by the temperature limits in the application system. (Stadler et al. 2019, 574) In the lower end the temperature range is limited again by the temperature of phase change of the storage material (unless already solid), as well as the lowest temperature available in the target application. The temperature range can be below ambient temperature if the process allows it; in this case heat losses are called heat gains. (Stadler et al. 2019, 565; 572; 574)

Generally speaking, sensible heat storages have a lower volumetric energy density than latent heat -based energy storages. This is because often the temperature range of the storage material or the system is limited, and materials that are not as limited in terms of temperature range have a lower volumetric heat capacity, so the product of temperature difference and volumetric heat capacity generally does not surpass the energy density of latent heat storage materials. (Stadler et al. 2019, 574-575) A list of materials commonly used in sensible heat storage, and their properties, can be found in Appendix II - Table of sensible heat TES materials.

In addition to a suitable temperature range for the chosen application and decent volumetric and specific heat capacities, several other qualities of the material must also

be considered, most importantly price, material stability and performance over extended use and multiple charging-discharging cycles, thermal diffusivity and conductivity, density changes over temperature, safety, and environmental effects. (Dincer et al. 2018, 60; Stadler et al. 2019, 571; 574-575) More about these considerations in chapter 3.2.2 Common characteristics. Some materials are also suitable for thermal layering (also known as “stratified” or “thermocline” storage), which enables using a single tank for both hot and cold storage materials, usually reducing costs (Dincer et al. 2018, 62-63; Stadler et al. 2019, 586).

Expanding the temperature range of the storage increases its storage capacity proportionally. This, however, also increases the temperature difference between the storage and the environment and thus leads to storage losses. These losses can be mitigated using insulation, which is particularly important in higher temperature storage systems. (Dincer et al. 2018, 60; Stadler et al. 2019, 573)

As explained in chapter 3.2.2 Common characteristics under the subchapter Heat losses, in addition to having insulation, reducing the surface area of the storage tank will reduce heat losses as well as usually manufacturing cost of the tank. Surface area can be reduced through choosing a storage material with a higher volumetric heat capacity or by reducing the surface-to-volume ratio of the storage tank geometry. The optimal geometry in terms of surface-to-volume ratio would be a sphere, but those are usually too complicated and expensive to be worth the energy savings, a common compromise being a cylindrical tank. (Stadler et al. 2019, 581; Dincer et al. 2018, 60)

Thermal layering would also be inefficient in a spherical tank as the mixing surface between the hot and cold liquid would be roughly at the center of the tank at the point of largest diameter and thus largest cross-sectional area. This would increase the amount of mixing and conduction in the tank and destroy the stratification. In terms of layering the best design would also be the upright cylinder with as high as possible height-to-diameter ratio, usually between 2:1 to 5:1 and optimally 3,5:1. (Stadler et al. 2019, 581; Ievers et al. 2009, 2604; 2612; 2614; Xu et al. 2012, 6; Furbo 2015, 38) In general, one wishes to minimize the thermocline layer between the hot and cold layers, as that part is effectively useless volume and leads to reduced storage efficiency (Dincer et al. 2018, 62-63). The

inlet and outlet of the tank (or the corresponding heat exchangers) should be placed as far as possible from each other with the hot inlet/outlet being at the top of the tank and cold inlet/outlet at the bottom, but in this case the top inlet must be insulated carefully to prevent it from acting as a thermal bridge. The layering inside the tank can also be helped by decreasing or dividing/diffusing flow rates in the inlets and with the use of baffles and similar concepts to reduce mixing within the tank volume. (Dincer et al. 2018, 63-64; Ievers et al. 2009, 2604; 2612; 2614; Furbo 2015, 31; 36-37; 40; 44) It is also not uncommon to use a cheap solid filler material to displace some of the liquid storage medium and to reduce natural convection inside the liquid, commonly called "packed bed" (Stadler et al. 2019, 588; Dincer et al. 2019, 69; Grirate et al. 2016, 262; Molina et al. 2018, 252-253). Single tank thermocline storage generally has a 30-35% lower capital cost than a two-tank sensible heat storage system (Grirate et al. 2016, 262; Strasser et al. 2014, 393; Xu et al. 2012, 1; Molina et al. 2018, 253). In addition to this significant economic advantage, the single tank system also has a technical advantage in that liquid level in the tank can be kept almost constant (Bruch et al. 2014, 117).

Sensible heat storage is currently the cheapest method of storing energy in most cases. Storage materials are usually cheap and abundant. In higher temperature systems, the requirement for insulation increases overall price. (Stadler et al. 2019, 607)

While sensible heat -based storages generally lose out to latent heat -based systems in terms of energy density, they are more well-known technology which makes them comparably simpler and thus cheaper to manufacture. On the other hand, this also means there is less room for further development. Some advances can be done in terms of insulation and heat losses, but reductions in manufacturing prices are likely minor. (Stadler et al. 2019, 568; 588; Sterner et al. 2019e, 660-661) As such, sensible heat -based storages can be seen as a safer but less rewarding option to invest in as a technology.

4.1.1 **Water mass**

Water is one of the most common materials for sensible heat -based thermal energy storage. Water mass sensible heat storages simply take advantage of the high density and specific heat capacity of liquid water which combined lead to a very good volumetric heat

capacity. Other positive traits of water include: low thermal conductivity that reduces unwanted heat losses and makes layering possible, flow properties that enable good convective heat transfer when needed, density variation based on temperature changes which leads to possibility of layering, decent solvent properties, cheapness, wide availability, global experience on working with it, safety for both workers and the environment and the ability to function as a common heat transport, storage and process medium. (Stadler et al. 2019, 567-568; 574-575; Furbo 2015, 31)

A major disadvantage of using water as a heat storage material is its low boiling point at atmospheric pressure, only 100 ℃. This means that either the storage system's pressure must be increased substantially, the system must be built to deal with vapor or the storage maximum temperature must be limited to around 90-95 ℃. (Stadler et al. 2019, 574; 576; 589; Furbo 2015, 31) Storage systems that utilise water vapor are discussed in chapter 4.2.3 Steam accumulators.

Unpressurized hot water storages are economically viable even in very large scale, increasing the storage pressure increases the technical and operational flexibility of the storage but increases the cost significantly (Stadler et al. 2019, 576; Sterner et al. 2019c, 156). Pressurized water can store heat in temperatures up to 180 ℃ at 30 bar (Stadler et al. 2019, 565; 568). Storages at higher temperatures than this typically utilize other storage materials, such as thermal oils, which are discussed in chapter 4.1.4 Thermal oils (Stadler et al. 2019, 576).

Other significant disadvantages of using water as a storage medium are its susceptibility to freezing in sub-zero temperatures and tendency to corrode steel over time. Both of these disadvantages can be overcome by dosing chemicals to the water, but this may have other adverse effects depending on application and whether the water is also used as a heat transport or process fluid. (Dincer et al. 2018, 61; Stadler et al. 2019, 568)

The current state-of-the-art technology for storing hot water is the thermocline storage tank that utilises the natural thermal stratification of water due to density difference over temperature gradient and low thermal conductivity (Stadler et al. 2019, 575; 581-582; 586-587; Ievers et al. 2009, 2604).

Common industrial level applications for simple water tanks include load-balancing buffer storages for hot water or district heating. With adequate insulation, it is also possible to use a hot water tank for seasonal storage for the purpose of storing water heated during summer to cover some of heating needs during early winter. In this application, large scale is important as larger volume also leads to smaller surface-to-volume ratio and thus lower heat losses. The tank also needs to be protected from freezing by adding alcohol or other freezing protection chemicals to the water. (Stadler et al. 2019, 568; 576; 581; Furbo 2015, 37)

Hot water storage tanks are commonly made of steel, stainless steel, or concrete. Concrete tanks are especially common in the largest scale storage units. (Stadler et al. 2019, 581; Furbo 2015, 31) Despite the low average temperatures, hot water storages are commonly insulated to reduce heat losses to retain as high energy output as possible (Furbo 2015, 31-32).

Hot water sensible heat storage is very simple, well-known, and well-established technology which makes it cheap and safe. However, the temperature range or energy density of the storage are not very high. (Stadler et al. 2019, 568; 574) With a temperature difference of 80 ℃ the energy density of the storage would be around 93 kWh/m3, while with a lower temperature difference of 20 ℃ it would be only around 23 kWh/m3 (Sterner 2019a, 40; Cabeza et al. 2015, 6). Stadler reports specific capital cost of large-scale seasonal hot water storage as 0.5-3 €/kWh (Stadler et al. 2019, 607).

4.1.2 **Minerals and packed beds**

Minerals and loose solids are often combined with a HTF to form a packed bed storage but can also be used as the main storage material with a heat exchanger (Fleischer 2015, 22; Zanganeh et al. 2014, 812; Grirate et al. 2016, 262; Laing et al. 2015, 67). The main benefit of using mineral-based heat storage materials is their simplicity; they are cheap and widely available as well as very safe materials to use (Zanganeh et al. 2014, 813; Grirate et al. 2016, 262; Laing et al. 2015, 79). For these reasons one of the common uses of a packed bed of such materials is to displace a part volume of a more expensive HTF or storage medium (Strasser et al. 2014, 393; Molina et al. 2018, 252-253). They are also

suitable for a very wide range of temperatures as minerals can withstand high temperatures, up to around 800 °C (Dincer et al. 2018, 69; Laing et al. 2015, 65; Zanganeh et al. 2014, 813) and possess little to no danger of unwanted freezing (Stadler et al. 2019, 568).

Mineral heat storage materials generally have a lower volumetric heat capacity compared to water, but the higher limits on temperature range make up for it (Dincer et al. 2018, 69; Stadler et al. 2019, 574; Laing et al. 2015, 65). Thermal conductivity of minerals on the other hand is higher than that of water, albeit still mediocre (Grirate et al. 2016, 263; 270; Dincer et al. 2018, 70; Furbo 2015, 34). However, while the thermal conductivity of the minerals affects the systems response rate, the volumetric storage capacity is deemed more important in terms of system efficiency and overall performance (Grirate et al. 2016, 269; 272) The potential for high maximum temperature possessed by mineral storage materials along with the high heat transfer area of packed beds enables good heat transfer dynamics, possibly high enough heat transfer rates to generate superheated steam (Laing et al. 2015, 79).

Since minerals are solid materials, transferring heat to and from them normally requires a separate HTF. This can be a gas or liquid, either in the form of an embedded HTF in a packed bed, or a separate HTF loop with heat exchangers sunk into the mineral bed. (Grirate et al. 2016, 262; Laing et al. 2015, 65; 67) The storage material can potentially be used in place of the HTF if its particle size is sufficiently small (Laing et al. 2015, 67; 81-82). The choice of heat transfer method has a noticeable effect on the price and operation of the system (Grirate et al. 2016, 262). Additionally, in the case of a packed bed, pressure drop and flow distribution caused by the bed must be considered and the compatibility of the HTF with the bed material needs to be verified (Grirate et al. 2016, 260; 262; 272; Laing et al. 2015, 68; 78; Molina et al. 2018, 252; 255). The compatibility and pressure drop issues with HTF and packed bed can be alleviated by a novel concept of using a secondary HTF loop for the storage that uses air to transfer heat between the main HTF and the packed bed storage (Laing et al. 2015, 80). The three main charging configurations for packed beds are demonstrated in Figure 4.1, with discharging working with the same concept apart from reversed flow direction.

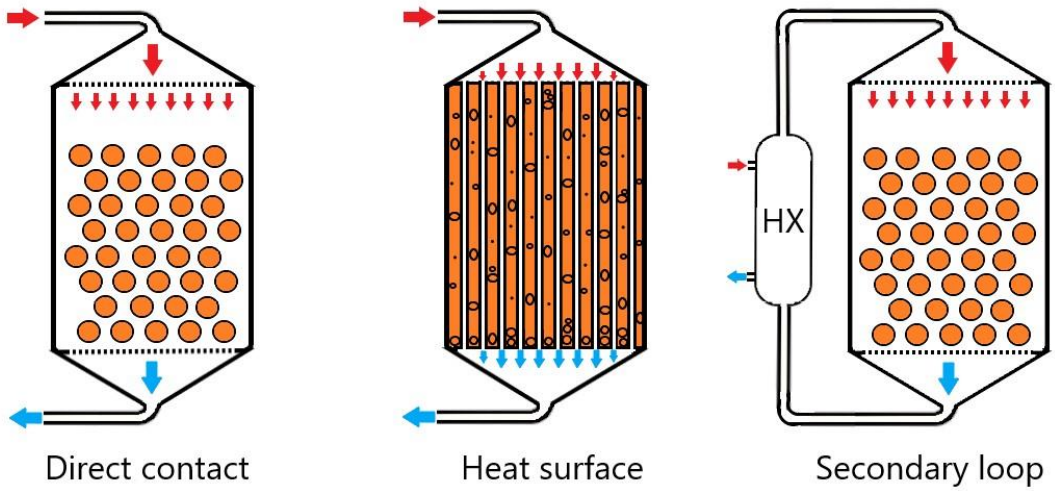

Figure 4.1. Main heat transfer configurations for packed bed systems.

Loose solids present a wide variety of options for storage materials, mostly inorganic minerals. In addition to density, specific heat and thermal conductivity, the thermal and chemical stability of the material are important criteria. Furthermore, in applications with high operational temperature ranges the thermal expansion coefficient should be considered. (Laing et al. 2015, 65-66) Grirate et al. evaluated various minerals in temperature ranges of 250 to 350 °C and emphasized basalt and quartzite as good materials based on their thermal properties. However, basalt is chemically incompatible with most thermal oils which must be considered when choosing the HTF. Quartzite is a good alternative for applications where basalt is not compatible and also has high conductivity which can prove useful in some scenarios. (Grirate et al. 2016, 260; 272) Quartzite, along with silica sand, have also been shown to be compatible with molten salt TES systems (Grirate et al. 2016, 262). Some materials on the other hand, such as granite and marble, have decent thermal properties but start losing their form at temperatures above 150-200 °C and thus are not usable as high-temperature storage materials. (Grirate et al. 2016, 262-263; 268; 272)

Thermal inertia of the packed bed can cause expansion of the thermocline layer during discharging, leading to a reduction in efficiency over multiple charging-discharging cycles (Bruch et al. 2014, 121-123; Bruch et al. 2016, 277-278; 282). This means that packed bed storages may be more suited to longer term storage than continuous cyclic charging and discharging or may have to be “overdimensioned” to balance storage size

with required discharging rate. An advantageous property for long-term storage applications would be that the packed bed reduces mixing and heat transfer within the tank, slowing down loss of stored energy (Dincer et al. 2018, 69).

Overall mineral-based packed bed storages can be very economical options as the materials are generally very cheap and the system design is fairly simple. For example, material cost of limestone is reported by Strasser et al. as $\$37/m^3$, which corresponds to 30.8 €/m^3 at the time of writing of this thesis, and the capacity specific cost as \$0.16/kWh, which corresponds to 0.13 €/kWh. This material cost is extremely low, however it is only a fraction of the overall system cost. Strasser reports the system cost of a typical packed bed storage with solar salt as HTF as \$30/kWh, which corresponds to 25 €/kWh. However, the issues discussed in the following paragraph are not taken into account in this value. (Strasser et al. 2014, 399-400)

One of the major disadvantages related to packed bed systems are stresses caused by the different thermal expansions of the storage vessel and the packed bed. During charging the tank, which is commonly made of steel, generally expands faster than the mineral bed, which then settles down to the expanded volume. During discharging, the opposite happens, except the packed bed does not naturally rise back to its original height, which leads to the tank walls compressing around the bed when they contract due to cooling. The issue is amplified the higher the temperature range of the system is, as thermal expansion is proportional to temperature change. (Strasser et al. 2014, 393; 400; Laing et al. 2015, 79)

Zanganeh et al. designed a sensible heat storage system of a packed bed of unknown rocks. The storage is designed to be charged with air up to a temperature of 650 °C and discharged to heat the air from 150 °C to up to 590 °C with an overall efficiency of up to 95% in continuous cyclic use. (Zanganeh et al. 2014, 812; 814; 816) The efficiency can be positively affected by increasing height-to-diameter ratio of the tank or decreasing pebble size in the packed bed, but will result in pressure losses increasing in the HTF (Zanganeh et al. 2014, 812; 819-821).

The design aims to solve the issues of thermal stress common for packed beds by molding the side walls in a conical shape to allow the tank and the packed bed to expand independently of each other (Zanganeh et al. 2014, 814; Strasser et al. 2014, 393-394). The design and thermal stress relieving effect of the tank are demonstrated in Figure 4.2, depicting the forces acting on the bed by the walls during discharge on a conceptual level.

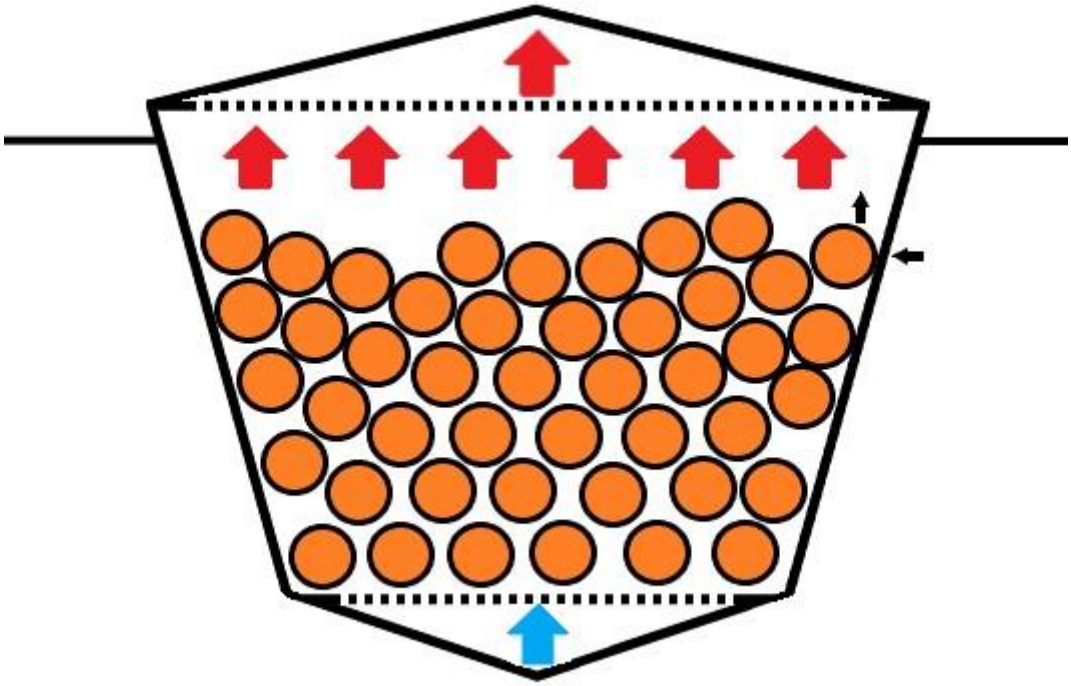

Figure 4.2. The novel conical design of the packed bed storage by Zanganeh et al. (Zanganeh et al. 2014, 814)

The tank is constructed from multi-layer concrete and sunk underground to both support the tank walls and reduce thermal losses. (Zanganeh et al. 2014, 814) Constructing the tank from anything but concrete would likely be costly due to the shape, while being made of concrete reduces compatibility with different HTF's (Strasser et al. 2014, 394). However, to compensate, very little insulation is required mostly due to the ground insulating the system (Zanganeh et al. 2014, 812; 814; 818). It should also be noted, that constructing with concrete is not necessarily very modular, which is one of the properties to consider in this review.

4.1.3 **Solid masses**

Solid masses such as concrete, metals and ceramics can also be used to store sensible heat. The difference between this type of storage system and the system consisting of loose particles described in the previous chapter is that solid masses generally cannot be made efficiently into packed beds, but instead require a type of heat exchanger to charge and discharge heat in the indirect method. (Stadler et al. 2019, 580; Strasser et al. 2014, 393-394; Grirate et al. 2016, 262) However, it is possible to arrange the storage material in such a way that leaves defined flow paths inside the storage akin to a heat exchange surface (Laing et al. 2015, 67).

Solid materials can be used for extremely high temperature storage, up to 1600 ℃. For this reason, they are popular in industrial applications such as steel and glass industries with respectively high temperatures. Recently interest in these systems has sparked to be used in combined cycle plants as well. Storage materials used for solid sensible heat storage are mostly inorganics, in particular, ceramic materials, different types of brick, concrete, and metals. (Laing et al. 2015, 65-68) These materials commonly have a low specific heat capacity, offset by their wide operational temperature range (Laing et al. 2015, 65).

Concrete is among the most used solid TES materials, it is cheap, widely available, simple to install by casting and safe in many ways. However, concrete used in TES is not the typical run-of-the-mill concrete, but rather a special composition with several added minerals to improve the mixtures thermal properties and ensure stability in high temperatures. Solid cast concrete is a viable sensible heat storage material up to at least 500 ℃, although its mediocre conductivity influences its heat transfer performance. (Laing et al. 2015, 70-71)

Structured concrete elements are proposed as a cheap option to packed bed storage, tested up to 400 ℃ with potential of maximum temperature of up to 600 ℃ (Strasser et al. 2014, 394). The tested concrete is reported to have a density of about 2240 kg/m^3 and specific heat of about 750 J/kgK (Strasser et al. 2014, 398). This option has slightly lower total efficiency and is slightly more expensive than a conventional packed bed system, but

largely avoids the issues caused by thermal expansion in packed beds (Strasser et al. 2014, 398-400).

Recycled waste materials such as inertized asbestos-containing ceramics can also be used as cheap options for solid mass sensible heat storage, reported to be safe to use up to 1000 °C (Laing et al. 2015, 66; Guillot et al. 2011, 174-176).

Capital cost of a solid sensible heat storage system is reduced by the fact that no pressure vessel is necessary since the storage volume does not need to contain fluid pressure. Furthermore, materials such as concrete can be cast directly around heat exchanger tubing, helping contain the stresses of the HTF pressure. (Laing et al. 2015, 65; 68) However, in place of fluid pressure in the storage volume the thermal expansion of the solid storage material needs to be considered instead and is an especially important consideration in the case of high temperature solid storage (Laing et al. 2015, 66; 68). The heat exchangers between the solid storage mass and the HTF increase price and contribute to heat transfer resistance (Grirate et al. 2016, 262).

Similar to loose mineral sensible heat storage materials, solid sensible heat storage materials are commonly very cheap. For example, the material cost of TES-grade concrete is reported by Strasser et al. as \$228.5/m^3, which corresponds to 190 €/m^3 at the time of writing, and by Cabeza et al. as 0.08 €/kg. Capacity specific cost is reported by Strasser et al. as \$1.46/kWh, which corresponds to 1.22 €/kWh, however at a lower temperature difference of only 100°C the capacity cost would be much higher, 3 €/kWh as reported by Cabeza et al. Ceramic storage materials reach somewhat higher prices, reported by Cabeza et al. as 4.5 €/kg and 188 €/kWh, although this capacity specific cost was also calculated with a temperature difference of only 100 °C, while ceramics in particular would be capable of handling much higher temperatures and temperature differences which would increase the energy storage capacity and thus reduce the specific price from that value if used to their full potential. The specific capital cost of a structured concrete thermocline system with solar salt as HTF is reported by Strasser et al. as \$34/kWh, which corresponds to 28.3 €/kWh. (Strasser et al. 2014, 399-400; Cabeza et al. 2015, 7)

4.1.4 **Thermal oils**

Thermal oils are liquid materials frequently used in TES applications. They tend to most commonly be used alongside other thermal energy storage methods either as a HTF in an indirect system with another storage material or as filler-HTF in a packed bed. They are also sometimes used as the sole sensible heat storage material in a two-tank system, although this is deemed expensive in comparison to other options. (Strasser et al. 2014, 393; Bruch et al. 2014, 116; Grirate et al. 2016, 262; Zavattoni et al. 2014, 125; Stadler et al. 2019, 566-576) As a storage material they are most suited to short-term storage (Stadler et al. 2019, 588).

Thermal oils are typically divided to mineral, synthetic and silicon oils. Their maximum temperature is generally 400 °C with thermal and chemical stability as the limiting factor. (Strasser et al. 2014, 393; Vignarooban et al. 2015, 385; 388; Stadler et al. 2019, 588) Mineral oils can be used up to 300 °C in atmospheric pressure with the lowest minimum operational temperatures out of the options as well. Synthetic oils are usable up to 350-400 °C, but they may need pressurizing in the top end of the range. Silicone oils are another option for storage up to 400 °C, but they pose slightly lower energy density and higher price than most synthetic oils. The energy density of all the oils is still relatively similar, between 50-60 kWh/m^3. (Stadler et al. 2019, 588; Ushak et al. 2015, 51)

For example, Therminol VP-1 is a commonly used organic synthetic oil with high thermal stability and a max temperature of 400 °C, but a boiling point of only 257 °C which causes high vapor pressure at higher temperatures, up to 10 bar at its maximum temperature. Because of this vapor phase VP-1 is also usable as a working fluid in two-phase processes, but likely a complicated and expensive option as a sensible heat storage material. (Grirate et al. 2016, 262; Therminol)

Therminol 66 is, according to its producer, the most commonly used thermal oil in the world. It is usable up to 345 °C at atmospheric pressure and with a specific heat capacity of 2.57 and density of around 800 kg/m3 at 300 °C it could be used as a sensible heat storage material, although it is designed as a HTF. Its lower temperature counterpart is

Therminol 55, usable up to 300 ℃ unpressurized, and pumpable as low as -28 ℃. (Therminol)

Thermal oils generally have a lower thermal conductivity (in the area of 0.1 W/mK) and specific heat capacity than water, but they can be used at atmospheric pressure in applications where water cannot. Minimum operational temperature for most oils is also low, around or below 0 ℃, low enough to avoid need for freezing protection in most cases. (Stadler et al. 2019, 576; Molina et al. 2018, 253; Vignarooban et al. 2015, 388; Ushak et al. 2015, 51) A downside for many thermal oils is that they are flammable (Stadler et al. 2019, 588).

Combining thermal oil with a packed bed can increase the storage capacity of the system and reduce thermal losses by reducing natural convection inside the tank, as well as reduce price since the solid storage material displaces part of the oil (Stadler et al. 2019, 576; 588; Grirate et al. 2016, 262; Bruch et al. 2014, 117). However, thermal oils have chemical compatibility and corrosion issues with certain common packed-bed materials, such as basalt (Grirate et al. 2016, 260; 262).

Thermal oils are quite expensive as materials. Mineral oils are the cheapest out of the three subtypes of thermal oils, costing about $0.3/kg as reported by Vignarooban et al., corresponding to 0.25 €/kg at the time of the writing of this thesis. Their capacity specific cost is reported by Ushak et al. as $4.2/kWh, which corresponds to about 3.5 €/kWh. Synthetic and silicone oils are roughly 10 times more expensive than mineral oils, reported by Vignarooban et al. as $3/kg and $5/kg (2.5€/kg and 4.2 €/kg), respectively, and their capacity specific costs reported by Ushak et al. as $43 and $80 per kWh (35.5 €/kWh and 66 €/kWh), respectively. Two-phase synthetic HTFs, as reported by Vignarooban et al., can reach prices as high as $100/kg, which corresponds to 83 €/kg at the time of writing. (Ushak et al. 2015, 51; Vignarooban et al. 2015, 387-388; Stadler et al. 588)

4.1.5 **Molten salts**

Molten salts are among the most promising technologies for both sensible and latent heat storage. Most research in the area is done in relation to centralized solar power (CSP) plants, in which molten salt storage has recently been adopted as the commercial norm. Evidence suggests that the same advances can be adapted and applied to other sectors dealing with thermal energy. (Stadler et al. 2019, 587-588; Ushak et al. 2015, 50) Molten salts are an interesting area of technology because they operate in a high range of temperatures, have a large storage capacity, are relatively simple and safe to work around and have a fairly low price in comparison to the amount of benefits they possess. (Stadler et al. 2019, 587; Ushak et al. 2015, 50; He et al. 2016, 1206; Lu et al. 2013, 98; Vignarooban et al. 2015, 385)

The most common salt mixtures used for thermal energy storage are nitrate salts, especially 60% $NaNO_3$ / 40% KNO_3 (weight percentage), commonly known as "solar salt" due to its use in early large-scale CSP plants, (Stadler et al. 2019, 587; Ushak et al. 2015, 52; Vignarooban et al. 2015, 389) and 53% KNO_3 / 40% $NaNO_2$ / 7% $NaNO_3$, commercially named "HITEC™" by its manufacturer (Ushak et al. 2015, 50-51; Guillot et al. 2011, 174; He et al. 2016, 1209). These two salt mixtures will hereafter be referred to as "solar salt" and "HITEC", respectively. Other salt mixtures and pure salts have also been researched and used, but to a lesser extent. For example, addition of $Ca(NO_3)_2$ to nitrate salts has been researched for its potential to lower the melting points of the mixtures to increase the operational temperature range. (Vignarooban et al. 2015, 390-391; Ushak et al. 2015, 55)

In terms of system layout, currently the most commercially advanced type of molten salt TES system is one with two separate molten salt tanks, a hot and a cold tank. The molten salt is then pumped between the tanks through a heat exchanger that either transfers heat from a HTF to the salt when charging the storage or from the salt to the HTF when discharging it. The molten salt can also be used directly as a HTF as it is typically in fully liquid form in both tanks, although indirect charging with thermal oil has been more common so far in this type of system. (Gaggioli et al. 2013, 781; Guillot et al. 2011, 174-

175; Stadler et al. 2019, 587-588; Strasser et al. 2014, 391-392; Ushak et al. 2015, 54; Fleischer 2015, 17)

The current research trend in molten salt storages is to reduce the number of tanks to one. This would be achievable by either utilizing thermal layering made possible by the low thermal conductivity of most salts, similar to water thermocline storage, or by using the latent heat of the salt, which is discussed in detail in chapter 4.2.1. (Stadler et al. 2019, 588; Fleischer 2015, 17; Gaggioli et al. 2013, 781) Benefits of reducing the number of tanks include decreases in costs in terms of tank manufacturing and auxiliary equipment as well as in the general size of the system, and improvements in reliability and modularity (Strasser et al. 2014, 393; Fleischer 2015, 17; Gaggioli et al. 2013, 787; 789). Gaggioli et al. are also testing the possibility of integrating the heat exchanger used for discharging of the storage inside the thermocline tank, which according to them would further improve the modularity, efficiency, and pricing of the system. (Gaggioli et al. 2013, 780; Gaggioli et al. 2015, 822)

The one-tank thermocline idea can be taken a step further by replacing part of the molten salt with solid mineral particles to form a packed bed system. The packed bed would help with maintaining thermal layering due to slowing down natural convection inside the tank, as well as replace some of the molten salt with a cheaper storage material, which could reduce the cost of the sensible heat storage by up to a third, however it can also result in problems related to impurities. (Stadler et al. 2019, 588; Strasser et al. 2014, 393; Xu et al. 2012, 1; Guillot et al. 2012, 175)

Properties of salts

The operational temperature range of molten salt sensible heat storage systems is quite high in comparison to most sensible heat storages. The lower limit of the temperature range is usually defined by the solidification temperature of the storage material (which is much higher than ambient temperature and generally higher than the boiling temperature of water in ambient pressure), as most sensible heat systems require the salt to stay in liquid form at all times. The upper limit is normally set by the thermal stability of the salt, which starts to deteriorate past certain temperatures. Salt mixtures can have a

lower melting temperature than single salts while still having a similar decomposition temperature, resulting in a wider operational temperature range. (Stadler et al. 2019, 587; Ushak et al. 2015, 50; 55; He et al. 2016, 1206) The high operational temperatures mean that heat stored in molten salt systems can be used for superheated steam generation, but similarly these systems require high temperature heat to fully charge (Ushak et al. 2015, 52).

The operational temperature range covered by the most common nitrate salt mixtures is in the area of 170 ℃ to 560 ℃, but even higher temperature salts are available. Specifically, the melting temperature of solar salt is between 220 ℃ and 240 ℃ depending on exact composition, making the lowest operational temperature for sensible heat applications that use solar salt normally around 290 ℃. (Stadler et al. 2019, 576; 587; Guillot et al. 2012, 175; Fleischer 2015, 17) The melting point of the HITEC salt is around 140-142 ℃, and thermal decomposition starts at around 535 ℃, although some sources state it can begin reducing in temperatures as low as 350 ℃ if subjected to oxygen. (Vignarooban et al. 2015, 390; He et al. 2016, 1209; Guillot et al. 2012, 175; Ushak et al. 2015, 51-52) Energy density of molten salts is quite decent thanks to their high operational temperature range, much larger than most common sensible heat storage methods such as thermal oil storage. Stadler estimates this value to be around 200 kWh/m^3 for solar salt. (Stadler et al. 2019, 587; Strasser et al. 2014, 391-392; Ushak et al. 2015, 50) With adequate insulation, molten salt storages are capable of storing heat for weeks or even months before the salt eventually begins to freeze, and even with poor insulation, hours up to days (Xu et al. 2012, 7; Sterner et al. 2019f, 724). However, the thermal layering in a thermocline storage can expand faster than this, reducing system efficiency (Xu et al. 2012, 6; 8-9).

Many material properties of common molten salts are somewhat comparable to liquid water, particularly in higher salt temperatures (Stadler et al. 2019, 587; Xiao et al. 2014, 23; He et al. 2016, 1206; 1212; Vignarooban et al. 2015, 389). As mentioned before, the thermal conductivity of most molten salts is fairly low, as low as around 0,2-0,5 W/mK (the thermal conductivity of liquid water is between 0.6 and 0.7 W/mK (Furbo 2015, 34)). Many references cite this as an issue for molten salt -based TES systems as it directly impedes heat transfer capabilities of the system, but it also means molten salt sensible

heat storages are capable of utilizing thermal layering, much like water. (Fleischer 2015, 17; Gaggioli et al. 2013, 781-782; Xiao et al. 2014, 23) In terms of viscosity, most molten nitrate salts behave somewhat like water in temperatures of about 100 ℃ above their melting point or higher (Ushak et al. 2015, 56-57). According to Xiao et al., HITEC salt at temperatures between 300 ℃ to 500 ℃ behaves much like liquid water in terms of viscosity and fluidity, with a Prandtl number close to 7 which is close to that of water in ambient conditions. At temperatures lower than 300 ℃, both the viscosity and Prandtl number of HITEC salt are noticeably higher than water's and the salt acts more like an oil than water. (Xiao et al. 2014, 23)

Equipment design and heat transfer

Due to high melting- and vaporization points and good thermal stability molten salts usually exhibit low vapor pressures in storage systems. This leads to viability of simple, unpressurized storage vessel designs which reduces manufacturing costs in that respect. However, high temperatures and temperature differences often present in molten salt systems can result in thermal stresses proving problematic, especially for heat exchanger design and in unsteady operation. (Stadler et al. 2019, 587; Ushak et al. 2015, 50; He et al. 2016, 1206; Gonzalez-Gomez et al. 2017, 228; 231)

As noted earlier, due to the high operational temperature range of molten salt -based TES systems these storages are often capable of being discharged to generate saturated or superheated steam, even in intermediate or higher pressures. The determining factors of heat transfer in this case are convection of salt and either boiling of water or convection of steam. (Ushak et al. 2015, 52; Yuan et al. 2016, 163; González-Gómez et al. 2017, 228) Since boiling of water provides very effective heat transfer, the heat flux of an evaporator is mainly limited by convection of the molten salt, and generally ends up having a good heat transfer efficiency (He et al. 2017, 1234-1235). In a superheater the heat transfer coefficient of the steam side is generally the more determinant factor to the total heat transfer coefficient, although the difference between the coefficients of steam and molten salt is not as broad as those in an evaporator (He et al. 2017, 1236). The low thermal conductivity of the salt reduces its convective heat transfer coefficient, but heat transfer can be helped by increasing the temperature difference between the molten salt

and water/steam. However, increasing this temperature difference too much reduces overall heat transfer efficiency due to increasing heat losses to environment. (Yuan et al. 2016, 163) Furthermore, too high a temperature difference in an evaporator leads to boiling heat transfer coefficient decreasing as per the boiling curve; according to He et al. the optimal average temperature difference between water/steam and molten salt would be between 60-100 °C. Both the boiling region and the temperature difference in an evaporator can be controlled by altering the boiling point of water. (He et al. 2017, 1235;1238; Yuan et al. 2016, 169) According to Gonzalez-Gomez et al., pinch point of molten salt steam generator can be quite low, between 2-10 °C, despite generally lower heat transfer capabilities of molten salts (Gonzalez-Gomez et al. 2017, 228; 237; 239).

The current trend of heat exchanger for steam generation with molten salt is a shell-and-tube heat exchanger with salt on shell-side and water/steam on tube-side. Reasons for this design include water practically always being in much higher pressure than the salt, so it is convenient to enclose it in the tubes, in addition to the possibility of salt freezing due to its high melting point and blocking or breaking the tubes. However, if water is not at a significantly higher pressure compared to the salt, putting the salt on tube-side may be a worthwhile option as tubes are much easier and cheaper to clean and replace, and also putting the higher temperature fluid in the tubes would reduce heat losses and the need for insulation. According to Gonzalez-Gomez et al., a natural circulation evaporator would be feasible for molten salt applications, but likely more expensive than a forced circulation evaporator. A variety of fairly conventional heat exchanger designs have been proposed with different benefits and drawbacks. (He et al. 2016, 1206; González-Gómez et al. 2017, 228-232; Moore et al. 2010, 23-26)

Gonzalez-Gomez et al. designed a model for a dual pressure steam cycle system for a CSP plant consisting of a superheater, reheater, evaporator and preheater, a two-tank molten salt TES unit and a 110 MWe turbine-generator. The steam generator was dimensioned to produce 87 kg/s superheated steam at 12.6 MPa, 550 °C using molten salt at a maximum temperature of 565 °C, with a pinch point as low as 3 °C for an estimated capital cost of around 5 m€. (González-Gómez et al. 2017, 230; 239-240)

Gaggioli et al. have researched the concept of integrating the heat exchanger inside the storage tank. Their once-through countercurrent heat exchanger consists roughly of a coaxial shell and tube bundle, the inner helical tube bundle acting as the evaporator and the outer shell acting as a flow channel for molten salt. The advantages of this design over a separate heat exchanger are reduced components and increased modularity, as the integrated heat exchanger helps maintain thermal layering in the storage tank and the molten salt flow on the shell-side of the heat exchanger is induced through natural convection. The design has been tested to generate superheated steam in small scale at 45 bar, up to 520 °C. The concept is depicted in Figure 4.3. (Gaggioli et al. 2013, 782-786; Gaggioli et al. 2015, 822-823; 825-826)

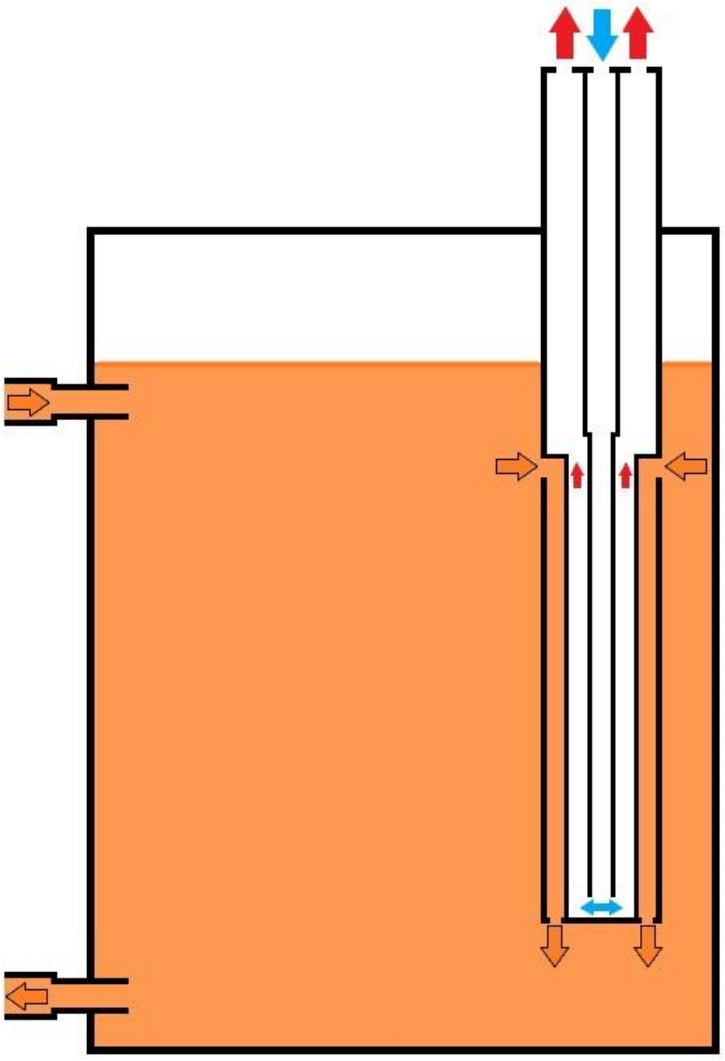

Figure 4.3. Integrated thermocline storage and natural circulation steam generator concept by Gaggioli et al. (Gaggioli et al. 2013, 784-785; Gaggioli et al. 2015, 823; 825-826)

Charging a molten salt storage comes down to two approaches, using the molten salt itself as heat transfer material from an external source or using a separate HTF, such as steam or thermal oil, to charge the storage (Guillot et al. 2011, 174-175). Indirect charging with a HTF such as thermal oil, common for two-tank systems, eliminates the possibility of salt freezing inside the larger charging loop. (Strasser et al. 2014, 393) Indirect storage charging from live steam, originally devised for needs of direct steam generation CSP plants, is an option that is relatively simple to integrate to the existing steam/power generation system without disrupting the operation and reliability of the process loop (Aga et al. 2013, 1098; 1101). However, additional exergy losses resulting from the extra heat transfer interface compared to direct charging generally leads to discharge steam pressure being significantly lower than charge steam pressure. Additional equipment for handling condensation of steam may also be required depending on system design. (Aga et al. 2013, 1100)

Direct charging using the molten salt as HTF, on the other hand, eliminates the charging heat exchanger from the system, reducing system cost. Additionally, most non-salt HTFs have a lower maximum operational temperature, meaning some of the molten salt's storage potential would be unused. (Strasser et al. 2014, 393; Ushak et al. 2015, 53) For thermocline storage systems using direct charging method, Gaggioli et al. suggest distributing inlet flow of hot molten salt from charging loop to avoid disturbing thermal layering in the tank (Gaggioli et al. 2013, 782; Gaggioli et al. 2015, 829). Direct and indirect charging methods in two-tank and thermocline systems are demonstrated in Figure 4.4. Figure 4.4 only displays charging configurations for molten salt storages, but discharging in these systems can be achieved by reversing the flow directions.

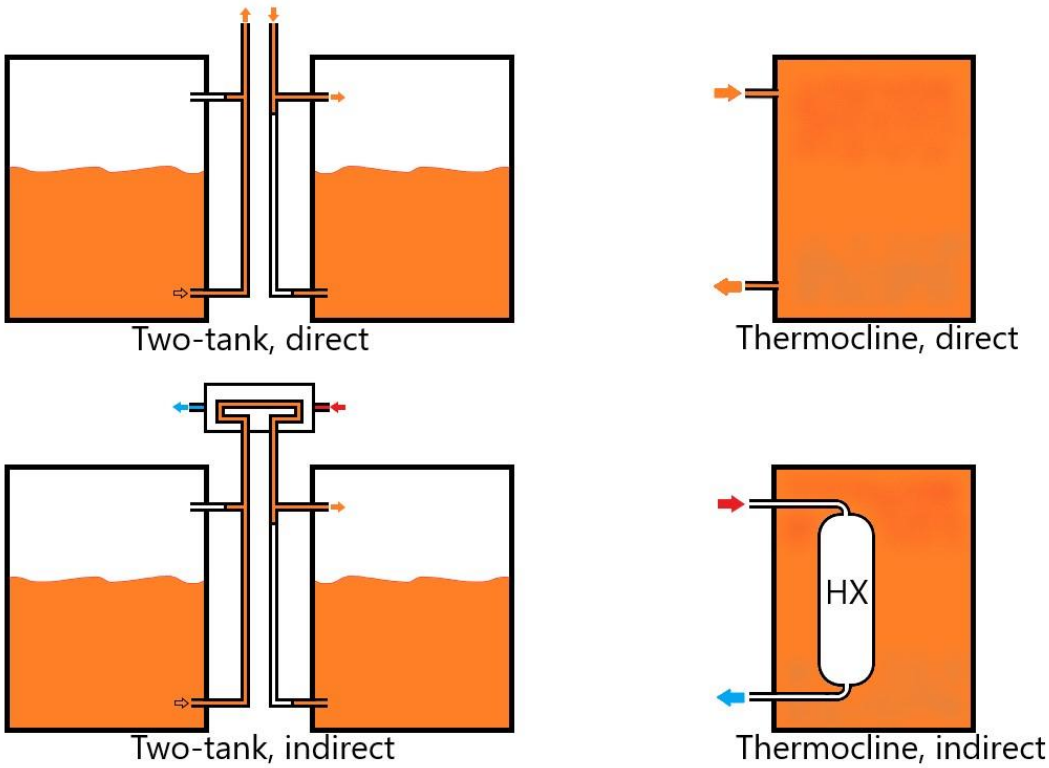

Figure 4.4. Examples of charging modes of two-tank and thermocline molten salt storages.

Common issues

The high melting temperature of molten salts can cause issues with tubes plugging or even breaking if the temperature of the salt is allowed to drop below melting point. This can happen in three scenarios (Stadler et al. 2019, 587; Strasser et al. 2014, 393; Gaggioli et al. 2013, 781; Moore et al. 2010, 18-19; Lu et al. 2013, 98):

- Molten salt is not heated enough, and ambient heat loss reduces the temperature.
- Molten salt is not drained properly from process tubes outside operational time.
- Molten salt at just above the melting temperature is pumped into a cold pipe.

Therefore care should be taken to avoid this unwanted freezing. In order to ensure pumpability of the molten salt and avoid the issues of tube plugging, the inlet temperature of the molten salt to heat exchanger tubing should be significantly higher than its melting point (Lu et al. 2013, 98). There is a range of temperature, where the initial molten salt is just cold enough to start freezing on the inner surface of the tube affecting flow

characteristics (mainly resulting in increasing pressure loss), but not cold enough to completely plug the tube before it warms up and the salt starts melting again (Lu et al. 2013, 101). A critical salt inlet temperature exists at the tipping point between the pipe completely plugging from freezing and the salt blockage melting off, dependent on pipe diameter, pipe temperature, the type of molten salt used and the mass flow of salt (Lu et al. 2013, 106). Molten salt freezing in cold pipes could be avoided by mixing some higher temperature salt in the cold molten salt when initially filling the charging heat exchanger pipes, if available. The phenomenon of molten salt freezing on surface of cold pipes at startup is demonstrated in Figure 4.5, where T_{crit} refers to the critical temperature of the tipping point between the pipe freezing completely shut and melting back fully open after warmup period.

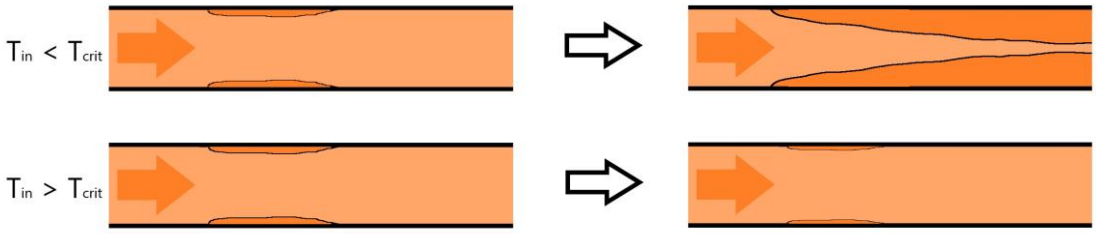

Figure 4.5. Molten salt freezing on inner surface of cold pipes at startup.

In any case, piping subjected to near-ambient temperatures should be drained of salt when not operated for an extended time (Moore et al. 2010, 19). Gaggioli et al. found a declination angle of 5 slope-permille (~0,3°) to be suitable for emptying and refilling piping using solar salt; this may be affected by other parameters such as pipe diameter and salt composition (Gaggioli et al. 2015, 824). In an evaporator-discharger freezing of salt can be avoided by maintaining the pressure of water high enough to keep the boiling point and inlet temperature of water above or at least close to the freezing point of the salt (Moore et al. 2010, 23) or integrating the heat exchanger inside the storage tank (Gaggioli et al. 2013, 782). A backup option in case of accidents is installing electric heaters in the piping and heat exchangers; electric heaters are capable of melting and heating the salt up to over 500 °C, however, their constant use is somewhat expensive for the overall efficiency of the process (Stadler et al. 2019, 587; Strasser et al. 2014, 393; Moore et al. 2010, 22).

Molten salts commonly come with problems of high corrosiveness, especially in higher temperatures (Fleischer 2015, 17; Guillot et al. 2011, 174; Sabharwall et al. 2014, 43). Heat exchangers in particular can be affected by stress corrosion in combination with thermal stresses (González-Gómez et al. 2017, 229). Corrosion is considered one of the most important technical issue to solve for salt-based energy technologies, including TES (Sabharwall et al. 2014, 49).

Nitrate salts in themselves are not overly corrosive while impurities in them, chlorides in particular, are corrosive. However, stainless steels are for the most part resistant enough to handle industrial-grade nitrate salts, with highest temperature components possibly requiring higher grade steels. (Moore et al. 2010, 15-16; Ushak et al. 2015, 52; Sabharwall et al. 2014, 49-50; Vignarooban et al. 2015, 389) Alkali chloride salts are more corrosive than nitrate salts (Guillot et al. 2011, 176). Fluoride salts are capable of removing the protective oxide layers of most stainless steels, however pure fluoride salts will not easily react with the metals themselves, impurities and other constituents of the salt on the other hand will (Sabharwall et al. 2014, 50). Corrosion by impurities in most salts will ultimately be limited as the impurities will be expended from the system over time, unless more impurities are leaked into the system during operation (Sabharwall et al. 2014, 51). Furthermore, corrosion by at least nitrate salt mixtures can be reduced by pretreating the salt to remove/reduce impurities and moisture before use (Moore et al. 2010, 16; Ushak et al. 2015, 52).

Price

The two-tank system is the established norm for molten salt sensible heat storage. As mentioned above, stainless steel is usually durable enough to use as tank and heat exchanger material for nitrate salt applications, so expensive special alloys are not necessary. However, building large storage tanks, and in the case of system with indirect charging the necessary heat exchangers, out of stainless steel is still costly (Strasser et al. 2014, 393). Stadler reports the specific capital cost of two-tank molten salt storage as 20-75 €/kWh depending on factors such as charging and discharging rate and operational temperature range (Stadler et al. 2019, 587). Strasser et al. reports capital cost of two-tank molten salt storage with indirect charging as $89/kWh and direct charging as $50/kWh,

which at the time of writing of this thesis correspond to about 74 €/kWh and 42 €/kWh, respectively (Strasser et al. 2014, 391).

Reducing the number of storage tanks to one by utilizing either thermal stratification or latent heat could reduce the cost of molten salt storage significantly, and as such is a heavily researched area. Latent heat -based salt storage is discussed in chapter 4.2.1 PCM salts. Having a system with only one storage tank instead of two would reduce the necessary salt inventory, heat exchangers in indirect systems, and simplify construction and installation to reduce overall costs. (Strasser et al. 2014, 393; Fleischer 2015, 17) Furthermore, utilizing an integrated steam generator in storage tank -concept designed by Gaggioli et al. shows promise to reduce the capital cost even further (Gaggioli et al. 2013, 781).

As mentioned above, González-Gómez et al. dimensioned a superheated steam generator system for a 110 MWe CSP plant, capable of producing superheated steam at 12.6 MPa and 550 °C for estimated 5 m€ capital cost. (González-Gómez et al. 2017, 228; 230; 239-240)

Molten salts as materials are relatively cheap in comparison to other liquid sensible heat storage materials of similar temperature area such as thermal oils (Vignarooban et al. 2015, 385). However, large scale production of molten salts may end up being a bottleneck due to availability of ground resources (Guillot et al. 2011, 175; Vignarooban et al. 2015, 389). The material cost of solar salt is reported by Strasser et al. as around \$2118/m^3, which corresponds to about 1765 €/m^3 at the time of writing of this thesis, and the capacity specific cost as \$10.83/kWh (9 €/kWh). Gaggioli et al. report prices in line with this amount. Vignarooban et al. on the other hand report the price of solar salt as \$0.5/kg, which corresponds to 0.41 €/kg and comparing it to common density values of solar salt of around 1800 kg/m^3, this price would be less than half of what Strasser et al. reported. Vignarooban et al. report the price of HITEC salt as around \$1/kg (0.83 €/kg), which would be close to the value reported by Strasser et al. Cabeza et al. report the cost of solar salt as 0.63 €/kg, and its capacity specific cost as 14 €/kWh albeit at a temperature difference of only 100 °C, which affects the price since molten salt storages are usually

capable of temperature differences higher than that. (Strasser et al. 2014, 399; Vignarooban et al. 2015, 387; Cabeza et al. 2015, 7; Gaggioli et al. 2013, 787)

4.2 Latent Heat -based solutions

Latent heat thermal energy storage systems are based around increasing the energy content of the system by storing energy in the heat of phase change (i.e., latent heat) of a storage material in addition to a minor amount of sensible heat. Latent heat achieves much higher energy densities than sensible heat in most cases, up to more than a tenfold higher at best, and is the main point of focus in these storage applications. (Dincer et al. 2018, 72-73; Stadler et al. 2019, 568; 588-589; Salunkhe et al. 2012, 5604) The concept of latent heat of phase change is explained in chapter 3.1 Thermodynamic definitions subchapter Latent heat. Comparison of storage capacity of general latent heat and sensible heat TES systems depending on storage temperature difference is displayed in Figure 4.6.

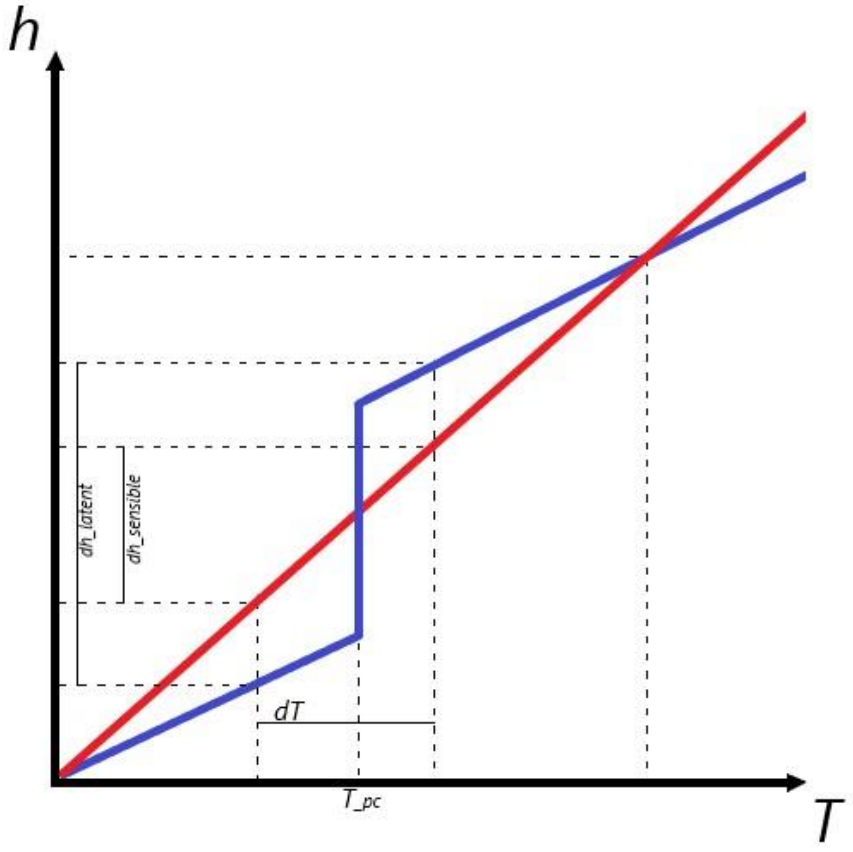

Figure 4.6. Comparison of latent and sensible heat TES at a constrained temperature difference *dT*. T_{pc} refers to temperature of phase change. (Fleischer 2015, 2; Dincer et al. 2018, 72; Stadler et al. 2019, 590)

The materials used in latent heat -based thermal energy storage applications are called Phase Change Materials (PCM) (Fleischer et al. 2015, 1; Dincer et al. 2018, 73). The solid-liquid phase change is much more popular in utilization of latent heat than the liquid-gas phase change, despite the latter generally having a higher latent heat value. This is due to the major change in density and thus volume, as well as other technical inconveniences, associated with vaporization. (Dincer et al. 2018, 72-73; Stadler et al. 2019, 568; 591-592; Fleischer 2015, 2; Salunkhe et al. 2012, 5604) Density changes by usually about 10 % but up to 20% in the solid-liquid phase change as well, which needs to be accounted for but is not as large of an issue than in the case of liquid-gas phase change. The phase change between liquid and solid is also a design challenge in itself, in terms of containing the liquid phase while taking the aforementioned density change into account without negatively affecting system performance and dynamics. (Fleischer 2015, 49; 63; Stadler et al. 2019, 568; 596; Pereira da Cunha et al. 2016, 228) Furthermore, some PCMs face issues with phase separation and subcooling, the phenomenon of the PCM cooling below its melting point before the onset of solidification, which is demonstrated in Figure 4.7 (Stadler et al. 2019 592-593; 596). Other material properties differ between the solid and liquid phases too and material properties in all phases should be considered in design. Most notably specific heat capacity of most materials is not the same in solid and liquid phases. The thermal stability of the PCM must also be researched and monitored, as the properties of the PCM may change over time in cyclic use or due to reactions with its container. (Dincer et al. 2018, 219; Farid et al. 2003, 1603)

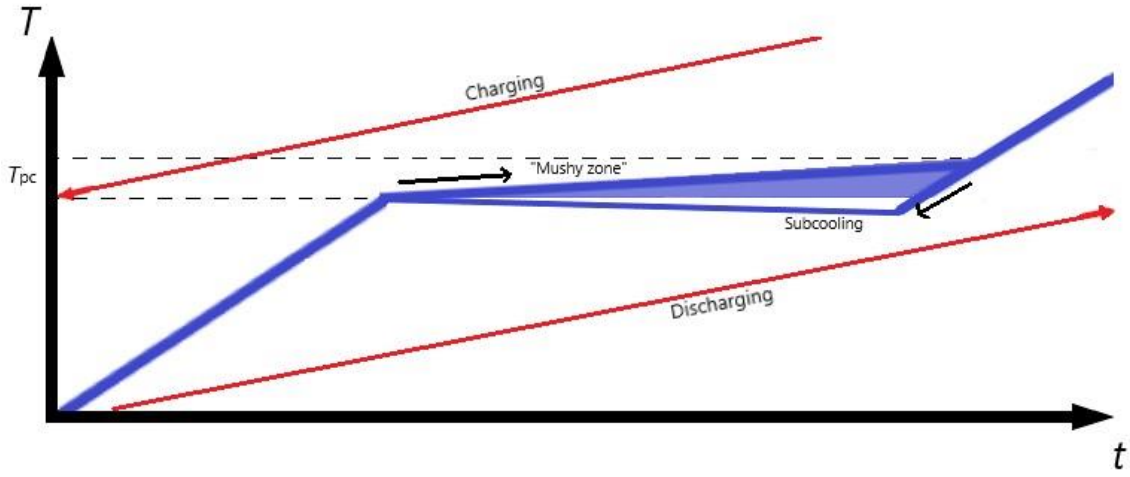

Figure 4.7. Temperature diagram of a latent heat TES system that experiences phase change temperature change within range T_{pc}, and subcooling (not always experienced together).

One of the main benefits of latent heat -based thermal energy storage (in addition to potentially high energy density) is that the storage system's temperature generally does not change during the phase transition, making it possible to store energy with minimal temperature difference and release it at a constant temperature (Stadler et al. 2019, 568; 590; Sterner et al. 2019c, 157; Longeon et al. 2013, 175; Salunkhe et al. 2012, 5604). However, some materials change phase over a range of temperatures rather than a clear-defined temperature. This kind of softening transition region of phase change is called a "mushy zone" in some literature. This phenomenon is demonstrated in Figure 4.7 (above). (Fleischer 2015, 39-40; 76; Martin et al. 2013, 160) That said, even if temperature stays unchanged for the entire process, heat transfer rate does affect the rate that phase change happens at (Fleischer 2015, 3). This means, that the temperature of the heat transfer fluid plays an important role in heat transfer efficiency of the system (Longeon et al. 2013, 178-182; Salunkhe et al. 2012, 5611-5612).

The phase change does not happen evenly throughout the volume of PCM, but rather as a moving front of phase transition, starting from the surfaces that transfer heat. The movement of this front is not even or easily predictable, but depends locally on the rate of heat transfer, which in turn is affected by, for example, temperature gradients and the presence of natural convection. Behavior of this phase change front is demonstrated in Figure 4.8. (Fleischer et al. 2015, 75-76; Longeon et al. 2013, 178-182)

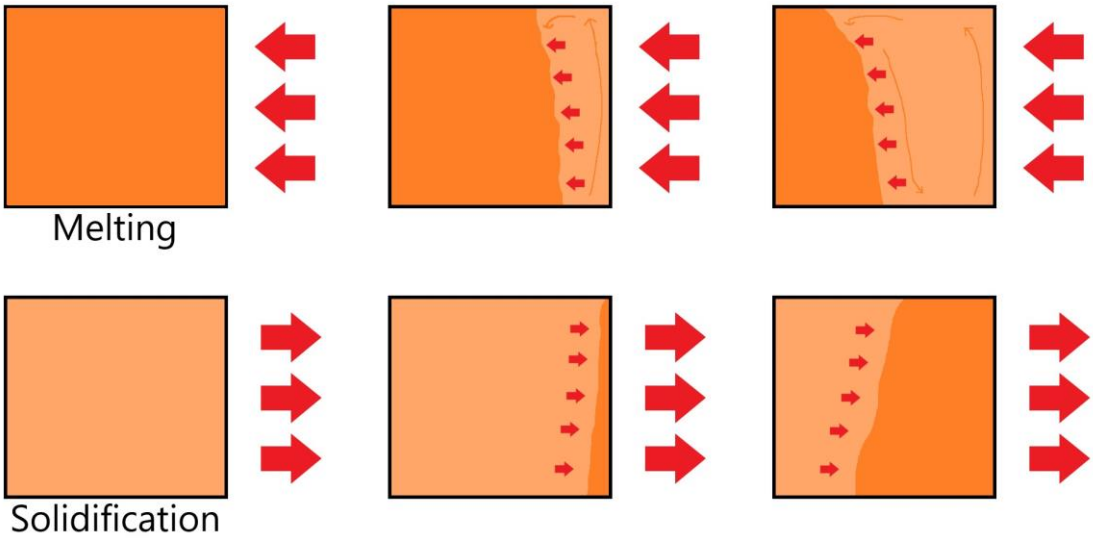

Figure 4.8. Demonstration of phase change as a front and natural convection in PCM. Heat is applied or withdrawn from the right-hand edge of the volume.

More information about solving the phase change boundary over time, also known as “the Stefan problem”, can be found in literature (Fleischer et al. 2015, 76-80).

Heat transfer of the melting of solid PCM is dominated by natural convection, while the heat transfer of solidification is dominated by conduction as the outer layers of the PCM release their heat first, leaving an increasingly thick resistive layer between the phase change front and the heat transfer surface, as demonstrated in Figure 4.8 (above). This leads to the discharge process often being the slower part of the cycle timewise, sometimes inhibitively slow for efficient system operation and thus requiring of different solutions. Poor heat transfer inside the PCM during melting, on the other hand, can lead to high temperature gradients and superheating of the molten layer of PCM before the phase change process is complete. (Fleischer et al. 2015, 11; 25-26; 50-51; 79; Longeon et al. 2013, 175-176; 178-183; Stadler et al. 2019, 597; 599; Salunkhe et al. 2012, 5603; 5611; 5613) Enhancing heat transfer of latent heat storage materials and systems is discussed later in this chapter.

In general, phase change materials pose similar requirements to sensible heat storage materials. Instead of specific heat, the storage capacity is mainly determined by the latent heat of the PCM, although having high specific heat and density are still very beneficial for a PCM. In addition, thermal conductivity often plays an emphasized part in the performance of a PCM. The general requirements for energy storage materials mentioned in chapter 3.2.2 Common characteristics should all be taken into consideration, notably density change over phase transition and thermal and chemical stability. The most important requirement, however, is a suitable phase change temperature. There is no single PCM in the market that would fulfill all these requirements in many scenarios, and as such compromises must be made and work should be done to develop new materials that would be more widely usable. (Fleischer 2015, 37-38; 87; Stadler et al. 2019, 590; 592; Dincer et al. 2018, 74; Farid et al. 2003, 1599)

Types of PCM

Phase change materials are often divided mainly to organics and inorganics. There are also eutectic mixtures that can consist of materials of either of these subtypes or a

combination of both. Water is also used in some latent heat applications, but generally not considered a part of any of the above categories. (Fleischer 2015, 37; Dincer et al. 2018, 74-75; Stadler et al. 2019, 593) A list of various PCMs and their properties can be found in Appendix III - Table of latent heat TES materials.

Organic phase change materials are defined by containing carbon. They consist mainly of paraffins, fatty acids and glycols. (Fleischer 2015, 39; Pereira da Cunha et al. 2016, 229; Dincer et al. 2018, 74) Organics are commonly used in a wide array of low to medium temperature applications, but most of them work in lower temperatures than desirable for industrial uses with melting points mainly under 100 °C and maximum of 170 °C. Their latent heat values are decent considering the temperature area, around 150-250 kJ/kg, with energy densities in the area of 50-150 kWh/m^3. (Fleischer 2015, 39-40; Dincer et al. 2018, 76; Pereira da Cunha et al. 2016, 230; Stadler et al. 2019, 595; Farid et al. 2003, 1599)

Main disadvantage of organic PCMs aside from their low melting temperatures is that they mostly have very poor conductivities (Pereira da Cunha et al. 2016, 229; Dincer et al. 2018, 76; Fleischer 40-41; Stadler 595-596; Farid et al. 2003, 1597; 1599). Some organic PCMs experience the “mushy zone” phenomenon of melting over a temperature range. Most organics are stable, non-corrosive, and safe to use apart from being very flammable. However, they do tend to be expensive especially in high purity. (Fleischer 2015, 39-40; Stadler et al. 2019, 595; Dincer et al. 2018, 76; Farid et al. 2003, 1599; Salunkhe et al. 2012, 5604)

Inorganic PCMs consist mainly of salts, salt hydrates and metals. PCM salts are uncommon in the lower end of their usable temperature range due to better options being available, but in higher temperatures they are the most popular choice of PCM due to available temperature options and low cost. Certain molten salts are also commonly used as sensible heat storage materials. Salts and salt hydrates are discussed in detail in chapter 4.2.1 PCM salts. (Fleischer 2015, 24; 42; Longeon et al. 2013, 175) Metallic PCMs, while technically also inorganic materials, are considered their own subcategory by some authors. (Dincer et al. 2018, 74-75; Fleischer 2015, 37). Metals generally have better

thermal conductivity than other potential PCMs, but lower latent heat and higher density (Fleischer 2015, 45). Metallic PCMs are discussed in chapter 4.2.2 Metallic PCMs.

Eutectic PCMs are combinations of multiple PCMs, either organic, inorganic or a combination of both. They have many favorable properties which can also be widely customized, but some of them are very expensive and research on the field is still underway. They are mostly suited for low to medium temperature storage, reportedly up to 250 °C. (Pereira da Cunha et al. 2016, 227; 230-231; Dincer et al. 2018, 74-75; 77)

System design and PCM containment

One of the key points of focus in development of latent heat storages is the heat transfer capabilities of the system; many PCMs suffer from an inherently low thermal conductivity which makes them less dynamic, most notably in the solidification/discharging phase. Increasing the thermal conductivity of the PCM is vital for efficient use and economic viability. In the worst case, the solidifying PCM acts as outright thermal insulation. (Dincer et al. 2018, 228-229; 232; Fleischer 2015, 5; 25; 49-50; Stadler et al. 2019, 596; Farid et al. 2003, 1604-1605; Pereira da Cunha et al. 2016, 228) A much researched solution is to increase conductivity of the PCM or to provide heat paths inside the volume by adding metallic or carbon fins, meshes or foams, nanoscale particle suspensions or other high-conductivity particles (Fleischer 2015, 11; 23; 25-26; 50-62; Dincer et al. 2018, 228; Stadler et al. 2019, 596; Farid et al. 2003, 1605; 1607; Salunkhe et al. 2012, 5607; Pereira da Cunha et al. 2016, 234-236). Carbon is an interesting option as it has good thermal conductivity and is resistant to corrosion and relatively light (Fleischer 2015, 55). Slow solidification and supercooling after phase change in particular are remedied by increasing conduction, as solidification is more conduction-based than melting and the additives often provide nucleation surfaces as an added benefit (Fleischer 2015, 23; 25-26; 43; 50; Dincer et al. 2018, 78; 242). Addition of particles can adversely affect other thermal qualities of the PCM, most notably by displacing the storage material itself and increasing manufacturing cost, albeit mass fraction of the additive rarely needs to exceed 10% (Fleischer 2015, 25; 53-54; Dincer et al. 2018, 229; 231-232). Additionally, it has been found that the natural convection -dominant melting process in a shell-and-tube heat exchanger can be sped up by a

considerable margin by angling the heat exchanger by around 5 degrees if PCM is on shell-side (Fleischer 2015, 26). An option for increasing the overall heat transfer coefficient is adding fins on the HTF side (Fleischer 2015, 25).

Another method to increase the heat transfer capabilities of the PCM system is encapsulation of the PCM. Encapsulation refers to dividing the PCM to smaller volumes and either covering them with a coating or encasing them inside shells. This results in increased heat transfer surface while also acting as a reliable container for the PCM. The smaller container units also better withstand the volume change associated with phase change. In some cases, encapsulation enables combining PCM with existing TES systems. (Fleischer 2015, 21-22; Salunkhe et al. 2012, 5604; 5607; Stadler et al. 2019, 596; 598; Farid et al. 2003, 1597; 1605)

Macroencapsulation refers to when the PCM is encapsulated in volumes ranging in size from roughly separable by eye up to relatively large. The capsules are usually either spheres, tubes or plates of metal, plastic, composites, or other durable material. They are often forming a packed bed or a similar stacked arrangement. (Fleischer 2015, 21; 62; 64-65; Stadler et al. 2019, 596; Farid et al. 2003, 1606-1607; Salunkhe et al. 2012, 5606; Wu et al. 2015, 1062) The sphere is considered a good option due to high surface-to-volume ratio and suitable packing ratio/void fraction in the packed bed leading to good heat transfer performance (Fleischer 2015, 65; Salunkhe et al. 2012, 5610). The ideal encapsulation material is structurally and thermally durable, leak and diffusion proof and non-reactive with the PCM and HTF, and has high thermal conductivity (Salunkhe et al. 2012, 5605; 5609; Fleischer 2015, 64). Metallic shell material in particular helps with heat transfer due to high conductivity and is suitable for high temperature use (Salunkhe et al. 2012, 5606; 5613). Stainless steel has been tested suitably corrosion resistant to a variety of PCMs, although its conductivity is lower than some other metal options (Fleischer 2015, 64-65). Further heat transfer enhancements like conductivity-increasing particles may be necessary (Fleischer 2015, 23-24; Salunkhe et al. 2012, 5607).

Capsules are often not fully filled to avoid problems with volume change, in cases of lesser volume change a strong enough encapsulation material can absorb the stresses caused by it (Stadler et al. 2019, 596; Salunkhe et al. 2012, 5605; Farid et al. 2003, 1607).

However, if the change in volume causes the PCM to partially separate from the capsule surface, it may result in a significant degradation of heat transfer capacity (Fleischer 2015, 63; Farid et al. 2003, 1607). Encapsulation shell material itself displaces some of the PCM leading to reduced storage capacity (Stadler et al. 2019, 598), and the space that is left between the encapsulated PCM volumes (so called "void fraction") reduces the volumetric capacity further (Wu et al. 2015, 1062). Thus, shell thickness is a balance between durability, and storage capacity and heat transfer resistance (Salunkhe et al. 2012, 5603; 5605; 5608; 5613).

A packed bed configuration of encapsulated PCM spheres may cause uneven flow distribution in HTF, leading to inconsistent heat transfer (Stadler et al. 2019, 598). Additionally, the packed bed can cause high pressure loss in HTF (Farid et al. 2003, 1607). Despite these considerations the PCM packed bed system generally results in a smaller storage volume than an equivalent sensible heat packed bed and possibly reduced investment cost (Fleischer 2015, 22).

Microencapsulation simply refers to PCM capsules of a significantly smaller size than macroencapsulated PCM, typically 1-1000 µm. Microencapsulated PCM behaves (and looks) like powder, making it easier to handle and less susceptible to damage. (Stadler et al. 2019, 596; Fleischer 2015, 66; Salunkhe et al. 2012, 5606) Microencapsulated PCM can also reach better heat transfer performance due to higher surface-to-volume ratio of the beads and the smaller size leads to less issues with PCM volume change and poor conductivity due to lesser temperature gradient inside the PCM (Salunkhe et al. 2012, 5606-5607; Fleischer 2015, 66).

Microencapsulation is often achieved through processes such as coating or polymerization (Fleischer 2015, 67; Salunkhe et al. 2012, 5605; Stadler et al. 2019, 597). Capsule material requirements are similar to those of macroencapsulation with an added requirement of suitability for above processes. Metallic shell materials are currently not viable for microencapsulation. (Salunkhe et al. 2012, 5610; 5613) So far microencapsulation is more common in applications of passive temperature control, such as embedding in building materials (Stadler et al. 2019, 596-597; Fleischer 2015, 66; Salunkhe et al. 2012, 5607). Also under research is nanoencapsulation, which is similar

to microencapsulation but in even smaller scale (Fleischer 2015, 68; Salunkhe et al. 2012, 5606).

Phase-change slurries are mixtures of HTF and PCM that behave like a fluid and can be pumped regardless of charge state (Stadler et al. 2019, 568; 600). They are produced by adding either micro- or nanoencapsulated PCM to a suitable HTF, or combining a PCM and HTF that do not mix naturally (Stadler et al. 2019, 600; Salunkhe et al. 2012, 5612). Slurries can be used either as higher-capacity HTF, or a storage material with better heat transfer capabilities (Fleischer 2015, 66; Salunkhe et al. 5603; 5612). The portion of PCM in the slurry affects the fluid viscosity and is typically between 20-40% to avoid increasing pressure drop and necessary pumping work too much (Stadler et al. 2019, 600; Salunkhe et al. 2012, 5603; 5612).

Aside from encapsulated PCMs, a conventional shell-and-tube type heat exchanger has been found a viable option as a latent heat storage unit. Shell-and-tube heat exchangers are simple, known and thus generally low-cost. Typically, the PCM is placed on the shell-side and HTF flows in the tubes. (Longeon et al. 2013, 175; Fleischer 2015, 24-26)

In applicable heat exchangers Longeon et al. recommend a general top-downward direction for HTF during charging (PCM melting), and bottom-upward direction for discharging. This is to retain a thermocline layering in the storage during partial charge/discharge cycling, increasing the system efficiency in irregular operation, as well as to avoid creating voids in the PCM during discharging. (Longeon et al. 2013, 183)

Optimizing temperature differences between TES and HTF is important for reaching high efficiency (Laing et al. 2012, 498). Heat transfer efficiency of a PCM storage can be optimized by using multiple PCMs with slightly different melting points in cascaded steps to both reduce exergy loss from temperature difference of HTF between charging and discharging and to make heat flux more consistent over the process (Fleischer 25-26; Wu et al. 2015, 1061; Farid et al. 2003, 1607; Pandiyarajan et al. 2011, 6017). This also allows for optimization of pinch points for higher charging and discharging rate overall, instead of optimizing for either-or (Wu et al. 2015, 1069; 1071-1072; Fleischer 2015, 25). If using only one type of PCM, system charging/discharging rates and efficiencies will suffer from

low logarithmic temperature differences and high exergy loss (Wu et al. 2015, 1061; 1071-1072). The more temperature steps the system has, the more complicated the heat transfer characteristics of the system are but closer to linear temperature distribution is in HTF (Wu et al. 2015, 1071). Furthermore, the ability of latent heat storage to store energy with minimal temperature difference can be utilized to avoid high maximum temperatures in the system and thus reduce heat losses to environment (Stadler et al. 2019, 590). Effect of multiple phase change temperature steps on HTF temperature difference is demonstrated in Figure 4.9.

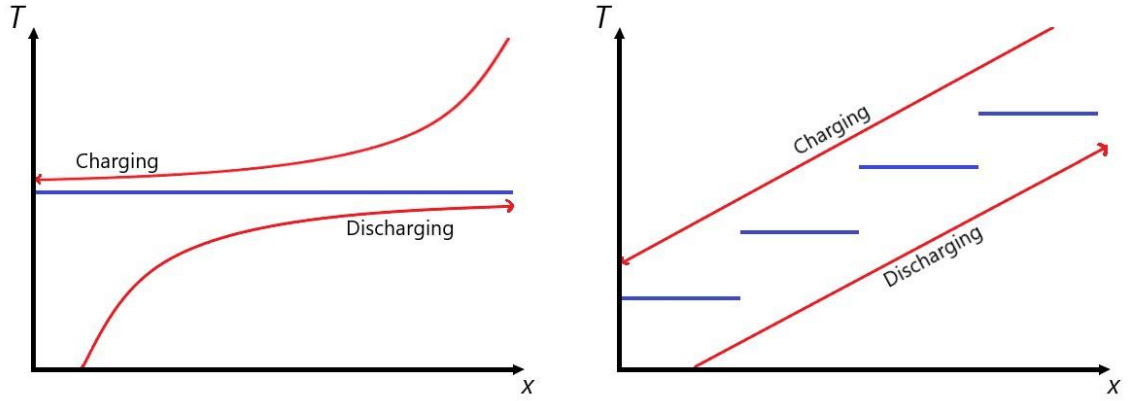

Figure 4.9. Temperature differences in single-PCM (left) and multi-PCM (right) systems. Purple lines represent PCM phase change temperatures and *x* refers to axial distance along the storage system.

Other system optimization option, for steam generation in particular, is to use sensible heat storage for preheating and superheating, and latent heat for evaporation (Guillot et al. 2011, 175).

Price

Generally speaking, latent heat storage is more expensive than an equivalent sensible heat storage, apart from special exceptions such as very tight temperature range where sensible heat storage is not viable. Reasons for this include early phase of research and market, complicated system designs that are often tailor-made and expensive materials. Stadler reports the typical specific capital cost of latent heat storage as 10-50 €/kWh, with potential of being even higher. (Stadler et al. 2019, 590; 607) PCM encapsulation is currently unfeasibly expensive, research is required to make all forms of encapsulation

more economically viable (Salunkhe et al. 2012, 5607; 5613). Stadler reports cost of microencapsulated PCMs on average as 10 €/kg (Stadler et al. 2019, 607).

4.2.1 **PCM salts**

In addition to being relatively widely used in sensible heat storage applications, salts (and by extension, salt hydrates) can be utilized for their high latent heat as PCMs. Salt hydrates are salts with water molecules amidst their molecular structures (Fleischer 2015, 17; 41-42). As with molten salts in sensible heat applications, most research on PCM salts is based on CSP applications, but they are also viable for higher temperature WHR applications (Stadler et al. 2019, 596; Fleischer 2015, 24; 42-43).

The melting points of salts and salt hydrates cover a wide range of temperatures, from as low as 10 °C to over 900 °C (Fleischer 2015, 42). In the lower end of the range, existence of simpler and/or cheaper options such as some organic PCMs as well as sensible heat storage using water or other cheap materials make the use of salts and salt hydrates rare (Fleischer 2015, 42). In particular, the melting points of salt hydrates fall mostly below 120 °C and for this reason the rest of this chapter will focus mainly on anhydrous salts (Dincer et al. 2018, 77; Pereira da Cunha et al. 2016, 230; Stadler et al. 2019, 593-594). Furthermore, salt hydrates suffer from problems related to subcooling, chemical instability and phase separation, which can be reduced by stirring, encapsulation or chemical additions (Stadler et al. 2019, 593; Fleischer 2015, 43; Dincer et al. 2018, 77-79; Farid et al. 2003, 1597). Aside from these shortcomings, salt hydrates have decent volumetric storage density and conductivity and are often competitive in storage capabilities and price with organic PCMs (Stadler et al. 2019, 593-595; Farid et al. 2003, 1597; 1601; Pereira da Cunha et al. 2016, 230; Dincer et al. 2018, 77).

Anhydrous salts on the other hand are the most popular type of PCM in high temperature applications (Fleischer 2015, 43; Adinberg et al. 2009, 9). Nitrate and nitrite salts are particularly useful in temperatures up to 350 °C and can, according to Stadler et al., beat most sensible heat systems in pricing in the area of 120-340 °C especially in situations with a tight temperature range (Stadler et al. 2019, 596). The melting temperature of PCM salts can be tailored to specific applications quite flexibly by mixing different salts

together to form eutectics (Wu et al. 2015, 1063). Most common cations used for PCM salt mixtures are alkali- and alkaline earth metals, while anions in addition to nitrates and nitrites are usually carbonates, sulfates, chlorides, or fluorides (Stadler et al. 2019, 596).

Latent heat of lower temperature salts and salt hydrates is decently high, comparable to organics, in the area of 150-300 kJ/kg. Higher melting temperature salts latent heat values are even higher, up to 700 kJ/kg. The relatively high density of most salts and salt hydrates acts to increase the energy density of these materials. (Fleischer 2015, 43-44; Cabeza et al. 2015, 6) PCM salts generally have a higher energy density than most sensible heat storage systems (Fleischer 2015, 17-18; Adinberg et al. 2009, 9).

Anhydrous salts generally have an average thermal conductivity that may need to be increased through external means (Fleischer 2015, 43; Laing et al. 2012, 497). Despite this, they are feasible to use for steam generation owing to their high temperature and the fact that simultaneous phase change in both side of the heat exchanger helps with achieving the necessary heat rate (Stadler et al. 2019, 596; Laing et al. 2012, 497-498). Additionally, constant temperature of discharge is efficient in designing temperature differences (Guillot et al. 2011, 175; Adinberg et al. 2009, 9; Laing et al. 2012, 498).

Laing et al. used sodium nitrate to generate superheated steam at up to 110 bar and 400 °C, with a sensible heat concrete storage as superheater. The storage had a capacity of 700 kWh and weighed approximately 14 tons. (Laing 2012, 497-498) Pure $NaNO_3$ is a decent candidate for a PCM salt with a melting temperature of 305 °C, latent heat of 178 kJ/kg, thermal conductivity of around 0.6 W/mK and density of 2100 as solid and 1900 as liquid near the melting point (~10% difference over phase change) (Laing et al. 2012, 501). Laing et al. also tested charging and discharging of the latent heat storage in constant and variable water/steam pressure; constant pressure results in decreasing heat flux over time in discharge mode in particular, as the salt solidifies around the heat exchanger, increasing thermal resistance, while variable pressure was able to keep heat flux and mass flow nearly constant (Laing et al. 2012, 498). System was able to perform with satisfactory results in forced circulation, natural circulation, and once-through modes (Laing et al. 2012, 498-501; 504).

A mixture of 70% $NaNO_3$ and 30% KNO_3 was studied by Martin et al. and found to have a larger melting range of 220-260 ℃ as opposed to about 222-240 ℃ of the traditional solar salt (60% $NaNO_3$, 40% KNO_3). The mixture has a specific heat capacity of around 1.5-1.6 kJ/kgK in both solid and liquid phase, latent heat of about 118 kJ/kg and average thermal conductivity of around 0.5 W/mK. (Martin et al. 2013, 160-161; 163-164) Latent heat is reported to be almost evenly distributed along the melting range, leading to a combined sensible and latent heat capacity in the melting range of 220-260 ℃ of about 4.5 kJ/kgK (Martin et al. 2013, 162-163; 165). The mixture did suffer from issues of phase separation in incomplete cycling which could reduce storage capacity by up to 75%, but full capacity could be restored by completely melting the PCM. The mixture would be at its best in applications that aim to utilize both sensible and latent heat of the salt around the respective temperature range. Furthermore, melting over a temperature range can be possibly advantageous if sharp change in temperature profile is to be avoided. (Martin et al. 2013, 159-160; 165)

Despite having less stability issues than salt hydrates, anhydrous salts are not by any means simple materials either. PCM salts generally show some density change at phase change, although in most cases small enough difference to not cause significant issues. Some salts have a tendency for supercooling, which can be partially mitigated with nucleating agents or other particles that help start solidification. Some salts are also chemically unstable over repeated cycling. On the positive side, salts are mostly non-flammable and non-combustible. (Fleischer 2015, 43; Stadler et al. 2019, 593) Possibility of corrosion should also be taken into account, particularly with cheaper materials (Fleischer 2015, 17; 43). Corrosion of salts commonly used in TES applications is discussed in chapter 4.1.5 Molten salts under the subchapter Common issues, some of which is also applicable to salts used as PCMs.

Efficient heat exchanger designs for PCM salts can be difficult; solidification of salt on the heat surface can cause issues with both heat transfer and corrosion (Adinberg et al. 2009, 10). Proposed solutions include macroencapsulation of the PCM salt, or usage of fins to increase heat surface particularly in the salt volume (Laing et al. 2012, 498; 501; Adinberg et al. 2009, 10)

Utilizing the latent heat of the salt increases energy density in comparison to sensible heat molten salt storage, reducing storage size and as such cost compared to a two-tank sensible system. In particular, encapsulated PCM salt packed bed storage is estimated to be competitive in comparison to both two-tank sensible heat molten salt storage and a shell-and-tube type PCM salt storage. (Fleischer 2015, 17-18)

4.2.2 **Metallic PCMs**

Some metals have melting points in temperatures that allow them to be useful for TES applications. They are still very much underused in the field of thermal energy storage despite years of collective experience with molten metals in other applications, so information about their use as PCMs is somewhat limited. (Fleischer 2015, 44-45; Fernández et al. 2017, 275)

Metals that have been used as PCMs cover a wide range of different melting temperatures from room temperature levels to around 1000 °C. Promising candidates for metal PCMs in useful temperature range include tin, zinc, aluminium, and their alloys. (Fleischer 2015, 44-46; Fernández et al. 2017, 277) Most of the viable metals have a fairly low latent heat value which results in high storage masses. Volumetric energy density is partially remedied by high density of most metals, but energy density is still often lower than PCM salts. (Fleischer 2015, 44-45; Fernández et al. 2017, 276) Metals of higher melting temperatures, however, tend to have higher latent heat values and as such can compete in volumetric storage capacity, and consequently costs, with salts of similar temperatures, particularly when maximum weight is not limited (Fleischer 2015, 45-46; Fernández et al. 2017, 275-276; Adinberg et al. 2009, 10; 12). The main draw of metals as PCMs, however, is the extremely high thermal conductivity that most metals pose. This high conductivity also means that metallic PCMs do not need conductivity-increasing additions that many other PCMs do, that would otherwise increase both weight and price of the system. (Fernández et al. 2017, 275-276; Fleischer 2015, 45)

Some properties of metals in high-temperature thermal cycling are still partially unknown. Generally, metals and metal alloys have shown good stability in high temperatures. However, slight reductions in latent heat values of some alloys have been

detected in extended cycling. Some metals experience supercooling, for example pure aluminium. Metals are rarely corrosive or otherwise incompatible with surrounding materials, but this is still possible. Thermal expansion as well as volume change over phase change pose a problem for some metals. (Fleischer 2015, 45; Fernández et al. 2017, 276; 279-280) Although metals are relatively easy to work with and there is a lot of experience in handling and using them in various applications, more research is needed on their use as PCMs (Fleischer 2015, 44-45; Fernández et al. 2017, 275; 280). In particular, the encapsulation of metal PCMs is a challenge and as such costly (Fernández et al. 2017, 280).

Adinberg et al. tested a 70% zinc-30% tin alloy as PCM for a buffer storage in generation of superheated steam at 350 °C. Storage temperature was held at 370 °C, although the PCM alloy changes phase at a temperature range of 200-370 °C. (Adinberg et al. 2009, 9) Due to how the molten metal alloy behaves when cooled, assessing the latent heat of the mixture was somewhat complicated; cooling the mixture down from 370 °C to 270 °C resulted in a total enthalpy change of 107 kJ/kg (Adinberg et al. 2009, 12). Unfortunately, this behavior means that the benefit of near-constant discharging temperature characteristic to most PCMs is lost. The alloy was used to lower the liquidus temperature of the PCM to below 400 °C; pure zinc would not only have at a constant phase change temperature of 420 °C, but also a higher latent heat value than the total enthalpy change of the used alloy over 100 °C of 112 kJ/kg (Adinberg et al. 2009, 12). Pure zinc does, however, have issues of potentially high vapor pressure which would reduce its usability as a PCM (Fernández et al. 2017, 279).

4.2.3 **Steam accumulators**

A steam accumulator can be roughly described as a steam drum that operates in variable pressures. Other names include “sliding-pressure water storage” or “Ruths storage”. It is particularly popular with process steam applications. (Stadler et al. 2019, 565; 585; Laing et al. 2012, 497). Steam accumulators are among the oldest forms of TES used in industrial applications, with earliest examples used in the 1920’s (Stevanovic et al. 2020, 1).

The steam accumulator is a cylindrical tank that is filled with water and steam in saturated condition. Charging the steam accumulator is done by feeding steam into the tank, which leads to pressure increase in the tank as the saturated water-steam mixture is heated in constant volume. In the discharging process, steam is taken from the accumulator, which then causes the pressure to decrease. This effectively means, that in addition to physical dimensions, the storage capacity of the accumulator is defined by the range of pressure it operates in, which in turn is limited by the operating pressures of the steam supplier and the steam consumer (while taking pressure losses into account). The general structural principle of a steam accumulator is depicted in Figure 4.10. (Stadler et al. 2019, 585; Sun et al. 2016, 1-4; Stevanovic et al. 2020, 4-6)

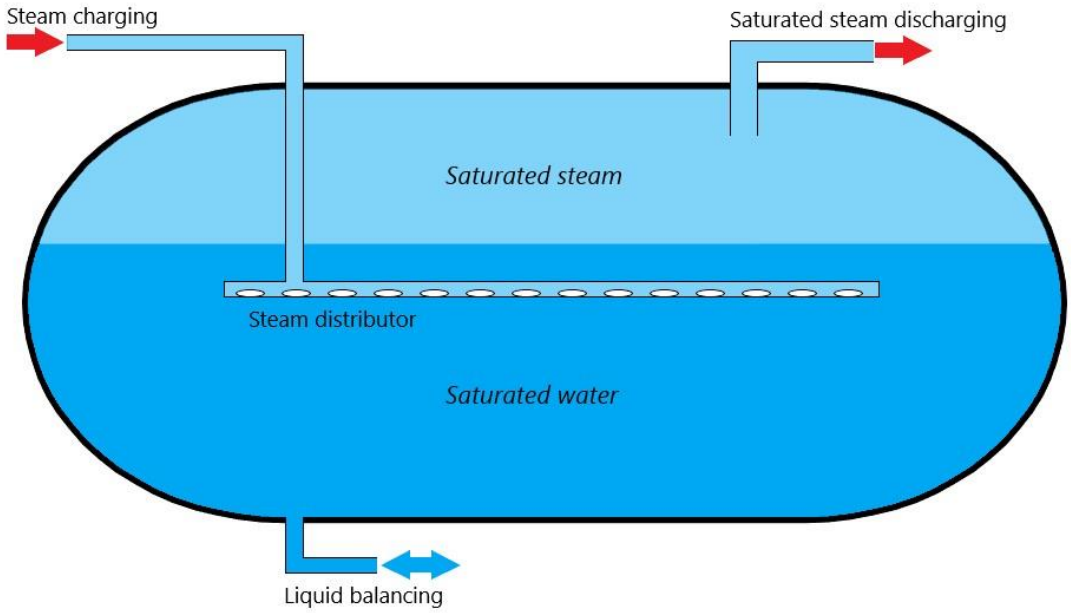

Figure 4.10. General structural principle of a steam accumulator. (Stadler et al. 2019, 586; Sun et al. 2017, 3)

These properties also make the steam accumulator a bit of an outlier in terms of classification in the energy storage field. Instead of storing heat through a heat exchanger, it directly stores live steam by condensing it into saturated liquid. On the other hand, the storage mechanism is based on pressure instead of temperature difference. Finally, the system is in saturated condition, making it classifiable as a latent heat -based storage technology utilizing liquid-vapor phase change in an isochoric reverse reaction (Stadler et al. 2019, 568), but the storage pressure and thus temperature are variable throughout

the storage cycle, so some authors such as Stadler ultimately classify steam accumulators as sensible heat storage despite above definition of isochoric liquid-vapor latent heat storage (Stadler et al. 2019, 585).

However, as opposed to solid-liquid latent heat storages, the steam accumulator stores heat by condensing steam to liquid. This is because in pressures between 4-40 bars the energy content of saturated steam is 2.5-4.5 times higher than that of saturated water, while the density of saturated water is around 40-400 times higher than that of saturated steam (Incropera et al. 2007, 949-950). This leads to saturated water having a much higher volumetric storage capacity than saturated steam (Sun et al. 2016, 4).

For a steam accumulator to function in a process, the operating pressure of the steam consumer must be notably lower than that of the steam supplier. This way steam will flow from supplier to accumulator and from the accumulator to consumer naturally by pressure difference. This also defines the operating range of the accumulator and thus the storage capacity: the maximum charge pressure of the accumulator is the operating pressure of the steam supply reduced by pressure loss between the supplier and the accumulator, and the lowest pressure the accumulator can be discharged to is similarly above the consumer pressure, by an amount equal to pressure loss between the consumer and the accumulator. This means, that the greater the difference in operating pressures of the steam supplier and consumer, the greater the volumetric storage potential of the steam accumulator will be. (Sun et al. 2016, 2-4; 10) However, if the absolute difference between charging and discharging pressures stays unchanged, higher overall pressure level of the system will lead to a lower storage capacity because saturated water energy content increases more along with pressure than energy content of saturated steam, while the difference in the densities of the two is reduced (Incropera et al. 2007, 949-950; Sun et al. 2016, 6). However, higher overall system pressure level may allow increasing the pressure difference between charging and discharging.

Steam accumulators are technically viable up to critical point of water (374 °C, 221 bar), above which vapor and liquid cannot be separated. However, due to diminishing increase in storage capacity in higher pressures and the effect of operating pressure on pressure vessel price they generally are not cost efficient in pressures as high, instead typically

limited to outputting steam at max 250 °C, 40 bar. This range is usually optimal for steam used by process applications. (Stadler et al. 2019, 565; 585-586; Sun et al. 2016, 6)

Due to the direct discharge method of steam generation from saturated water via pressure decrease and lack of surface heat exchanger, steam accumulators are capable of high discharging rates fast response times (Stadler et al. 2019, 585; Sun et al. 2016, 2-3). Owing to this, in addition to acting as a buffer storage for intermittent steam sources, a steam accumulator can be used to momentarily exponentially boost steam supply to cover a sudden spike in demand (Sun et al. 2016, 4; 14). Some evidence suggests saturated steam quality in nominal operation could be high enough for low-efficiency turbine. However, although saturated condition exists in storage, in actual operation the conditions can momentarily deviate from equilibrium due to rapid charging or discharging resulting in wet steam. (Sun et al. 2016, 2; Stevanovic et al. 2020, 7) Discharged steam can be moisture-proofed by superheating it using another TES module (Stevanovic et al. 2020, 2).

Sun et al. considers investment cost of steam accumulators high, comparing it to a boiler of same size (Sun et al. 2016, 1-2). Careful optimization of the accumulator to the target application can help reduce investment cost, as it is highly dependent on steam accumulator volume (Sun et al. 2016, 1). In addition, as mentioned, higher pressure increases pressure vessel price (Stadler et al. 2019, 586). As such it cannot be considered a very competitive option for larger capacity storage (Laing et al. 2012, 497). However, steam accumulators can be competitive options in situations where a steam process requires fast response to load changes, when both operational and economic factors are taken into consideration (Stevanovic et al. 2020, 2).

5 PROPOSED TES SYSTEMS

Several different sensible and latent heat TES systems have been reviewed in the previous chapter. Sensible heat storages offer well-established and relatively simple options for TES in different temperature ranges. Latent heat storages, on the other hand, offer potentially high energy densities in low temperature differences as well as often a consistent discharge temperature, but research is still needed to solve some issues, most importantly with thermal conductivity, stability, and containment, as well as to make them overall cheaper to manufacture as they can be quite costly in comparison to most sensible heat storages. The objective of this chapter is to assess the options that Alfa Laval Aalborg might be most interested in for the most common applications out of the technologies reviewed previously.

The technical viability of each technology for a given application depends heavily on the prevailing conditions. The most important determining factor is temperature range of heat sources and consumers. Common temperature ranges for various sensible heat storage systems are displayed Figure 5.1.

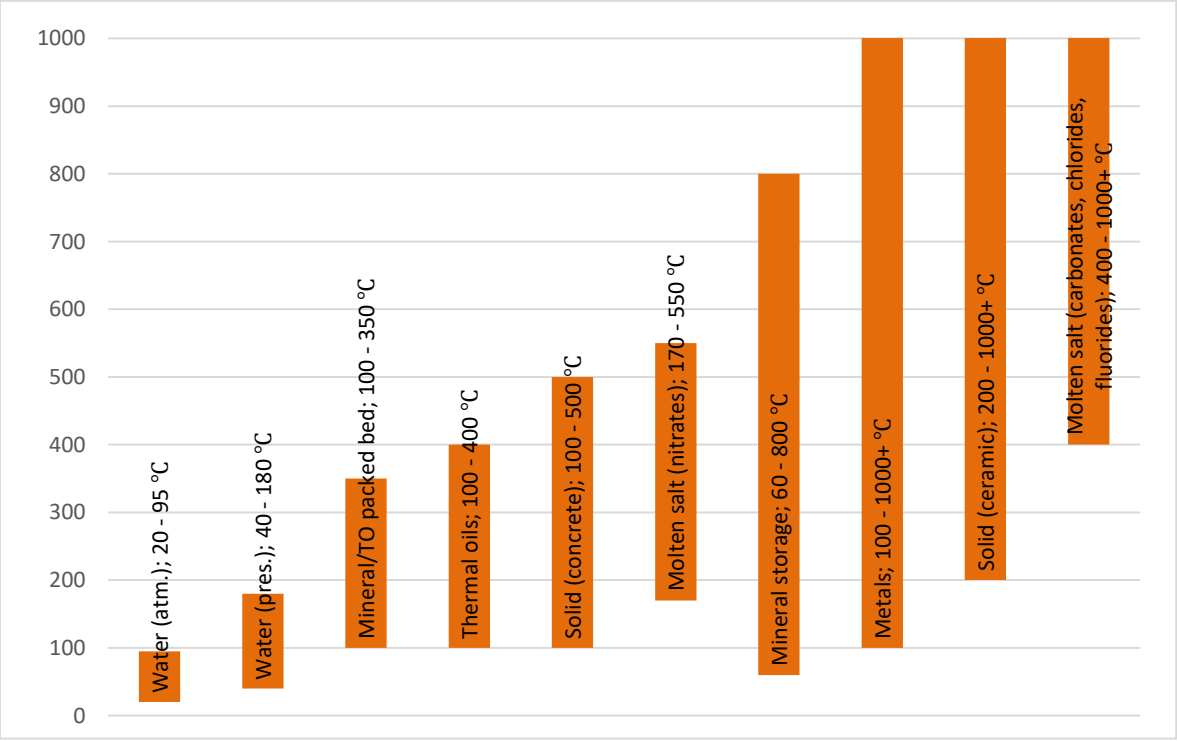

Figure 5.1. Common temperature ranges for sensible heat TES systems.

Common general ranges for phase-change temperatures of various types of PCM are displayed in Figure 5.2. It should be noted that despite displaying temperature ranges in the figure, the majority of these PCMs still change phase at a constant temperature; each range is representing the overarching category of PCM.

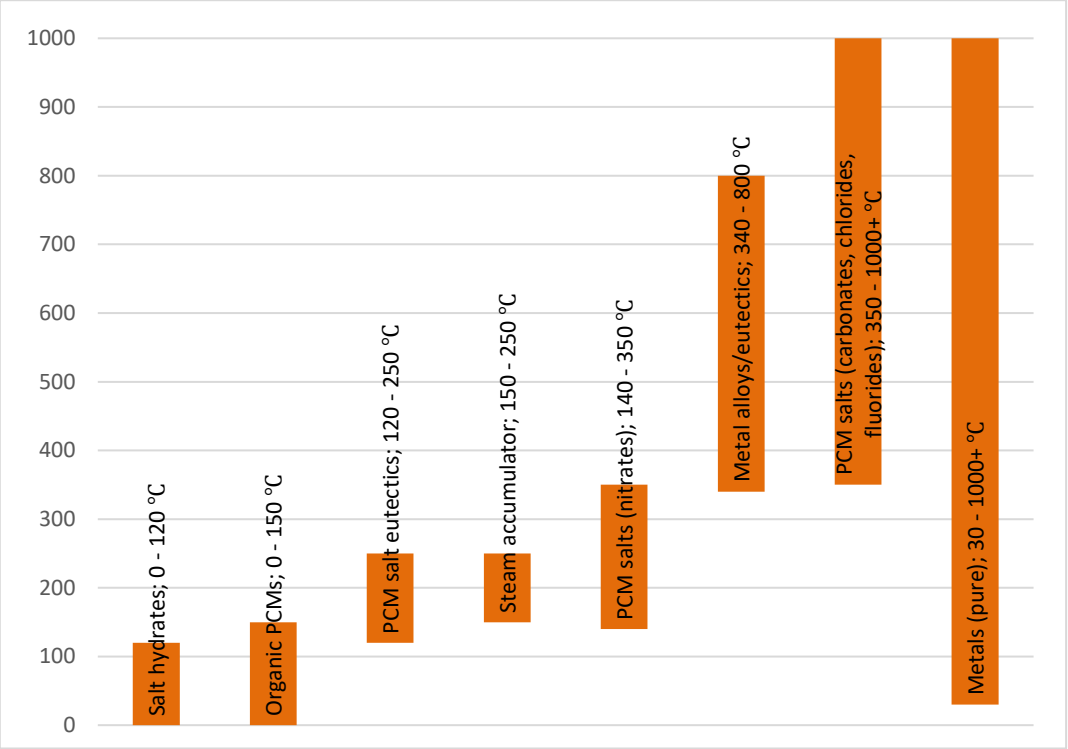

Figure 5.2. Common temperature ranges for phase change temperatures of each type of PCM.

The second factor in determining the options for viable TES methods is the type and required heat transfer capability of the discharge, for example whether the heat is required as saturated or even superheated steam or if process heat in any form is usable, whether the discharge needs to happen at a high heat rate and/or fast response to load, and once again the temperature level of the storage output.

The third set of factors that must be taken into account is special constraints set by the existing process and heat source and utilization of possible synergies. These could include unavailable (or readily available) materials, space constraints (or existing unused structures) and/or logistics. These factors are mainly case-specific and will not be considered in this general comparison of options.

The reference applications selected in chapter 3.4.3 for comparing outputs of TES systems were as follows:

- Saturated steam generation at ~160-250 ℃
- Superheated steam generation at up to 350 ℃
- Process heating at various temperatures using water or other heat transfer fluids if applicable

Naturally, other applications exist, and the viability of different technologies also depends on the heat source, but the heat sources are very case specific and thus difficult to generalize. The heat source mainly sets a maximum limit on the temperature level of the storage in terms of technology options.

For low temperature process- or district heating applications the most common TES system is a thermocline water tank storage (Gadd et al. 2015, 473). This is a sensible choice, as water tanks are among the cheapest storage systems available while still having an adequate storage capacity. Water is a widely used and simple HTF for both charging and discharging the storage. Additionally, due to the low temperature level of the system heat losses are inherently reduced. Pressurizing the storage can extend the temperature range above 100 ℃ if necessary. If space or mass of the storage are a critical issue, such as in marine applications, latent heat storage using salt hydrates or organic PCMs could be an option, but otherwise they are typically not economically competitive with thermocline water tank storage.

For higher temperature process heating, thermal oils would be a step up from the simple water storage. Thermal oils on their own are fairly expensive, so they could be combined with a packed bed of minerals to reduce cost of the system. However, thermal inertia of minerals may cause thickening of the thermocline layer and thus reduction of storage capacity in frequent cyclic use. If packed bed is not a viable option, mineral oil would be the most affordable type of thermal oil, usable up to 300 ℃. In temperatures above these, minerals, solid materials, or salt-based PCMs would be the next likely options. In marine applications in particular, PCM nitrate salts and salt mixtures could store energy in high

enough density to be useful options. These salt-based latent heat storages are also potentially able to output saturated steam.

For saturated steam output up to 250 °C (40 bar), steam accumulators would be an option worth considering. Steam accumulators have the advantages of high discharging capabilities and fast response rates, making them especially useful for covering sudden peaks in load (Stevanovic et al. 2020, 1-2; 9). As an additional benefit, ALA has extensive experience in steam systems which can be very useful in design of steam accumulator storages.

If superheated steam output is desired from the TES, temperature level and heat transfer capability criteria are emphasized. Molten salt sensible heat storages have been found capable of generating superheated steam. The molten salt thermocline storage with integrated steam generator -concept by Gaggioli et al. could be an interesting option due to its claimed modularity and ability to produce superheated steam. In addition, latent heat storages using salt- or metal-based PCMs are possible options, but still somewhat unproven technology. The constant temperature of phase change helps in managing temperature differences in steam generation, and either a separate sensible heat storage or a cascaded PCM system can be used for efficient pre- and superheating if deemed necessary. High temperature solid sensible heat storage could also be viable, provided high enough charging temperatures are available.

Connecting the TES to the heat source is also a technical question that should be answered. As the precedent is to utilize TES along with waste heat recovery, the main point of interest would be system connection options to a WHR boiler or system.

The most straightforward option would be to charge the TES with the flue gases from the heat source using an embedded heat surface inside the storage. This would avoid the need for an intermediate HTF loop and thus one step of exergy losses and a secondary heat exchanger. However, gases have poor heat transfer compared to liquids, so adequate heat surface is harder to install inside the storage. (Pandiyarajan et al. 2010, 79) Fouling of the heat surface would also likely become a problem, as cleaning the heat surfaces inside the TES would be challenging.

Other charging options all involve a secondary loop of heat transfer fluid. This HTF can either be the storage material in a direct charging scheme, or another HTF in an indirect charging scheme as visualized in Figure 3.3 of chapter 3.2.1. (Pandiyarajan et al. 2010, 79)

From CSP technology development we can learn that storage can be charged with steam generated in the heat source, or we can use an intermediary HTF or the storage material itself as additional circulating fluids to transfer heat from the heat source to the storage (Fleischer 2015, 16). It has been shown that even charging of molten salt storages, which generally have below average heat transfer properties and require fairly high temperatures to take full advantage of, can be charged using steam as the HTF (Aga et al. 2013, 1097-1098; 1100).

For ALA, suitable options to charge the storage are using steam, storage fluid or separate HTF in a secondary loop. This is due to mentioned difficulties of using direct heat transfer from flue gases and because ALA already has established products for recovering the waste heat from said flue gases to various HTFs, especially steam and water.

As a closing statement it should be reiterated that overall sensible technologies are safer investments, but latent heat has more room for development and thus more room for establishing a position at a new market with potentially high profit, albeit with higher risk.

6 SUMMARY

A wide range of thermal energy storage technologies have been reviewed for purposes of being used in conjunction with waste heat recovery systems. The aim of waste heat recovery is to recover heat from sources that generate it as a byproduct and to use the heat to for example benefit a process or to generate power.

Reviewed thermal energy storage technologies can be divided to sensible and latent heat -based solutions. Sensible heat storage technologies store energy by increasing the temperature of the storage material. Latent heat storage technologies store energy in the latent heat of phase change, commonly melting.

Sensible heat storage systems are characterized by simplicity and cheap materials, and as such they are the more common thermal energy storage systems. Applicable sensible heat storage technologies include water thermocline tanks, thermal oil storage with or without a packed bed of mineral filler, mineral and solid mass storages, and molten salt sensible heat storages.

Latent heat storage systems are characterized by higher energy densities in comparison to sensible heat systems. They also have a benefit of constant or near-constant temperature when charging and discharging. However, they are generally more expensive than sensible heat storages, and have certain issues that require further research, such as poor conductivity that reduces heat transfer especially during discharging. Applicable latent heat storage technologies, or phase-change materials (PCMs), include organic PCMs, salt hydrates, salts, and metals. Additionally, steam accumulators have characteristics of both sensible and latent heat storages, but in this thesis, they are categorized as a latent heat storage technology.

Most promising options for different applications are water thermocline storage for low-temperature process- or district heating, thermal oils with or without a packed bed of mineral filler for mid or high temperature process heat, steam accumulators for mid-temperature saturated process steam applications especially in cases where high heat rates and fast response to load changes are required, and molten salt sensible heat storages for higher temperature applications including superheated steam generation. PCM salts and

metals show development potential for mid to high temperature heat or steam generation. All of these technologies can be used in conjunction with waste heat recovery boilers.

Overall sensible technologies are more established and as such safer investments, but latent heat has more room for development and thus for potential profit, albeit with higher risk.

REFERENCES

Adinberg, R.; Zvegilsky, D.; Epstein, M. 2009. Heat transfer efficient thermal energy storage for steam generation. Energy Conversion and Management. Vol. 51(2010) P. 9–15. DOI: 10.1016/j.enconman.2009.08.006

Aga, V.; Ehrsam, A.; Boschek, E.; Simiano, M. 2013. Adaptation of a direct steam solar tower plant with molten salt storage for optimum value creation under different incentive schemes. Energy Procedia. Vol. 49(2014) P. 1097–1106. DOI: 10.1016/j.egypro.2014.03.119

Alfa Laval. 2015 (a). Alfa Laval Aalborg. Website. Available at: https://www.alfalaval.fi/tietoa-alfa-lavalista/our-company/alfa-laval-suomessa/alfa-laval-aalborg-oy-rauma/ (Accessed: 6.8.2020.)

Alfa Laval. 2015 (b). Aalborg AV-6N Exhaust gas heat recovery boiler. Product leaflet. Available at: https://www.alfalaval.com/globalassets/images/products/heat-transfer/boilers/exhaust-gas-economizer/aalborg-av-6n-heat-recovery-boiler.pdf (Accessed: 6.8.2020.)

Boretti, A.A. 2012. Transient operation of internal combustion engines with Rankine waste heat recovery systems. Applied Thermal Engineering. Vol. 48(2012) P. 18–23. DOI: 10.1016/j.applthermaleng.2012.04.043

Bruch, A.; Fourmigué, J.F.; Couturier, R. 2014. Experimental and numerical investigation of a pilot-scale thermal oil packed bed thermal storage system for CSP power plant. Solar Energy. Vol 105(2014) P. 116–125. DOI: 10.1016/j.solener.2014.03.019

Bruch, A.; Molina, S.; Esence, T.; Fourmigué, J.F.; Couturier, R. 2016. Experimental investigation of cycling behaviour of pilot-scale thermal oil packed-bed thermal storage system. Renewable Energy. Vol. 103(2017) P. 277–285

Cabeza, L.F.; Martorell, I.; Miró, L.; Fernández, A.I.; Barreneche, C. 2015. Introduction to thermal energy storage (TES) systems. In: Cabeza, L.F. (edit.) Advances in Thermal Energy Storage Systems – Methods and Applications. Woodhead Publishing Series in Energy: Number 66. Cambridge, UK: Woodhead Publishing. Ch. 1, P. 1–28. ISBN 978-1-78242-096-5.

Dincer, I.; Ezan, M.A. 2018. Heat Storage: A Unique Solution for Energy Systems. Cham, Switzerland: Springer. Green Energy and Technology. ISBN 978-3-319-91892-1.

Farid, M.M.; Khudhair, A.M.; Razack, A.K.; Al-Hallaj, S. 2003. A review on phase change energy storage: materials and applications. Energy Conversion and Management. Vol. 45(2004). P. 1597–1615. DOI: 10.1016/j.enconman.2003.09.015

Fernández, A.I.; Barreneche, C.; Belusko, M.; Segarra, M.; Bruno, F.; Cabeza, L.F. 2017. Considerations for the use of metal alloys as phase change materials for high temperature applications. Solar Energy Materials and Solar Cells. Vol. 171(2017) P. 275–281. DOI: 10.1016/j.solmat.2017.06.054

Fleischer, A.S. 2015. Thermal Energy Storage Using Phase Change Materials – Fundamentals and Applications. Cham, Switzerland: Springer. Thermal Engineering and Applied Science. ISBN 978-3-319-20922-7. DOI: 10.1007/978-3-319-20922-7

Furbo, S. 2015. Using water for heat storage in thermal energy storage (TES) systems. In: Cabeza, L.F. (edit.) Advances in Thermal Energy Storage Systems – Methods and Applications. Woodhead Publishing Series in Energy: Number 66. Cambridge, UK: Woodhead Publishing. Ch. 2, P. 31–47. ISBN 978-1-78242-096-5. DOI: 10.1533/9781782420965.1.31

Gadd, H.; Werner, S. 2015. Thermal energy storage systems for district heating and cooling. In: Cabeza, L.F. (edit.) Advances in Thermal Energy Storage Systems – Methods and Applications. Woodhead Publishing Series in Energy: Number 66. Cambridge, UK:

Woodhead Publishing. Ch. 18, P. 467–478. ISBN 978-1-78242-096-5. DOI: 10.1533/9781782420965.4.467

Gaggioli, W.; Fabrizi, F.; Fontana, F.; Rinaldi, L.; Tarquini, P. 2013. An innovative concept of a thermal energy storage system based on a single tank configuration using stratifying molten salts as both heat storage medium and heat transfer fluid, and with an integrated steam generator. Energy Procedia. Vol 49(2014) P. 780–789. DOI: 10.1016/j.egypro.2014.03.085

Gaggioli, W.; Fabrizi, F.; Tarquini, P.; Rinaldi, L. 2015. Experimental validation of the innovative thermal energy storage based on an integrated system “storage tank/steam generator”. Energy Procedia. Vol 69(2015) P. 822–831. DOI: 10.1016/j.egypro.2015.03.091

González-Gómez, P.A.; Gómez-Hernández, J.; Briongos, J.V.; Santana D. 2017. Thermo-economic optimization of molten salt steam generators. Energy Conversion and Management. Vol. 146(2017) P. 228–243. DOI: 10.1016/j.enconman.2017.05.027

Grirate, H.; Agalit, H.; Zari, N.; Elmchaouri, A.; Molina, S., Couturier, R. 2016. Experimental and numerical investigation of potential filler materials for thermal oil thermocline storage. Solar Energy. Vol. 131(2016) P. 260–274. DOI: 10.1016/j.solener.2016.02.035

Guillot, S.; Faik, A.; Rakhmatullin, A.; Lambert, J.; Veron, E.; Echegut, P.; Bessada, C.; Calvet, N.; Py, X. 2011. Corrosion effects between molten salts and thermal storage material for concentrated solar power plants. Applied Energy. Vol. 94(2012) P. 174–181. DOI: 10.1016/j.apenergy.2011.12.057

He, C.; Lu, J.; Ding, J.; Wang, W.; Yuan, Y. 2017. Heat transfer and thermal performance of two-stage molten salt steam generation system. Applied Energy. Vol. 204(2017) P. 1231–1239. DOI: 10.1016/j.apenergy.2017.04.010

He, Y.-L.; Zheng, Z.-J.; Du, B.-C.; Wang, K.; Qiu, Y. 2016. Experimental investigation on turbulent heat transfer characteristics of molten salt in a shell-and-tube heat exchanger. Applied Thermal Engineering. Vol. 108(2016) P. 1206–1213. DOI: 10.1016/j.applthermaleng.2016.08.023

Ievers, S.; Lin, W. 2009. Numerical simulation of three-dimensional flow dynamics in a hot water storage tank. Applied Energy. Vol. 86(2009) P. 2604–2614. DOI: 10.1016/j.apenergy.2009.04.010

Incropera, F.P.; DeWitt, D.P.; Bergman, T.L.; Lavine, A.S. 2007. Fundamentals of Heat and Mass Transfer. 6th edition. New York, USA: Wiley. 997 P. ISBN 978-0-471-45728-2.

Jäpölä, Mika. 2020. Personal conversations with M.Sc. and general manager of Technology at Alfa Laval Aalborg Oy.

Laing, D.; Bauer, T.; Breidenbach, N.; Hachmann, B.; Johnson, M. 2012. Development of high temperature phase-change-material storages. Applied Energy. Vol. 109(2013) P. 497–504. DOI: 10.1016/j.apenergy.2012.11.063

Laing, D.; Zunft, S. 2015. Using concrete and other solid storage media in thermal energy storage (TES) systems. In: Cabeza, L.F. (edit.) Advances in Thermal Energy Storage Systems – Methods and Applications. Woodhead Publishing Series in Energy: Number 66. Cambridge, UK: Woodhead Publishing. Ch. 4, P. 65–86. ISBN 978-1-78242-096-5. DOI: 10.1533/9781782420965.1.65

Longeon, M.; Soupart, A.; Fourmigué, J.-F.; Bruch, A.; Marty, P. 2013. Experimental and numerical study of annular PCM storage in the presence of natural convection. Applied Energy. Vol. 112(2013) P. 175–184. DOI: 10.1016/j.apenergy.2013.06.007

Lu, J.; Ding, J.; Yang, J. 2013. Filling dynamics and phase change of molten salt in cold receiver pipe during initial pumping process. International Journal of Heat and Mass Transfer. Vol. 64(2013) P. 98–107. DOI: 10.1016/j.ijheatmasstransfer.2013.04.021

Läiskä, Pekka. 2020. Personal conversations with M.Sc. and general manager of Power business at Alfa Laval Aalborg Oy.

Martin, C.; Bauer, T.; Müller-Steinhagen, H. 2013. An experimental study of a non-eutectic mixture of KNO_3 and $NaNO_3$ with a melting range for thermal energy storage. Applied Thermal Engineering. Vol. 56(2013) P. 159–166. DOI: 10.1016/j.applthermaleng.2013.03.008

Miró, L., Gasia, J., Cabeza, L.F. 2016. Thermal energy storage (TES) for industrial waste heat (IWH) recovery: A review. Applied Energy. Vol. 179(2016) P. 284–301. DOI: 10.1016/j.apenergy.2016.06.147

Molina, S.; Haillot, D.; Deydier, A.; Bedecarrats, J.P. 2018. Material screening and compatibility for thermocline storage systems using thermal oil. Applied Thermal Engineering. Vol. 146(2019) P. 252–259. DOI: 10.1016/j.applthermaleng.2018.09.094

Moore, R.; Vernon, M.; Ho, C.K.; Siegel, N.P.; Kolb, G.J. 2010. Design Considerations for Concentrating Solar Power Tower Systems Employing Molten Salt. Report. Sandia National Laboratories. Albuquerque, New Mexico. SAND2010-6978.

Pandiyarajan, V.; Chinna Pandian*, M.; Malan, E.; Velraj, R.; Seeniraj, R.V. 2010. Experimental investigation on heat recovery from diesel engine exhaust using finned shell and tube heat exchanger and thermal storage system. Applied Energy. Vol. 88(2011) P. 77–87. DOI: 10.1016/j.apenergy.2010.07.023

Pandiyarajan, V.; Chinnappandian*, M.; Raghavan, V.; Velraj, R. 2011. Second law analysis of a diesel engine waste heat recovery with a combined sensible and latent heat

storage system. Energy Policy. Vol. 39(2011) P. 6011–6020. DOI: 10.1016/j.enpol.2011.06.065

Pereira da Cunha, J.; Eames, P. 2016. Thermal energy storage for low and medium temperature applications using phase change materials – A review. Applied Energy. Vol. 177(2016) P. 227–238. DOI: 10.1016/j.apenergy.2016.05.097

Sabharwall, P.; Clark, D.; Glazoff, M.; Zheng, G.; Sridharan, K.; Anderson, M. 2014. Advanced heat exchanger development for molten salts. Nuclear Engineering and Design. Vol. 280(2014) P. 42–56. DOI: 10.1016/j.nucengdes.2014.09.026

Sala, J.M. 2015. Thermal energy storage (TES) systems for cogeneration and trigeneration systems. In: Cabeza, L.F. (edit.) Advances in Thermal Energy Storage Systems – Methods and Applications. Woodhead Publishing Series in Energy: Number 66. Cambridge, UK: Woodhead Publishing. Ch. 20, P. 493–509. ISBN 978-1-78242-096-5. DOI: 10.1533/9781782420965.4.493

Salunkhe, P.B.; Shembekar, P.S. 2012. A review on effect of phase change material encapsulation on the thermal performance of a system. Renewable and Sustainable Energy Reviews. Vol. 16(2012) P. 5603–5616. DOI: 10.1016/j.rser.2012.05.037

Shu, G.; Zhao, M.; Tian, H.; Wei, H.; Liang, X.; Huo, Y.; Zhu, W. 2016. Experimental investigation on thermal OS/ORC (Oil Storage/Organic Rankine Cycle) system for waste heat recovery from diesel engine. Energy. Vol. 107(2016) P. 693–706. DOI: 10.1016/j.energy.2016.04.062

Stadler, I.; Hauer, A.; Bauer, T. 2019. Thermal Energy Storage. In: Sterner, M.; Stadler, I. (edit.) Handbook of Energy Storage. Transl. of 2nd edition. Berlin, Germany: Springer. Ch. 10, p. 563-609. ISBN 978-3-662-55504-0.

Sterner, M. 2019. Energy Storage Through the Ages. In: Sterner, M.; Stadler, I. (edit.) Handbook of Energy Storage. Transl. of 2nd edition. Berlin, Germany: Springer. Ch. 1, P. 1–22. ISBN 978-3-662-55504-0.

Sterner, M. and Bauer, F. 2019 (a). Definition and Classification of Energy Storage Systems. In: Sterner, M.; Stadler, I. (edit.) Handbook of Energy Storage. Transl. of 2nd edition. Berlin, Germany: Springer. Ch. 2, P. 23–47. ISBN 978-3-662-55504-0.

Sterner, M.; Breuer, C.; Drees, T.; Eckert, F.; Maaz, A.; Pape, C.; Rotering, N.; Thema, M. 2019 (b). Storage Demand in Power Supply. In: Sterner, M.; Stadler, I. (edit.) Handbook of Energy Storage. Transl. of 2nd edition. Berlin, Germany: Springer. Ch. 3, P. 51–136. ISBN 978-3-662-55504-0.

Sterner, M.; Eckert, F.; Gerhardt, N.; Henning, H.-M.; Palzer, A. 2019 (c). Heating Supply Storage Requirements. In: Sterner, M.; Stadler, I. (edit.) Handbook of Energy Storage. Transl. of 2nd edition. Berlin, Germany: Springer. Ch. 4, P. 137–163. ISBN 978-3-662-55504-0.

Sterner, M.; Bauer, F.; Crotogino, F.; Eckert, F.; von Olshausen, C.; Teichmann, D.; Thema, M. 2019 (d). Chemical Energy Storage. In: Sterner, M.; Stadler, I. (edit.) Handbook of Energy Storage. Transl. of 2nd edition. Berlin, Germany: Springer. Ch. 8, P. 325–482. ISBN 978-3-662-55504-0.

Sterner, M.; Thema, M. 2019 (e). Comparison of Storage Systems. In: Sterner, M.; Stadler, I. (edit.) Handbook of Energy Storage. Transl. of 2nd edition. Berlin, Germany: Springer. Ch. 12, P. 637–672. ISBN 978-3-662-55504-0.

Sterner, M.; Stadler, I.; Eckert, F.; Thema, M. 2019 (f). Storage Integration in Individual Energy Sectors. In: Sterner, M.; Stadler, I. (edit.) Handbook of Energy Storage. Transl. of 2nd edition. Berlin, Germany: Springer. Ch. 13, P. 675–755. ISBN 978-3-662-55504-0.

Sterner, M.; Stadler, I.; Eckert, F.; Gerhardt, N.; von Olshausen, C.; Thema, M.; Trost, T. 2019 (g). Storage Integration for Coupling Different Energy Sectors. In: Sterner, M.; Stadler, I. (edit.) Handbook of Energy Storage. Transl. of 2nd edition. Berlin, Germany: Springer. Ch. 14, P. 757–803. ISBN 978-3-662-55504-0.

Stevanovic, V.D.; Petrovic, M.M.; Milivojevic, S.; Ilic, M. 2020. Upgrade of the thermal power plant flexibility by the steam accumulator. Energy Conversion and Management. Vol. 223(2020) Article 113271. DOI: 10.1016/j.enconman.2020.113271

Strasser, M.N.; Selvam, R.P. 2014. A cost and performance comparison of packed bed and structured thermocline thermal energy storage systems. Solar Energy. Vol. 108(2014) P. 390–402. DOI: 10.1016/j.solener.2014.07.023

Sun, W.; Hong, Y.; Wang, Y. 2016. Operation Optimization of Steam Accumulators as Thermal Energy Storage and Buffer Units. Energies. Vol. 10(2017):1 Article 17. ISSN 1996-1073. DOI: 10.3390/en10010017

Takasuo, Matti. 2020. Personal conversations with M.Sc. and general manager of Offshore business at Alfa Laval Singapore Pte Ltd.

Therminol. Therminol 55 product information and technical data sheets. Available at: https://www.therminol.com/product/71093433; https://productcatalog.eastman.com/tds/ProdDatasheet.aspx?product=71093433; https://www.eastman.com/Literature_Center/T/TF8994.pdf (Accessed: 26.4.2021.)

Therminol. Therminol 66 product information and technical data sheets. Available at: https://www.therminol.com/product/71093438; https://productcatalog.eastman.com/tds/ProdDatasheet.aspx?product=71093438; https://www.eastman.com/Literature_Center/T/TF8695.pdf (Accessed: 26.4.2021.)

Therminol. Therminol VP-1 product information and technical data sheets. Available at: https://www.therminol.com/product/71093459;

https://productcatalog.eastman.com/tds/ProdDatasheet.aspx?product=71093459; https://www.eastman.com/Literature_Center/T/TF9141.pdf (Accessed: 26.4.2021.)

Ushak, S.; Fernández, A. G.; Grageda, M. 2015. Using molten salts and other liquid sensible storage media in thermal energy storage (TES) systems. In: Cabeza, L.F. (edit.) Advances in Thermal Energy Storage Systems – Methods and Applications. Woodhead Publishing Series in Energy: Number 66. Cambridge, UK: Woodhead Publishing. Ch. 3, P. 49–63. ISBN 978-1-78242-096-5.

Vignarooban, K.; Xu, X.; Arvay, A.; Hsu, K. Kannan, A.M. 2015. Heat transfer fluids for concentrating solar power systems – A review. Applied Energy. Vol. 146(2015) P. 383–396. DOI: 10.1016/j.apenergy.2015.01.125

Wu, M.; Xu, C.; He, Y. 2015. Cyclic behaviors of the molten-salt packed-bed thermal storage system filled with cascaded phase change material capsules. Applied Thermal Engineering. Vol. 93(2016) P. 1061–1073. DOI: 10.1016/j.applthermaleng.2015.10.014

Wärtsilä Oy. 2020. (a) UK Energy Storage: How is energy storage making more money in 2020 than before? Webinar. Available at: https://www.wartsila.com/energy/learn-more/downloads/webinar/uk-energy-storage-live-session (Accessed: 22.5.2020.)

Wärtsilä Oy. 2020. (b) The lessons of Covid-19 pandemic for the European electricity market. Article. 7.7.2020. Available at: https://www.wartsila.com/energy/transition-lab/weekly-updates/07072020 (Accessed: 3.8.2020.)

Wärtsilä Oy. 2020. (c) A new normal for the energy industry. Article. 16.7.2020. Available at: https://www.wartsila.com/energy/transition-lab/weekly-updates/16072020 (Accessed: 3.8.2020.)

Xiao, P.; Guo, L.; Zhang, X. 2014. Investigations on heat transfer characteristic of molten salt flow in helical annular duct. Applied Thermal Engineering. Vol. 88(2015) P. 22-32. DOI: 10.1016/j.applthermaleng.2014.09.021

Xu, C.; Wang, Z.; He, Y.; Li, X.; Bai, F. 2012. Parametric study and standby behavior of a packed-bed molten salt thermocline thermal storage system. Renewable Energy. Vol. 48(2012) P. 1–9. DOI: 10.1016/j.renene.2012.04.017

Yuan, Y.; He, C.; Lu, J.; Ding, J. 2016. Thermal performances of molten salt steam generator. Applied Thermal Engineering. Vol. 105(2016) P. 163–169. DOI: 10.1016/j.applthermaleng.2016.03.080

Zanganeh, G.; Pedretti, A.; Haselbacher, A.; Steinfeld, A. 2014. Design of packed bed thermal energy storage systems for high-temperature industrial process heat. Applied Energy. Vol. 137(2015) P. 812–822. DOI: 10.1016/j.apenergy.2014.07.110

Zavattoni, S.A.; Barbato, M.C.; Pedretti, A.; Zanganeh, G.; Steinfeld, A. 2014. High temperature rock-bed TES system suitable for industrial-scale CSP plant – CFD analysis under charge/discharge cyclic conditions. Energy Procedia Vol. 46(2014) P. 124–133. DOI: 10.1016/j.egypro.2014.01.165

APPENDIX I - CALCULATION OF THERMAL PROPERTIES

Available data of material properties is often incomplete and needs to be expanded upon. In material property tables of this work mainly values of volumetric heat capacities and energy densities are calculated for certain materials where they have been possible to calculate and have been viewed relevant to find out.

Volumetric heat capacity is easy to calculate by multiplying the specific heat capacity of a material with its density. As an example, assuming common values of a density of 1800 kg/m^3 and a specific heat capacity of 1,5 kJ/kgK, the volumetric heat capacity of solar salt would be

$$C_{\mathrm{vol}} = 1800\,\frac{\mathrm{kg}}{\mathrm{m^3}} \cdot 1.5\,\frac{\mathrm{kJ}}{\mathrm{kgK}} = 2700\,\frac{\mathrm{kJ}}{\mathrm{m^3 K}}.$$

For the energy density of a sensible heat storage, the applicable temperature range must be chosen. This temperature is constrained by the viable temperature range of the storage material, but also depends on the charging and discharging temperatures of the energy system that the storage is linked to. As an example, solar salt has a freezing point of around 220 °C and a thermal stability maximum temperature of around 565 °C (sometimes up to 600 °C). Its usable temperature range might then be, for example, 290-540 °C to leave a safety factor in both ends of the range. Energy density of solar salt can then be calculated by combining equations (10) and (11) as explained in chapter 3.1:

$$Q_{\mathrm{vol}} = 1800\,\frac{\mathrm{kg}}{\mathrm{m^3}} \cdot 1.5\,\frac{\mathrm{kJ}}{\mathrm{kgK}} \cdot (540 - 290)\mathrm{K} = 675\,\frac{\mathrm{MJ}}{\mathrm{m^3}} = 187{,}5\,\frac{\mathrm{kWh}}{\mathrm{m^3}}.$$

The energy density value of 187.5 kWh/m^3 at a temperature range of 250 K is close to the value 200 kWh/m^3 reported by Stadler et al. (Stadler et al. 2019, 587; Gaggioli et al. 2013, 786-787)

In a similar fashion, the volumetric latent heat of a material can be calculated by multiplying its latent heat value by its density. If the density of the material changes by a

significant margin in phase change, it might be good practice to use the lower of the values in calculating the volumetric latent heat in order to not be misleading about the practical energy density of the material. For example, $NaNO_3$ has a latent heat value of around 175 kJ/kg and a density of around 2150 in solid phase and 1900 in liquid phase. Calculating the volumetric latent heat using the density in solid phase would yield

$$175\,\frac{\mathrm{kJ}}{\mathrm{kg}} \cdot 2150\,\frac{\mathrm{kg}}{\mathrm{m}^3} = 376\,\frac{\mathrm{kJ}}{\mathrm{m}^3},$$

while calculating it using the density in liquid phase would result in

$$175\,\frac{\mathrm{kJ}}{\mathrm{kg}} \cdot 1900\,\frac{\mathrm{kg}}{\mathrm{m}^3} = 332\,\frac{\mathrm{kJ}}{\mathrm{m}^3}.$$

As can be seen, calculating the volumetric latent heat of $NaNO_3$ using the density in solid phase would imply that a smaller storage vessel is sufficient to hold the necessary amount of PCM than is required in reality.

The energy density of PCM storage can be increased by adding a factor of sensible heat to the latent heat capacity. In this case the energy content in equation (10) would be calculated using equation (12). However, in this thesis it is assumed that energy content of PCM consists only of the latent heat portion unless otherwise specified in a source. As such, energy density values of latent heat storages are not calculated separately as they would be consistent with volumetric latent heat values listed. The exceptions to this rule are the few PCMs that change phase over a range of temperatures rather than at a consistent phase change temperature.

APPENDIX II - TABLE OF SENSIBLE HEAT TES MATERIALS

The data on this table should be treated as estimates, as there is some variance in the data and its accuracy between different sources, and actual properties may vary due to precise composition, manufacturing method and so forth. Calculated, interpolated, estimated or otherwise unsure values are bolded. Note that decimal separator used in this table is comma (,) instead of period (.).

Type	Material	Limiting temp	Common temp	Density	Specific heat capacity	Volumetric heat capacity	Energy density	Conductivity	Source
		℃	℃	kg/m^3	kJ/kgK	kJ/m^{3}K	kWh/m^3	W/mK	
	Water	0-100	20-90	960-1000	4,18-4,21	4050-4200	23-93	0,58-0,68	Stadler et al. 2019, 575; Dincer et al. 2018, 22; Sterner 2019a, 40; Cabeza et al. 2015, 6; Furbo 2015, 32
	Gravel-water fill	0-100		2200	1,32	2904	40		Stadler et al. 2019, 575
Mineral/solid	Basalt			2210-2770	0,80-0,90	1750-2500		2,0	Grirate et al. 2016, 263
Mineral/solid	Basalt (Moroccan)			3020	1,193	3000-3850		2,0-2,2	Grirate et al. 2016, 268-270
Mineral/solid	Brick	0-1000		1400-1900	0,80-0,84	1176-1510	**150**	0,5-5,0	Stadler et al. 2019, 575; Laing et al. 2015, 67; Cabeza et al. 2015, 6; Furbo 2015, 32; Dincer et al. 2018, 22
Mineral/solid	Brick (fire clay)	0-1450		2050-2645	0,96			1,0-1,8	Incropera et al. 2007, 939
Mineral/solid	Brick (magnesite)	0-1200			1,13			1,9-5,0	Incropera et al. 2007, 939
Mineral/solid	Brick (silica)			2340	0,86-1,13	**2019-2637**		1,5-2,1	Laing et al. 2015, 67; Dincer et al. 2018, 22
Mineral/solid	Ceramics			3500	0,87			1,35	Cabeza et al. 2015, 7
Mineral/solid	Cipolin			2610-2870	0,80-1,47	1680-2520		3,2	Grirate et al. 2016, 263
Mineral/solid	Cipolin (Moroccan)			2800	1,14	2600-3600		1,6	Grirate et al. 2016, 268-270
Mineral/solid	Clay			1450-1458	0,88	1280		1,3	Cabeza et al. 2015, 6; Laing et al. 2015, 67; Incropera et al. 2007, 939; Dincer et al. 2018, 61
Mineral/solid	Cofalite			3120	0,80-1,03			1,4-2,1	Cabeza et al. 2015, 7
Mineral/solid	Concrete	0-500		1900-2300	0,75-1,01	1672-2100	**125**	1,2-2,0	Stadler et al. 2019, 575; Strasser et al. 2014, 398; Laing et al. 2015, 67; Dincer et al. 2018, 22; 61
Mineral/solid	Concrete (high temperature)			2750	0,92			1	Cabeza et al. 2015, 7
Mineral/solid	Gabbro			2911	0,62-0,67	**1805-1950**		1,97-2,13	Dincer et al. 2018, 70
Mineral/solid	Glass			2710	0,80-0,84	2200-2270			Cabeza et al. 2015, 6; Furbo 2015, 32; Dincer et al. 2018, 61
Mineral/solid	Granite	0-800		2530-2750	0,75-0,89	2060-**2400**	**170-200**	2,2-2,9	Stadler et al. 2019, 575; Laing et al. 2015, 67; Incropera et al. 2007, 940; Grirate et al. 2016, 263
Mineral/solid	Granite (Moroccan)	0-375	X-200	2820	1,11	2300-3200	**150**	3,0-3,7	Grirate et al. 2016, 267-270
Mineral/solid	Gravelly earth			2050	1,84	3770			Cabeza et al. 2015, 6; Dincer et al. 2018, 61
Mineral/solid	Hornfels			2400-2800	0,7-0,9	2560-2880		1,5	Grirate et al. 2016, 263
Mineral/solid	Hornfels (Moroccan)			2740	1,04	2400-3400		5-6,5	Grirate et al. 2016, 267-270
Mineral/solid	Limestone			2320-2700	0,67-0,81	**1800-1880**		2,2-2,9	Dincer et al. 2018, 70; Laing et al. 2015, 67; Incropera et al. 2007, 940; Strasser et al. 2014, 398
Mineral/solid	Limestone (silicious)			2776	0,65-0,68	**1815-1900**		3,4-3,8	Dincer et al. 2018, 70
Mineral/solid	Magmatic rock			3023	0,838-1,118	**2533-3380**		1,9-2,45	Laing et al. 2015, 67
Mineral/solid	Magnetite			5177	0,75-0,80	3890-4100			Cabeza et al. 2015, 6; Furbo 2015, 32; Dincer et al. 2018, 61
Mineral/solid	Marble	0-325	X-200	2610-2680	0,83-1,470	1680-2520		2,9	Incropera et al. 2007, 940; Grirate et al. 2016, 263

Mineral/solid	Marble (Moroccan)			2680	1,128	2300-3320		2,0-2,8	Grirate et al. 2016, 267-270
Mineral/solid	Quartzite			2510-2860	0,61-1,0	**1605-2660**		5,3-7,7	Dincer et al. 2018, 70; Incropera et al. 2007, 940; Grirate et al. 2016, 263
Mineral/solid	Quartzite (Moroccan)			2570	1,185	2100-3300		3,0-5,5	Grirate et al. 2016, 268-270
Mineral/solid	Rock (unspecified)			2735	0,65-1,1	**1778-3000**		0,5-5,0	Zanganeh et al. 2014, 815; Grirate et al. 2016, 269
Mineral/solid	Sand, gravel	0-800		1454-2000	0,71-1,2	1200-1420		0,25-1,0	Stadler et al. 2019, 575; Laing et al. 2015, 67; Incropera et al. 2007, 940; Dincer et al. 2018, 22; Furbo 2015, 32
Mineral/solid	Sandstone			2200-2661	0,62-0,71	1570		4,21-4,51	Cabeza et al. 2015, 6; Dincer et al. 2018, 61; 70
Mineral/solid	Silica gravel			2500	0,90	**2250**		0,10	Bruch et al. 2014, 123
Mineral/solid	Slag (mineral waste)			2700	0,84	**2268**		0,57	Laing et al. 2015, 67
Thermal oil	Mineral oils	-20 - 300	200-300	770	2,60	**2002**	55-**83**	0,10-0,12	Ushak et al. 2015, 51; Dincer et al. 2018, 22; Vignarooban et al. 2015, 387
Thermal oil	Mineral oil (Xceltherm 600)	0-315			2,44			0,10	Vignarooban et al. 2015, 387
Thermal oil	Silicone oils	-20 - 400	300-400	900	2,10	**1890**	52-**79**	0,10	Ushak et al. 2015, 51; Dincer et al. 2018, 22; Vignarooban et al. 2015, 387
Thermal oil	Synthetic oils	-20 - 350	250-350	900	2,3	**2070**	57-**86**	0,10-0,11	Ushak et al. 2015, 51; Dincer et al. 2018, 22; Vignarooban et al. 2015, 387
Thermal oil	Synthetic oil (Biphenyl/Diphenyl oxide)	12-393			1,93			0,10	Vignarooban et al. 2015, 387
Thermal oil	Synthetic oil (Therminol VP-1)	12-400		700-1070	1,53-2,63	**1640-1850**	**73**	0,075-0,136	Therminol
Thermal oil	Synthetic oil (Therminol 55)	-28 - 315	X-300	670-900	1,8-2,9	**1620-1940**	**75**	0,095-0,13	Therminol
Thermal oil	Synthetic oil (YD-350)	0-350		850-1020	1,70-2,42	**1750-2050**	**80**	0,10-0,135	He et al. 2016, 1209
Thermal oil	Thermal oils	0-400		766-1020	1,5-2,55	1360-1700	**75**	0,10-0,12	Stadler et al. 2019, 575; Bruch et al. 2014, 117; 123; Furbo 2015, 32
Thermal oil	Thermal oil (Therminol 66)	-3 - 359	X-345	770-1020	1,5-1,75	**1530-2110**	**75**	0,09-0,12	Therminol
Molten salt	Nitrate salt (Solar salt)	220-600	290-550	1720-1900	1,1-1,5	2700	188-200	0,5-0,55	Stadler et al. 2019, 587; Vignarooban et al. 2015, 387; Strasser et al. 2014, 395; 398; Guillot et al. 2011, 175; Gaggioli et al. 2013, 780-782; 786-787
Molten salt	Nitrate salt (HITEC)	140-550	200-450	1680-2000	1,5-2,0	**2460-3000**	**190**	0,25-0,63	Ushak et al. 2015, 50; Vignarooban et al. 2015, 387; Guillot et al. 2011, 175; He et al. 2016, 1209; He et al. 2017, 1234; Yuan et al. 2016, 165; Xiao et al. 2014, 23
Molten salt	Nitrate salt (HITEC XL)	120-500			1,45			0,52	Vignarooban et al. 2015, 387
Molten salt	Nitrate salt (14%NaNO3-50%KNO3-18%LiNO3-18%NaNO2)	99-500			1,66				Ushak et al. 2015, 57; Vignarooban et al. 2015, 387
Molten salt	Nitrate salt (15%NaNO3-43%KNO3-42%Ca(NO3)2)	140-460							Ushak et al. 2015, 57
Molten salt	Nitrate salt (16%NaNO3-48%KNO3-36%Ca(NO3)2)	134-500							Ushak et al. 2015, 57
Molten salt	Nitrate salt (18%NaNO3-52%KNO3-30%LiNO3)	120-550							Ushak et al. 2015, 57
Molten salt	Nitrate salt (18%NaNO3-70%KNO3-12%LiNO3)	200-550							Ushak et al. 2015, 57

Molten salt	Nitrate salt (20%NaNO3-54%KNO3-26%LiNO3)	116-435							Ushak et al. 2015, 57
Molten salt	Nitrate salt (24%NaNO3-46%KNO3-30%Ca(NO3)2)	160-480							Ushak et al. 2015, 57
Molten salt	Nitrate salt (28%NaNO3-52%KNO3-20%LiNO3)	130-600			1,091				Vignarooban et al. 2015, 387; Ushak et al. 2015, 57
Molten salt	Nitrate salt (33%NaNO3-40%KNO3-27%LiNO3)	160-550							Ushak et al. 2015, 57
Molten salt	Nitrate salt (34%NaNO3-50%KNO3-16%Ca(NO3)2)	190-500							Ushak et al. 2015, 57
Molten salt	Nitrate salt (6%NaNO3-23%KNO3-8%LiNO3-19%Ca(NO3)2)-44%CsNO3) (Halotechnics SS-500)	65-500			1,22				Vignarooban et al. 2015, 387
Molten salt	Nitrate salt (NaNO3-KNO3-LiNO3-Ca(NO3)2) (Sandia Mix)	95-500			1,16-1,44			0,654	Vignarooban et al. 2015, 387
Molten salt	Nitrate salt (KNO3-LiNO3-Ca(NO3)2)	80-500						0,43	Vignarooban et al. 2015, 387
Molten salt	Carbonate salts	450-850		2100	1,8	**3780**	430	2	Ushak et al. 2015, 51; Dincer et al. 2018, 22
Molten salt	Carbonate salt (33%Na2CO3-35%K2CO3-32%Li2CO3)	400-850	400-800		1,4-1,5				Vignarooban et al. 2015, 387
Molten salt	Carbonate/fluoride salts (Li-Na-K)	400-900						1,17	Vignarooban et al. 2015, 387
Molten salt	Chloride salt (7%NaCl-24%KCl-69%ZnCl)	204-850			0,81			0,325	Vignarooban et al. 2015, 388
Metal	Aluminium			2710	0,8-1,15	2430-2500		204-238	Cabeza et al. 2015, 6; Dincer et al. 2018, 61; Laing et al. 2015, 67; Furbo 2015, 32; Incropera et al. 2007, 929; Grirate et al. 2016, 269
Metal	Bismuth (Bi) (liquid)	271-1670		9500-10000	0,144-0,165	**1500**	**165,7**	16,3	Ushak et al. 2015, 59; Incropera et al. 2007, 951
Metal	Copper			8300-8933	0,38-0,48	3500		340-401	Laing et al. 2015, 67; Incropera et al. 2007, 929; Furbo 2015, 32
Metal	Gallium (Ga) (liquid)	30-2237		6090	0,36	**2192**	**243,6**	50	Ushak et al. 2015, 59
Metal	Gold			19300	0,1-0,13	2500		255-317	Furbo 2015, 32; Incropera et al. 2007, 930
Metal	Indium (In) (liquid)	157-2072		6670	0,24	**1601**	**177,9**	47,2	Ushak et al. 2015, 59
Metal	Iron	0-800		7850-7900	0,4-0,6	3570-**3700**	**400**	32-80	Stadler et al. 2019, 575; Dincer et al. 2018, 22; 61; Laing et al. 2015, 67; Cabeza et al. 2015, 6; Incropera et al. 2007, 930
Metal	Kalium (K) (liquid)	64-766		705	0,76	**536**	**59,5**	34,9	Ushak et al. 2015, 59

Metal	Lead (Pb) (liquid)	327-1743		**10320**	0,15	**1548**	**172,0**	14,9-18,8	Ushak et al. 2015, 59; Incropera et al. 2007, 951
Metal	Lithium (Li) (liquid)	180-1342		475	4,16	**1976**	**219,6**	49,7	Ushak et al. 2015, 59
Metal	Metal eutectic (56%Bi-44%Pb) (liquid)	125-1533		9660	0,15	**1449**	**161,0**	12,8	Ushak et al. 2015, 59; Vignarooban et al. 2015, 388; Incropera et al. 2007, 951
Metal	Metal eutectic (78%K-22%Na) (liquid)	-12 - 785		750	0,87	**653**	**72,5**	26,2	Ushak et al. 2015, 59; Vignarooban et al. 2015, 388; Incropera et al. 2007, 951
Metal	Sodium (Na) (liquid)	98-883	270-530	800-1200	1,25-1,35	750-**1100**	80	46-86	Stadler et al. 2019, 575; Ushak et al. 2015, 51; Vignarooban et al. 2015, 388; Incropera et al. 2007, 951; Dincer et al. 2018, 22; 59
Metal	Steel			7840-8030	0,44-1,1	3600-3680		16,3-50,0	Cabeza et al. 2015, 6; Dincer et al. 2018, 22; 61; Furbo 2015, 32; Lu et al. 2013, 101; Incropera et al. 2007, 930; Grirate et al. 2016, 269
Metal	Stainless steel			7930-8050	0,48-0,6	3900		15-25	Furbo 2015, 32; Incropera et al. 2007, 931; He et al. 2017, 1234
Metal	Tin (Sn) (liquid)	232-2687		6330	0,24	**1519**	**168,8**	33,8	Ushak et al. 2015, 59
Others	Sodium Chloride (NaCl)			2165	0,86	**1862**		6,5-7,0	
Other	Wood			700	1,80-2,39	900-1670			Cabeza et al. 2015, 6; Dincer et al. 2018, 61; Furbo 2015, 32

APPENDIX III - TABLE OF LATENT HEAT TES MATERIALS

The data on this table should be treated as estimates, as there is some variance in the data and its accuracy between different sources, and actual properties may vary due to precise composition, manufacturing method and so forth. Calculated, interpolated, estimated or otherwise unsure values are bolded. Calculated energy densities only take energy bound in phase change into account, capacity can in some cases be increased by additional sensible heating. In salt hydrates, "w" refers to hydrate number, e.g., “CaCl2 6w” means $CaCl_2 \cdot 6H2O$, Calcium chloride hexahydrate. Note that decimal separator used in this table is comma (,) instead of period (.).

Type	Material	Phase change temperature	Density	Latent heat	Volumetric latent heat	Specific heat capacity	Energy density	Conductivity	Source
		℃	kg/m3	kJ/kg	MJ/m3	kJ/kgK	kWh/m3	W/mK	
	Water (ice)	0	920 (s) – 1000 (l)	334	**310**-330	3,3 (s) - 4,2 (l)	109	0,6-1,6	Pereira da Cunha et al. 2016, 230; Stadler et al. 2019, 575, 594; Cabeza et al. 2015, 7
Organic	Acetamide	82	1160 (s)	260	**302**	2 (s) - 3 (l)	93	0,25-0,4	Pereira da Cunha et al. 2016, 230
Organic	Acetic acid	17	1214 (s)	192	**233**	1,33 (s) – 2,04 (l)	71	0,19-0,26	Pereira da Cunha et al. 2016, 230
Organic	Adipic acid	152	1360 (s)	275	**374**	1,87 (s) – 2,72 (l)	109		Pereira da Cunha et al. 2016, 230
Organic	Alcohols	20-450			200-450		120		Cabeza et al. 2015, 7; Ushak et al. 2015, 58
Organic	Capric acid	32	1004 (s) – 878 (l)	153	**134**	1,95 (s) – 1,72 (l)		0,153	Fleischer 2015, 41
Organic	d-Mannitol	165	1490 (s)	300	**447**	1,31 (s) – 2,36 (l)	139	0,11-0,19	Pereira da Cunha et al. 2016, 230
Organic	Erythritol	117-120	1450 (s) – 1300 (l)	340	**442-490**	2,25 (s) – 2,61 (l)	130-148	0,32-0,73	Pereira da Cunha et al. 2016, 230; Stadler et al. 2019, 595; Ushak et al. 2015, 58
Organic	Formic acid	8	1227 (s)	277	**340**	1 (s) – 1,17 (l)	96	0,27-0,3	Pereira da Cunha et al. 2016, 230
Organic	HDPE (high density polyethylene)	130	952 (s)	255	**243**	2,6 (s) – 2,15 (l)	80	0,44-0,48	Pereira da Cunha et al. 2016, 230
Organic	Heneicosane	41	773 (l)	294,9	**228**	2,386 (l)		0,145	Fleischer 2015, 41
Organic	Hydroquinone	172	1300 (s)	258	**335**	1,59 (s) – 1,64 (l)	105		Pereira da Cunha et al. 2016, 230
Organic	Lauric acid	44	1007 (s) – 870-965 (l)	178-212	**155-213**	1,76-2,02 (s) - 2,15-2,27 (l)	66	0,15-0,22	Pereira da Cunha et al. 2016, 230; Fleischer 2015, 41; Stadler et al. 2019, 595
Organic	Maleic acid	141	1590 (s)	385	**612**	1,17 (s) – 2,08 (l)	184		Pereira da Cunha et al. 2016, 230
Organic	Myristic acid	58	861 (l)	186	**160**				Stadler et al. 2019, 595
Organic	Octadecane	29	814 (s) – 724-777 (l)	244	**177-190**	2,15 (s) – 2,18 (l)		0,15-0,36	Fleischer 2015, 41; Stadler et al. 2019, 595
Organic	Oleic acid	13	871 (l)	75,5	**66**	1,744 (l)		0,103	Fleischer 2015, 41
Organic	Oxalic acid	105	1900 (s)	356	**676**	1,62 (s) – 2,73 (l)	211		Pereira da Cunha et al. 2016, 230
Organic	Palmitic acid	61-64	989 (s) – 850 (l)	185-222	**157-220**	1,69-2,2 (s) - 2,2-2,48 (l)	67	0,16-0,21	Fleischer 2015, 41; Pereira da Cunha et al. 2016, 230
Organic	Paraffins	-20 - 100	880-950 (s)	150-250	150-250	3 (s) - 2 (l)	50-70	0,2	Pereira da Cunha et al. 2016, 230; Cabeza et al. 2015, 7
Organic	Phthalic anhydride	131	1530 (s)	160	**245**	1,85 (s) - 2,2 (l)	85		Pereira da Cunha et al. 2016, 230
Organic	Polyethylene	130					50		Ushak et al. 2015, 58
Organic	Stearic acid	54-69	940-965 (s) - 848 (l)	157-202	**148-171**	1,76-2,83 (s) - 2,27-2,38 (l)	49	0,17-0,29	Pereira da Cunha et al. 2016, 230; Fleischer 2015, 41
Organic	Tricosane	48,4	777,6 (l)	302,5	**235**	2,181 (l)		0,124	Fleischer 2015, 41

APPENDIX III, 2

Organic	Tetracosane	51,5	773,6 (l)	207,7	**161**	2,924 (l)		0,137	Fleischer 2015, 41
Organic	Urea	134	1320 (s)	250	**330**	1,8 (s) - 2,11 (l)	97	0,6-0,8	Pereira da Cunha et al. 2016, 230
Organic	2-Chlorobenzoic acid	142	1544 (s)	164	**253**	1,3 (s) - 1,6 (l)	83		Pereira da Cunha et al. 2016, 230
Organic	Stearic acid (36%) – Palmitic acid (64%)	53	971 (s)	182	**177**	1,72 (s) – 2,23 (l)	46	**0,169-0,234**	Pereira da Cunha et al. 2016, 231
Salt	Nitrates	120-300			200-700				Cabeza et al. 2015, 7; Stadler et al. 2019, 593
Salt	Carbonates	400-900			600-1100				Cabeza et al. 2015, 7; Stadler et al. 2019, 593
Salt	Chlorides	350-800			550-900				Cabeza et al. 2015, 7; Stadler et al. 2019, 594
Salt	Fluorides	700-1000			1000+				Cabeza et al. 2015, 7; Stadler et al. 2019, 595
Salt	Hydroxides	150-450			500-700				Cabeza et al. 2015, 7; Stadler et al. 2019, 596
Salt	CaCl2	770					145		Ushak et al. 2015, 58
Salt	K2CO3	900					100		Ushak et al. 2015, 58
Salt	KCl	765					150		Ushak et al. 2015, 58
Salt	KF	857	2370 (s)	452	**1071**		280		Fleischer 2015, 44; Ushak et al. 2015, 58
Salt	KNO3	333	2110 (s) – 1900 (l)	266	**505-561**		60	0,5	Fleischer 2015, 44; Stadler et al. 2019, 594; Ushak et al. 2015, 58
Salt	KOH	360					90		Ushak et al. 2015, 58
Salt	Li2CO3	720					290		Ushak et al. 2015, 58
Salt	LiCl	620					200		Ushak et al. 2015, 58
Salt	LiF	845					530		Ushak et al. 2015, 58
Salt	LiNO3	254	1800 (l)	360	**648**		180	0,6	Stadler et al. 2019, 594; Ushak et al. 2015, 58
Salt	LiOH	460					330		Ushak et al. 2015, 58
Salt	MgCl2	714	2140 (s)	452	**967**		205		Fleischer 2015, 44; Ushak et al. 2015, 58
Salt	Na2CO3	850					150		Ushak et al. 2015, 58
Salt	Na2SO4	884	2680 (s)	167	**448**				Guillot et al. 2011, 176-177
Salt	NaCl	802	2160 (s)	492	**1063**		200	5	Fleischer 2015, 44; Ushak et al. 2015, 58
Salt	NaNO2	280					110		Ushak et al. 2015, 58
Salt	NaNO3	305-307	2110-2260 (s) - 1900-1908 (l)	172-178	**327-389**		100	0,5-0,6	Fleischer 2015, 44; Stadler et al. 2019, 594; Laing et al. 2012, 501; Ushak et al. 2015, 58
Salt	NaOH	325					80		Ushak et al. 2015, 58
Salt hydrate	Salt hydrates	-20 - 80			200-600				Cabeza et al. 2015, 7; Stadler et al. 2019, 593
Salt hydrate	Ba(OH)2 8w	78	2180 (s)	280	**610**	1,34 (s) – 2,44 (l)	171	0,66-1,26	Pereira da Cunha et al. 2016, 230
Salt hydrate	CaCl2 6w	29	1710-1802 (s) - 1562 (l)	125-192	**214-281**	1,42 (s) - 2,2 (l)	64	0,53-1,1	Pereira da Cunha et al. 2016, 230; Fleischer 2015, 44; Stadler et al. 2019, 594
Salt hydrate	Mg(NO3)2 6w	89	1640 (s)	140-149	**230**	2,5 (s) - 3,1 (l)	74	0,49-0,65	Pereira da Cunha et al. 2016, 230; Stadler et al. 2019, 594
Salt hydrate	MgCl2 6w	117	1569 (s) – 1450 (l)	150-169	**236-244**	2,4	72	0,57-0,7	Fleischer 2015, 44; Pereira da Cunha et al. 2016, 230; Stadler et al. 2019, 594
Salt hydrate	Na(CH3COO) 3w	58	1450 (s) – 1280 (l)	226-266	**289-386**	1,68 (s) – 2,37 (l)	113	0,34-0,43	Pereira da Cunha et al. 2016, 230; Stadler et al. 2019, 594
Salt hydrate	Na2HPO4 12w	35-40	1442 (l)	280	**404**			0,476	Stadler et al. 2019, 594
Salt hydrate	Na2S2O3 5w	46-48	1666-1670 (s)	187-210	**312-350**	1,46 (s) – 2,39 (l)	103	0,38-0,76	Pereira da Cunha et al. 2016, 230; Stadler et al. 2019, 594
Salt hydrate	NaSO4 10w (Glauber's salt)	32	1485 (s)	180-251	**267-373**	1,93 (s) - 2,8 (l)	82	0,45-0,56	Pereira da Cunha et al. 2016, 230; Fleischer 2015, 44
Salt hydrate	Oxalic acid 2w	105	1653 (s)	264	**436**	2,11 (s) – 2,89 (l)	133	0,7-0,9	Pereira da Cunha et al. 2016, 230
Salt mixture	CaCl2 6w (67%) – MgCl2 6w (33%)	25	1661 (s)	**127**	**211**	1,62 (s) – 2,27 (l)	**57**	**0,55-0,93**	Pereira da Cunha et al. 2016, 231
Salt mixture	HCOONa(45%)-HCOOK(55%)	176	1913 (s)	175	**335**	1,15 (s) – 0,93 (l)	92	0,43-0,63	Pereira da Cunha et al. 2016, 231
Salt mixture	K3PO4(55%)-Li3PO4(45%)	833							Guillot et al. 2011, 176

Salt mixture	KNO3(56%)-NaNO2(44%)	141	1994 (s)	97	**193**	1,18 (s) – 1,74 (l)	52	0,57-0,73	Pereira da Cunha et al. 2016, 231
Salt mixture	KNO3(66%)-LiNO3(34%)	133	2018 (s)	**150**	**303**	1,17 (s) – 1,35 (l)	**82**	**0,52-0,96**	Pereira da Cunha et al. 2016, 231
Salt mixture	KNO3(80%)-KOH(20%)	214	1905 (s)	83	**158**	1,03 (s) – 1,35 (l)	43	0,54-0,88	Pereira da Cunha et al. 2016, 231
Salt mixture	LiNO3(58%)-KCl(42%)	160	2196 (s)	**272**	**597**	1,26 (s) – 1,35 (l)	**161**	**0,59-1,31**	Pereira da Cunha et al. 2016, 231
Salt mixture	LiNO3(62%)-NaNO2(38%)	156	2296 (s)	233	**535**	1,57 (s) – 1,91 (l)	143	0,66-1,12	Pereira da Cunha et al. 2016, 231
Salt mixture	LiNO3(73%)-LiBr(27%)	228	2603 (s)	279	**726**	1,34 (s) – 1,38 (l)	196	0,57-1,14	Pereira da Cunha et al. 2016, 231
Salt mixture	LiNO3(81%)-LiOH(19%)	183	2124 (s)	352	**748**	1,6 (s) - 2 (l)	202	0,69-1,33	Pereira da Cunha et al. 2016, 231
Salt mixture	LiNO3(87%)-CaCl2(13%)	238	2362 (s)	317	**749**	1,5 (s) - 1,53 (l)	204	0,69-1,37	Pereira da Cunha et al. 2016, 231
Salt mixture	LiNO3(87%)-NaCl(13%)	208	2350 (s)	**369**	**867**	1,54 (s) – 1,56 (l)	**235**	**0,63-1,35**	Pereira da Cunha et al. 2016, 231
Salt mixture	LiNO3(91%)-LiCl(9%)	244	2351 (s)	342	**804**	1,58 (s) – 1,61 (l)	218	0,64-1,37	Pereira da Cunha et al. 2016, 231
Salt mixture	Mg(NO3)2 6w (59%) - MgCl2 6w (41%)	59	1610 (s)	**132**	**213**	2,29 (s) – 2,81 (l)	**58**	**0,53-0,67**	Pereira da Cunha et al. 2016, 231
Salt mixture	Mg(NO3)2 6w (61%) - NH4NO3 (39%)	52	1672 (s)	**125**	**209**	2,13 (s) – 2,67 (l)	**58**	**0,5-0,59**	Pereira da Cunha et al. 2016, 231
Salt mixture	MgNO3 6w (86%) – LiNO3 (14%)	72	1713 (s)	**180**	**308**	2,38 (s) - 2,9 (l)	**84**	**0,51-0,7**	Pereira da Cunha et al. 2016, 231
Salt mixture	Na2CO3(48%)-Li2CO3(52%)	500	2320 (s)	370	**858**				Guillot et al. 2011, 176
Salt mixture	Na2CO3(59%)-K2CO3(41%)	710	2400 (s)	163	**391**				Guillot et al. 2011, 176
Salt mixture	NaNO3(18%)-KNO3(52%)-LiNO3(30%)	123	2068 (s)	**140**	**290**	1,17 (s) – 1,44 (l)	**79**	**0,53-0,79**	Pereira da Cunha et al. 2016, 231
Salt mixture	NaNO3(45%)-KNO3(55%)	222	2028 (s)	**110**	**223**	1,01 (s) – 1,49 (l)	**61**	**0,51-0,73**	Pereira da Cunha et al. 2016, 231
Salt mixture	NaNO3(45%)-NaNO2(55%)	233	2210 (s)	**163**	**360**	1,31 (s) – 2,13 (l)	**97**	**0,59-0,64**	Pereira da Cunha et al. 2016, 231
Salt mixture	NaNO3(50%)-KNO3(50%)	221	1733 (s)	105	**182**				Guillot et al. 2011, 176
Salt mixture	NaNO3(50%)-LiNO3(45%)-KCl(5%)	160	2297 (s)	**266**	**611**	1,32 (s) – 1,69 (l)	**166**	**0,59-0,88**	Pereira da Cunha et al. 2016, 231
Salt mixture	NaNO3(51%)-LiNO3(49%)	194	2317 (s)	**262**	**607**	1,35 (s) – 1,72 (l)	**165**	**0,59-0,87**	Pereira da Cunha et al. 2016, 231
Salt mixture	NaNO3(52%)-KNO2(48%)	149	2080 (s)	124	**258**	1,05 (s) – 1,63 (l)	70	0,52-0,58	Pereira da Cunha et al. 2016, 231
Salt mixture	NaNO3(6%)-KNO3(53%)-NaNO2(41%)	142	2006 (s)	**110**	**221**	1,17 (s) – 1,73 (l)	**60**	**0,57-0,72**	Pereira da Cunha et al. 2016, 231
Salt mixture	NaNO3(67%)-NaOH(27%)-LiOH(6%)	230	2154 (s)	**184**	**396**	1,3 (s) - 2 (l)	**107**	**0,67-0,78**	Pereira da Cunha et al. 2016, 231
Salt mixture	NaNO3(70%)-KNO3(30%)	220-260		118		1,6 (s) - 1,5 (l)	**95**	0,5	Martin et al. 2013, 160-161; 163-164
Salt mixture	NaNO3(86%)-NaOH(14%)	250	2241 (s)	**160**	**359**	1,19 (s) – 1,86 (l)	**97**	**0,60-0,66**	Pereira da Cunha et al. 2016, 231
Salt mixture	NaNO3-KNO3	222	1900 (l)	100	**190**			0,5	Stadler et al. 2019, 595
Salt mixture	NaNO3-KNO3-NaNO2	140	1980 (s) – 1940 (l)	59	**114**	1,51 (l)		0,47-0,60	Lu et al. 2013, 100-101; He et al. 2017, 1234
Salt mixture	NaNO3-LiNO3	194	1900 (l)	265	**504**			0,5	Stadler et al. 2019, 595
Metal	Al	661	2700 (s)	388	**1048**	0,9		237	Fleischer 2015, 46; Fernández et al. 2017, 277
Metal	Bi	271,4	979 (s)	53,3	**52**	0,122 (s)		8,1	Fleischer 2015, 46
Metal	Cs	28,65	1796 (s)	16,4	**29**	0,236 (s)		17,4	Fleischer 2015, 46
Metal	Cu	1077		71					Fernández et al. 2017, 277
Metal	Ga	29,8	5907 (s)	80,1	**473**	0,237 (s)		29,4	Fleischer 2015, 46
Metal	In	156,8	7030 (s)	28,6	**201**	0,23 (s)		36,4	Fleischer 2015, 46
Metal	Mg	648	1740 (s)	365	**635**	1,27 (s) – 1,37 (l)		156	Fleischer 2015, 46; Fernández et al. 2017, 277
Metal	Pb	330					80		Ushak et al. 2015, 58
Metal	Sn	232	730 (s)	60,5	**44**	0,221	115	15,08	Fleischer 2015, 46; Ushak et al. 2015, 58
Metal	Zn	419	7140 (s)	112	**800**	0,39 (s) – 0,48 (l)	**220-222**	116	Fleischer 2015, 46; Fernández et al. 2017, 277; Ushak et al. 2015, 58
Metal alloy	Al(20%)-Si(80%)	585		460					Fernández et al. 2017, 277

Metal alloy	Al(88%)-Si(12%)	557-577	2540-2700 (s)	462-560	**1265**-1512	0,939-1,04 (s) - 1,74 (l)		160-181	Fernández et al. 2017, 277; Fleischer 2015, 46
Metal alloy	Ca(16%)-Mg(84%)	790	1380 (s)	272	375,36				Fernández et al. 2017, 277
Metal alloy	Ca(21%)-Mg(30%)-Si(49%)	865	2250 (s)	305	**686**				Fernández et al. 2017, 277
Metal alloy	Cu(45%)-Mg(6%)-Zn(49%)	703	8670 (s)	176	**1526**	0,42 (s)			Fernández et al. 2017, 277
Metal alloy	Cu(56%)-Mg(17%)-Si(27%)	770	4150 (s)	420	**1743**	0,75 (s)			Fernández et al. 2017, 277
Metal alloy	Cu(69%)-P(14%)-Zn(17%)	720	7000 (s)	368	**2576**				Fernández et al. 2017, 277
Metal alloy	Cu(74%)-Si(7%)-Zn(19%)	765	7170 (s)	125	**896**				Fernández et al. 2017, 277
Metal alloy	Cu(80%)-Si(20%)	803	6600 (s)	197	**1300**	0,5 (s)			Fernández et al. 2017, 277
Metal alloy	Cu(83%)-P(10%)-Si(7%)	840	6880 (s)	92	**633**				Fernández et al. 2017, 277
Metal alloy	Cu(91%)-P(9%)	715	5600 (s)	134	**750**				Fernández et al. 2017, 277
Metal alloy	Mg(44%)-Si(56%)	946	1900 (s)	757	**1438**	0,79 (s)			Fernández et al. 2017, 277
Metal alloy	Mg(47%)-Si(38%)-Zn(15%)	800		314					Fernández et al. 2017, 277
Metal alloy	Mg2Cu	841		243					Fernández et al. 2017, 277
Metal alloy	Zn2Mg	588		230					Fernández et al. 2017, 277
Metal mixture	Al(4%)-Zn(96%)	381	6630 (s)	138	916				Fernández et al. 2017, 277
Metal mixture	Al(46%)-Cu(49%)-Si(5%)	571	5560 (s)	406	**2257**				Fernández et al. 2017, 277
Metal mixture	Al(54%)-Cu(22%)-Mg(18%)-Zn(6%)	520	3140 (s)	305	**958**	1,51 (s) – 1,13 (l)			Fernández et al. 2017, 277; Fleischer 2015, 46
Metal mixture	Al(60%)-Mg(34%)-Zn(6%)	443-450,3	2380 (s)	310-312	**738-743**	1,63 (s) – 1,46 (l)			Fernández et al. 2017, 277; Fleischer 2015, 46
Metal mixture	Al(61%)-Cu(33%)-Mg(6%)	506	3050 (s)	365	**1113**				Fernández et al. 2017, 277
Metal mixture	Al(64%)-Cu(29%)-Mg(2%)-Si(5%)	507	4400 (s)	374	**1646**				Fernández et al. 2017, 277
Metal mixture	Al(64%)-Cu(34%)-Sb(2%)	545	4000 (s)	331	**1324**				Fernández et al. 2017, 277
Metal mixture	Al(65%)-Cu(30%)-Si(5%)	571	2730 (s)	422	**1152**	1,3 (s) - 1,2 (l)			Fernández et al. 2017, 277; Fleischer 2015, 46
Metal mixture	Al(65%)-Mg(53%)	497	2155 (s)	285	615				Fernández et al. 2017, 277
Metal mixture	Al(67%)-Cu(33%)	548	3600 (s)	372	**1339**				Fernández et al. 2017, 277
Metal mixture	Al(69%)-Cu(26%)-Si(5%)	525	2938 (s)	364	**1069**				Fernández et al. 2017, 277
Metal mixture	Al(83%)-Mg(5%)-Si(12%)	555	2500 (s)	485	**1213**				Fernández et al. 2017, 277
Metal mixture	Al(86%)-Sb(4%)-Si(10%)	575	2700 (s)	471	**1272**				Fernández et al. 2017, 277
Metal mixture	Ca(23%)-Cu(25%)-Mg(52%)	453	2000 (s)	184	**368**				Fernández et al. 2017, 277
Metal mixture	Cu(25%)-Mg(60%)-Zn(15%)	452	2800 (s)	254	**711**				Fernández et al. 2017, 277
Metal mixture	Mg(48%)-Zn(52%)	340-342	2850-4600 (s)	155-185	**442-851**	0,73 (s)		75	Fernández et al. 2017, 277
Metal mixture	Mg(55%)-Zn(17%)-X(28%)	400	2260 (s)	146	**330**				Fernández et al. 2017, 277

APPENDIX IV - TABLE OF INSULATION MATERIALS

The data on this table should be treated as estimates, as there is some variance in the data and its accuracy between different sources, and actual properties may vary due to precise composition, manufacturing method and so forth. Note that decimal separator used in this table is comma (,) instead of period (.).

Material	**Max temperature**	**Density**	**Thermal conductivity**	**Source**
	°C	kg/m^3	W/mK	
Vacuum		0	0	Stadler et al. 2019, 573
Asphalt		2115	0,062	Incropera et al. 2007, 939
Bakelite		1300	1,4	Incropera et al. 2007, 939
Brick, fire clay		2050-2645	1,0-1,5	Incropera et al. 2007, 939
Brick, magnesite			2,8-3,8	Incropera et al. 2007, 939
Cellular glass	430	145	0,046-0,079	Incropera et al. 2007, 936-938
Clay		1460	1,3	Incropera et al. 2007, 939
Concrete		2300	1,4-2,1	Incropera et al. 2007, 939; Stadler et al. 2019, 573
Cork (board)		120	0,039	Incropera et al. 2007, 936
Cork (loose fill)		160	0,035-0,045	Incropera et al. 2007, 936; Stadler et al. 2019, 573
Cotton		80	0,06	Incropera et al. 2007, 939
Foamglas		120	0,05	Zanganeh et al. 2014, 816
Glass		2225-2500	0,76-1,4	Incropera et al. 2007, 939; Stadler et al. 2019, 573
Glass fiber (organic bonded)		105	0,036	Incropera et al. 2007, 936
Glass fiber (poured/blown)		16	0,043	Incropera et al. 2007, 936
LD		1500	0,35-0,40	Zanganeh et al. 2014, 816
Microtherm		250	0,019-0,030	Zanganeh et al. 2014, 816
Mineral fiber cement	985	430	0,071-0,123	Incropera et al. 2007, 938

Mineral fiberboard		265	0,049	Incropera et al. 2007, 936
Mineral wool		190	0,046	Incropera et al. 2007, 936
Pipe insulation (Calcium silicate)	650	190	0,051-0,061	Incropera et al. 2007, 937
Pipe insulation (Magnesia)	320	185	0,055-0,104	Incropera et al. 2007, 937
Polystyrene	80	35-56	0,023-0,029	Incropera et al. 2007, 936
Polyurethane			0,021-0,035	Stadler et al. 2019, 573
Rock		2150-2680	2,15-2,8	Incropera et al. 2007, 940
Rubber	70	70	0,029-0,033	Incropera et al. 2007, 938
Soil		2050	0,50-0,52	Incropera et al. 2007, 940; Zanganeh et al. 2014, 816
UHPC		2500	1,9-2,2	Zanganeh et al. 2014, 816
Urethane (foam)		70	0,026	Incropera et al. 2007, 936
Wood		350-640	0,087-0,19	Incropera et al. 2007, 936; 940
Wool			0,035	Stadler et al. 2019, 573